ABSTRACT

Paleoenvironmental Variability across the Cretaceous-Tertiary Boundary in the Alberta Foreland Basin, as Interpreted from Fluvial Deposits and Paleosols, Red Deer River Valley, Alberta, Canada

Robert M. Forkner

Advisor: Lee C. Nordt, Ph.D.

The integration of sedimentological, paleotectonic and paleopedogenic data across the Cretaceous-Tertiary (KT) boundary of south-central Alberta indicates fluvial aggradation and variability of paleosol morphology in response to foreland orogenesis. The depositional history records an evolution from amalgamated, multi-story, braided sand bodies to accretionary, single-story, overbank-prone meandering deposits. The distribution of paleosols throughout the section is also cyclic. Immature, well-drained paleosols are associated with the braided deposits, whereas mature, poorly-drained paleosols are interbedded with the meandering deposits.

Two large-scale aggradational fluvial cycles are observed within the study interval and are interpreted to record variations in sediment supply and tilt of the depositional profile associated with foreland tectonism. Orogenic pulses are reflected in outcrop by amalgamated fluvial deposits interbedded with immature paleosols. Waning orogenesis is characterized by reduced fluvial sedimentation rates and an increase in the

number of mature paleosols. Orogenic quiescence is associated with an increase in channel sinuosity, and poorly drained, gleyed, coal-capped paleosols.

The KT boundary is located three meters above the tectono-stratigraphic transition from amalgamated, braided fluvial systems with well-drained paleosols to accretionary, meandering fluvial systems with poorly-drained paleosols. A gradual shift towards a more poorly-drained paleosol morphologies and increasingly accretionary fluvial styles suggests that the KT event was not the cause of increasingly cool and wet conditions across the boundary, but that the boundary lies at the inflection point between a well-drained to poorly-drained depositional cycle.

Paleoenvironmental Variability across the Cretaceous-Tertiary Boundary in the Alberta Foreland Basin, as Interpreted from Fluvial Deposits and Paleosols, Red Deer River Valley, Alberta, Canada.

A Thesis Submitted to the Graduate Faculty of

Baylor University

in Partial Fulfillment of the

Requirements of the Degree

of

Master of Science

By

Robert Murchison Forkner

Waco, Texas

August 2002

TABLE OF CONTENTS

LIST OF FIGURES

CHAPTER ONE

Background

Introduction

The stratigraphic interval spanning the Cretaceous-Tertiary (KT) boundary in south-central Alberta has been the subject of numerous palynological, paleontological, and geological studies (Lerbekmo and Coulter, 1984; Sweet and Braman, 1992; Lerbekmo et al., 1992; Lerbekmo et al., 1995; Eberth and O'Connell, 1995; Sweet, 2001). Whereas each of these studies has added to the knowledge-base surrounding paleoenvironmental change through the Cretaceous-Tertiary (KT) interval in Alberta, none of these studies have focused on the numerous well-preserved paleosols found within the deposits. Paleosols are unique among lithologic units because their morphology and chemistry reflect the combined influences of biota, climate, and topographic relief on sediments during a period of surficial exposure. By isolating pedologic features that are indicative of climatic processes, such as the occurrence of pedogenic carbonate, evidence of clay translocation, matrix color, the occurrence of coaly surface horizons, and the oxidation state of iron, conclusions about paleoclimatic variability can be made (Jenny, 1941; Buol et al., 1997; Retallack, 2001). Additionally, comparison of the paleosol record to active foreland tectonism and resultant base level and accommodation change will provide a unique framework for interpreting pedogenic response to tectonism, sedimentation, evolving fluvial styles, and paleoclimatic variability through the KT interval.

Late Cretaceous to earliest Tertiary paleosol-bearing non-marine deposits have been documented and measured by Irish (1970), Gibson (1977), Richardson et al., (1988), Eberth and O'Connell (1995), and Jerzykiewicz (1997) along the walls of the Red Deer River valley in south-central Alberta (Figure 1). Gibson (1977) focused primarily on section measurement and description, with an emphasis on calibrating local stratigraphy to regionally pervasive coal seams. Eberth and O'Connell (1995) added in-depth sedimentologic observations and analysis to the initial conclusions of Gibson (1977), and suggest that a cooler, wetter paleoclimate may have given rise to both increased coal seam occurrence and increased paleochannel sinuosity across the KT boundary. Jerzykiewicz (1997) added more description and interpretation, suggesting climatic instability in the area during, and possibly associated with, regression of the interior seaway 68 Ma ago. Jerzykiewicz and Sweet (1988), Sweet and Braman (1992), and Jerzykiewicz (1997) documented caliche-rich paleosols within time-equivalent strata of southern Alberta, an indication of regional paleoclimatic variability. Although these previous works document lithostratigraphic distribution of paleosols within the study interval, the paleosols were not rigorously described or interpreted for their climatic implications. KT boundary studies by Hildebrand and Boynton (1988), Sweet and Braman (1992), and Sweet (2001) recognize extraterrestrial bolide impact as coincident with massive plant extinctions at the end of the Maastrictian in Alberta. Palynological studies by Sweet and Braman (1992), and Sweet (2001) suggest that aerosol debris from the bolide impact may have led to decade-scale global cooling that is overprinted on a millennial-scale cooling trend.

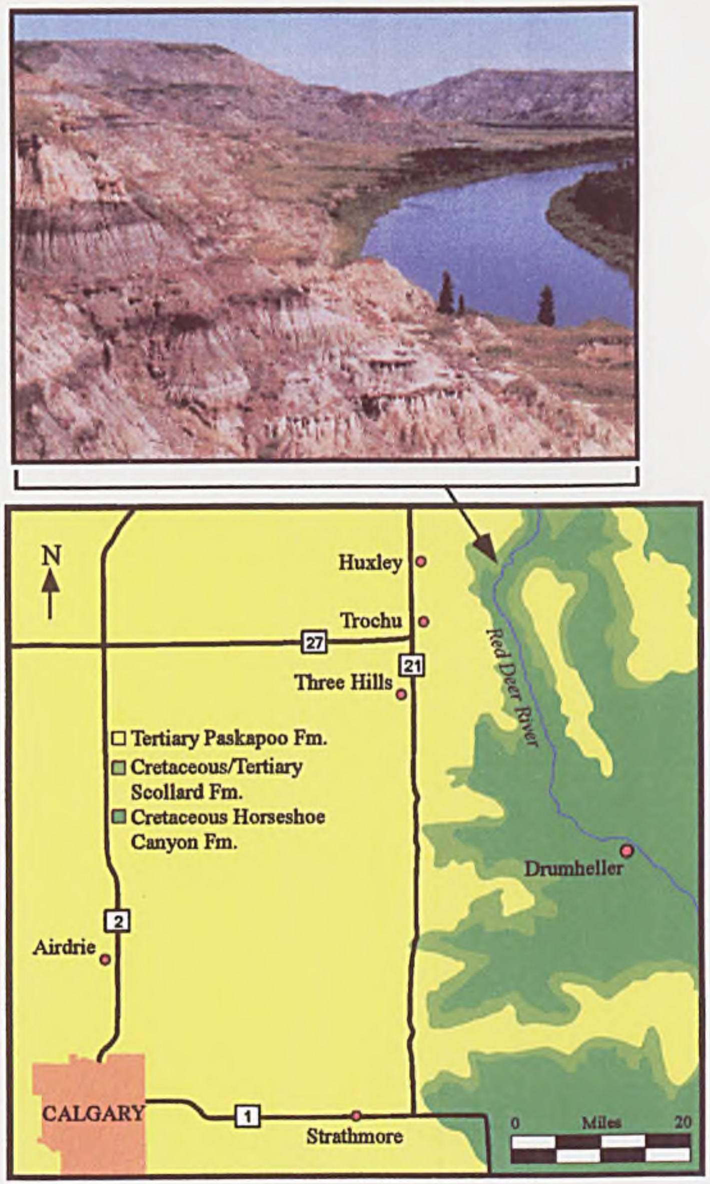

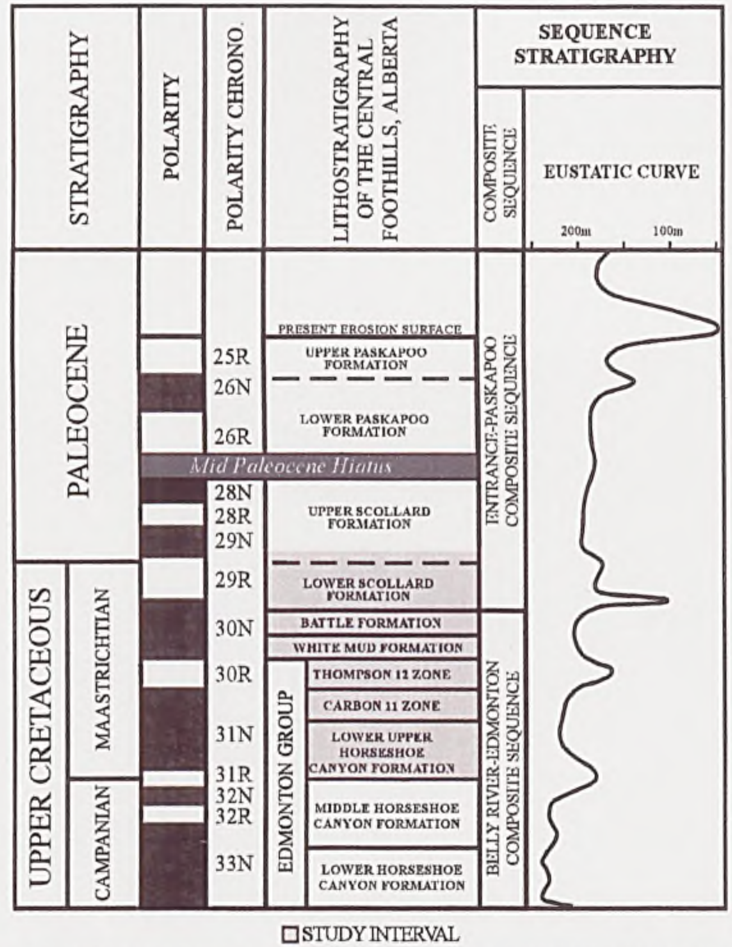

Figure 1. Location map, outcrop photograph and stratigraphic correlation chart for the Knudson's Farm locality. Geologic map adapted from the Canadian Society of Petroleum Geologists (1975); stratigraphic correlation chart adapted from Jerzykiewicz (1997) and Lerbekmo et al. (1992). Paleosol-bearing late Cretaceous to earliest Tertiary non-marine strata are well exposed along the walls of the Red Deer River Valley.

Whereas paleosols can be analyzed for paleoclimatic implications, they also can be analyzed for response to tectono-stratigraphic events (including tilt of the depositional profile, changing sediment supply, etc.) that directly affect pedogenesis. Extensive work by Catuneanu et al., (1997, 1999, 2000) describes and models the timing and stratigraphic response to active foreland processes in Alberta during the Late Cretaceous and early Paleocene (Figure 2). Foreland processes, including orogenic uplift, variable rates of sediment supply, and subsidence likely had pronounced effects on pedogenesis in the region. Integration of pedo-climatic data with the tectono-eustatic model for sedimentation and subsidence in the Alberta foreland basin may lead to the discovery of tectonic inputs that influenced pedogenesis as significantly as climate. For example, changes in the slope of the depositional profile induced by periods of foreland orogenesis combined with fluctuations in base level may have influenced fluvial morphology, sediment supply, topography, and drainage, thereby producing wetter or drier morphological characteristics in active soils that may or may not reflect true paleoclimatic variability. Additionally, accommodation change within the basin related to local and global base level fluctuations may be indicated by tracking variability of aggradational cycle thickness of fluvial deposits through the section (McCarthy et al., 1999). Analysis of the effects of foreland tectonism and base level change on the tilt of the depositional profile, rates of sedimentation, and evolving fluvial styles provides a framework from which to approach the paleopedogenic record in central Alberta.

The pedotype method is one of the most efficient ways to generate paleoenvironmental interpretations from a large number of paleosols within a single interval. Retallack (1994) utilized the pedotype approach in a study of KT paleosols in

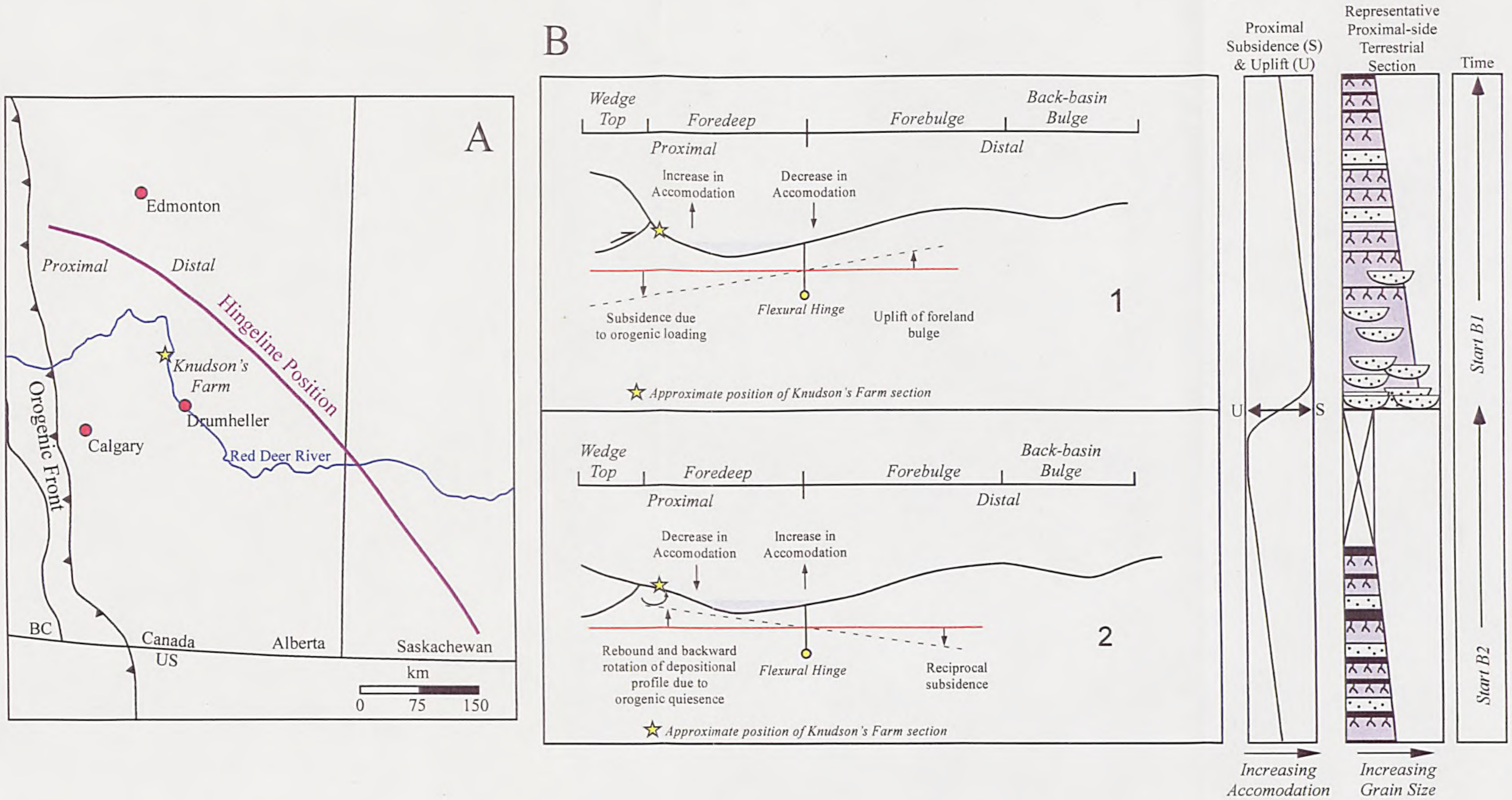

Figure 2. Tectono-stratigraphic model of foreland basin evolution of the Alberta basin. A) Tectonic map of the region depicting tectonic provinces including orogenic front and approximate position of flexural hinge during the Maastrichtian. Tectonic map modified from Catuneanu et al. (2000). B) Diagrammatic cross section of Alberta foreland basin tectonism with subsidence/accomodation plot and synthetic proximal-side stratigraphic section to the right. 1) Orogenic loading in wedge top causes foredeep subsidence, higher slopes on the proximal depositional profile, proximal base level rise and distal base level fall. Initial orogen-induced subsidence and shedding leads to aggradational channel filling that slows with time (see synthetic stratigraphic section). 2) Orogenic quiesence causes wedge top unloading and rebound, leading to backward rotation and flattening of the foreslope, proximal base level fall and distal base level rise. Flattening of the depositional profile, increasingly poor drainage, and decreasing rates of sedimentation lead to the formation of organic-rich paleosols (see synthetic stratigraphic section).

eastern Montana, roughly 500 miles southeast of the Red Deer River valley exposures. By viewing morphologically similar soils as paleoenvironmental "trace fossils", Retallack is able to determine that the paleoclimate of eastern Montana became increasingly humid during the KT transition. While these interpretations are well-supported by extensive field description and geochemical study, they do not account for constituent mass transport, which aids in the interpretation of soil development and exposure time. Retallack's study also does not address the relationship between soil development, local tectonism, and base level change on paleo-landscape stability, drainage, and the stacking of paleosol-capped fluvial aggradational cycles (McCarthy and Plint, 1998, McCarthy et al., 1999). Accounting for tectonic inputs is important because the effects of changing rates of landscape stability and drainage on paleosols can be identical to paleosol response to climate change.

The integration of lithofacies analysis, paleosol description, and geochemical analysis of measured sections in the Red Deer River valley will compliment earlier works by refining the history of paleoclimatic variability and response to foreland tectonism through the KT interval. The outcrop exposure at Knudson's Farm was chosen as the study locality because of the preservation of a complete non-marine section spanning the KT boundary, as well as ease of access. Grouping representative paleosols into pedotypes serves to constrain paleoenvironmental conditions related to climate, drainage, degree of organic matter accumulation, and general soil development to soils of similar descriptive morphology.

Location and Geologic Setting

Late Cretaceous and early Paleocene deposits in central Alberta are well known for their excellent preservation of the Late Cretaceous and early Tertiary sedimentary record (Jerzykiewicz and Sweet, 1988; Sweet and Braman, 1992; Lerbekmo et al., 1995). A wide valley cut into the plains of central Alberta by the Red Deer River exposes these deposits and allows their study (Figure 1).

The deposition of Late Cretaceous and early Paleocene sediments in central Alberta was the result of clastic infilling of the actively subsiding Alberta foreland basin that formed during Laramide orogenesis (Jerzykiewicz, 1985, 1997; Catuneanu et al., 1997; 2000). A study of the Saunders group of western Alberta by Jerzykiewicz (1985) recognizes six major basin-filling cyclothems related to Campanian through the early Paleocene Laramide uplift. Individual cyclothems form fining-upward couplets that are dominated by channel sandstones at the base and overbank muds, coals and paleosols at the top. Whereas Jerzykiewicz (1985) identifies sediment provenance and depositional cyclicity for major sandstone bodies in the Saunders group, no correlation is made to base level. Subsurface and outcrop studies by Catuneanu et al. (1997, 1999, 2000) reveal that the Alberta basin has a reciprocal stratal architecture as a result of orogenically-induced subsidence and rebound (Figure 2). Subsidence and rebound associated with foreland basin development alters local base level, and therefore sedimentary accommodation space. Variability in accommodation space may have influenced pedogenic pathways for paleosol development in the Knudson's Farm section.

Determination of the time-stratigraphic position of terrestrial sediments deposited in the Alberta basin has been confidently established through regional palynological and paleomagnetic studies (Lerbekmo et al., 1985, 1992, 1995). Formational boundaries and regionally pervasive coal seams at Knudson's Farm allow the section to be placed within a time-stratigraphic context (Figure 1). The base of the Knudson Farm section is roughly equivalent with the number 10 "Marker" coal seam of Gibson (1977) (Braman, 2001, personal communication). Work by Lerbekmo and Braman (in press) has placed the base of the number 10 Marker coal seam at the top of the *Baculites eliasi* ammonite biozone, which is roughly equivalent to the 31r-32n magnetic reversal at the Campanian-Maastrichtian boundary. The section is continuous through the early Paleocene, and is separated into several zones (base to top) based on paleopedogenic and depostional features: the Horseshoe Canyon Formation, including the lower upper unit (HSC), the Carbon 11 coal zone (C11), and the Thompson 12 coal zone (T12); the Whitemud Formation (Wm); the Battle Formation (Bat); the Lower Scollard Formation (L. Scol.), and the Upper Scollard Formation (U.Scol.) (Figure 1). The Battle-Scollard contact is the only recognized erosional unconformity in the Knudson's Farm section, but the extent and duration of exposure and incisement is not well constrained (Russell, 1983; Eberth and O'Connell, 1995). The Knudson Farm section is continuous through the KT transition, coincident with the Nevis 13 coal seam, and is capped by the early Paleocene Ardley 14 coal seam (Jerzykiewicz, 1997). The KT boundary itself has been recognized as a globally-pervasive claystone layer that is preserved near the base of the Nevis 13 coal seam in the Knudson's Farm section (Sweet and Brahman, 1991; Eberth and O'Connell, 1995; Sweet, 2001). Uppermost Cretaceous and earliest Tertiary deposits in the Red Deer River valley have not been buried deeply ($\leq$ 1000 m), as inticated by non-compacted biological remains such as roots, pollen, trees, and dinosaur bones (Lerbekmo and Coulter, 1983). Constraint of lithostratigraphic surfaces and excellent preservation of the terrestrial record at Knudson's Farm allows for detailed study of paleoenvironmental change through the KT transition.

Methods

During summer, 2000, a 150 meter composite section was identified and subsequently measured during the summer of 2001. This section has been called the "Knudson's Farm" section in previous works and is located adjacent to Kent and Marion Knudson's farm near Trochu, Alberta. Palynologist Dennis Braman of the Royal Tyrrell Museum of Palaeontology was consulted to insure accurate placement of stratigraphic surfaces including the KT boundary, marker coals described by Gibson (1977), and formation boundaries. Key stratigraphic surfaces were photographed and labelled during the walkthrough with Braman. The section was measured using a hand level and Jacob's staff, with each lithostratigraphic unit being measured and described. Paleosols were numbered and marked with survey flags as the outcrop section was described, and were annotated as to their stratigraphic position on the graphical outcrop description. Paleosols were not described in detail until the outcrop section had been completed. Observations documented on the outcrop description include lithology, texture, bed thickness, mechanical and biological sedimentary structures, paleocurrent, and position of paleosols. Paleocurrents measured from trough crossbeds and ripple sets were plotted on a rose diagram. Alluvial facies were described and interpreted using the methods of Miall (1996) and Walker and James (1992), and compared to the findings of Eberth and O'Connell (1995).

The second phase of section description involved the field description and sampling of paleosols. Initially, paleosols were recognized by the presence of a dark or coaly surface horizon, rooting, or recognizable soil structure. Detailed field description followed USDA standards, including horizon nomenclature, boundary distinction and topography, horizon thickness, Munsell color, reaction with HCl, type and degree of structural development, root and animal traces, evidence of clay translocation, and presence of nodules or other secondary minerals and oxides (Soil Survey Staff, 1998).

Paleosols with similar descriptive characteristics were grouped into pedotypes. Representative paleosols from each pedotype were sampled for bulk geochemical and thin section analysis at 10 centimeter intervals or for each horizon if the horizons were less than 10 centimeters thick. Key morphological features of pedotypes have been condensed into a pedotype summary table for Knudson's farm paleosols (Table 1).

Paleosol geochemistry was determined per horizon by triple-acid digestion ICP-AES analysis and reported in weight percent of single elements per horizon. Single element weight percentages were converted to oxide weight percents by the equation:

$$\text{Wt. \% Oxide} = \text{Wt. \% Element} / (^{\text{Mol. Mass of Element}}/_{\text{Mol. Mass Oxide}})$$

Recording weight percentages as oxides is preferred to single elements due to the natural occurrence of oxides in soil (Chadwick et. al., 1990; Buol et al., 1997). Weight percent SiO_2 was determined independantly and reported as an oxide.

Following the determination of weight percentages of oxides, stoichiometric molecular ratios were calculated as a proxy for several pedogenic processes (Retallack,

Table 1. Pedotype summary table for paleosols at Knudson's Farm. Parameters for pedogenic development from Soil Survey Staff (1998), Birkeland (1999) and Retallack (2001)

Pedotypes →	Milktoast	Gloom	Trochu	Cow 1	Oreo	Cow 2	Ramp	Doom
Epipedon / Endopedon	Ochric / Cambic	Ochric / Cambic	Ochric / Cambic	Ochric / Cambic	Ochric / Argillic	Ochric / Argillic	Ochric / Cambic	Ochric / Cambic
USDA Taxonomic Classification of Representative Profile	Lithic or Lamellic Dystrudept	Haplohemist	Typic Dystrudert	Typic Dystrochrept	Typic Endoaqualf	Typic Hapludalf	Typic Dystrudert	Troposaprist *or* Medisaprist
Representative Horizonation	A-Bw-C	OA-Bg1-Bg2-BC	A-Bw-Bss1-Bss2-BC	A-Bt1-Bt2-Bt3-BC-C	A-Bg-Btg1-Btg2-BC	A-Bw-Bt1-Bt2-BC	A-Bss1-Bss2-Bss3-BC	O-OA-Bg-BC
Paleoclimatic Implications	- MAP 125-150 cm/yr - Wet/dry seasonality - Free drainage	- MAP 150-250 cm/yr - Periodic drainage and/or seasonality	- MAP125-150 cm/yr - Pronounced wet/dry seasonality - Free drainage	- MAP 75-125 cm/yr - Wet/dry seasonality - Free drainage	- MAP 70-125 cm/yr - Moderate wet/dry seasonality - Variable drainage	- MAP 70-125 cm/yr - Wet/dry seasonality - Free drainage	- MAP125-150 cm/yr - Pronounced wet/dry seasonality - Free drainage	- MAP 250+ cm/yr - Poor, periodic drainage
Topographic Position	Overbank or floodplain proximal to channel	Backswamp	Overbank or floodplain	Overbank or floodplain	Overbank or floodplain, possibly swamp	Overbank or floodplain	Overbank or floodplain	Backswamp
Duration of Exposure	100 - 500 years	1,400 - 2,800 years	1,000+ years	3,000 - 5,000 years	5,000+ years	5,000+ years	500-1,000 years	3,000-12,000 years by coal thickness
Representative Photographs	Figure 15	Figure 16	Figure 17	Figure 18	Figure 19	Figure 20	Figure 21	Figure 22

1997). The ratio Al_2O_3/SiO_2 was used as proxy for clay translocation, Al_2O_3 representing the formation of silicate clays relative to stable silica. The ratio Al_2O_3/SiO_2 is typically between 0.1 and 0.3 in most soils, but can be greater than 0.3 in clay-rich soils (Retallack, 1997). Fe_2O_3/SiO_2 was used to represent oxidation of iron to iron oxide in the soil. Soils formed in reducing (waterlogged) conditions ought to have markedly lower ratios than do soils that formed in drier, oxidizing environments. Calcification was determined using $CaO+MgO/Al_2O_3$. Both CaO and MgO were used because pedogenic carbonate may contain both low-magnesium calcite and dolomite (Retallack, 1997). The ratio for calcification is typically below 2 in non-calcareous soils, but may exceed 10 within carbonate nodules (Retallack, 1997). The ratio $Al_2O_3/CaO+MgO+K_2O+Na_2O$ was used as proxy for base formation and weathering, and compares the stoichiometric concentration of soluble products of hydrolytic weathering ($CaO+MgO+K_2O+Na_2O$) to less-soluble clays (Al_2O_3) (Retallack, 1997). Deeply weathered soils (oxisols and ultisols) may have a $CaO+MgO+K_2O+Na_2O/Al_2O_3$ ratio of near 0.01, but most soils have ratios near 0.5 (Retallack, 1997). Na_2O/K_2O is the ratio used as a proxy for salinization, with soils affected by salt input having a ratio near 1.0 (Retallack, 1997). Finally, Ba/Sr was used as proxy for leaching, most rocks having a Ba/Sr ratio near 2 and highly leached soils having a ratio near 10 (Retallack, 1997).

Reconstruction of mass transport of mobile constituents was attempted with the assumption that post-pedogenic compaction affected bulk densities in a uniform manner throughout the profile, as suggested by Driese et al. (2000). With this assumption, trends in constituent concentration per horizon may not be quantitatively realistic, but relative trends in constituent concentration should be preserved (Driese et al., 2000). Determination of bulk density per horizon was done in triplicate by using the paraffincoating method of Blake and Hartge (1986). After bulk densities were determined, dilation or collapse of the soil relative to the parent material (strain) could be estimated. Strain was calculated per horizon using:

$$\varepsilon_{I,w} = (\rho_p C_{i,p}/\rho_w C_{i,w})\text{-}1$$

where $\varepsilon_{I,w}$ equals strain, ρ_p and ρ_w bulk density of parent material and soil, and $C_{i,p}$ and $C_{i,w}$ concentration of an immobile element (Ti) in parent material and soil (Chadwick et. al., 1990). Finally, the mass transport function of mobile elements was calculated per horizon using:

$$\tau_{j,w} = (\rho_w C_{j,w}/\rho_p C_{j,p})(\varepsilon_{I,w}+1) - 1$$

where $\tau_{j,w}$ is the unitless proportion of the element gained or lost in the horizon in question (w), and $C_{j,w}$ and $C_{j,p}$ are the weight percentages of mobile element j in the soil and parent material (Chadwick et. al., 1990).

Weight percentages of organic and inorganic carbon were determined using a ThermoFinnegan elemental analyzer. Samples were analyzed in duplicate, with one sample having been pre-treated with HCl and the other not pre-treated. The bulk carbon contents of the duplicate samples were then compared to determine inorganic carbon by difference. This analysis showed that the total carbon present in all analyzed samples was of organic origin. All chemical data were later tabulated in spreadsheet and graphical format using Microsoft Excel so that depth trends could be more easily observed.

Thin section analysis was done for textural determination and for recognition of micromorphological properties. Textural analysis was accomplished by counting 300 points per slide using an automated slide-moving mechanism and normalizing counts to percent sand (.05mm-2mm), silt (.05mm-.002mm), and clay (<.002mm). Differentiation between coarse clay and very fine silt was somewhat problematic because the textural break between these grain sizes is very difficult to determine visually, even at high magnification. Questionable point-counts were tabulated as clay if a true grain could not be identified and the point was associated with highly birefringent, directionally oriented matrix or wall-coating material (Brewer, 1976). Other properties identified in thin section analysis include: type and degree of primary mineral weathering, and description of iron oxides, concretions and/or nodules, plasma and granular microfabrics, voids, description of argillans, and biological traces (Brewer, 1976; Retallack, 1997, 2001; Birkeland, 1999).

Calculations for the duration of pedogenesis were estimated for each paleosol. For paleosols with coal surface horizons, Retallack et al., (1996) used modern analogues to determine average rate of peat accumulation of 0.50 – 1.0 mm yr^{-1} for woody peats, which are dominant in the fossil record. Compaction of organic litter to coal varies from .050-0.1 times former peat thickness, depending on overburden thickness (Retallack et al., 1996). While it is true that subtle climatic variability can significantly alter the rates at which peat accumulates, it is assumed here that peat accumulation was constant unless coals are noticeably stratified. Work by Lerbekmo and Coulter (1984), and observation of non-deformed biological traces in the lithologic units at Knudson's farm suggest minimal compaction by overburden (≤ 1,000 m). Therefore, coal compaction has been assumed to be low, at 0.1 times former peat thickness. Other more qualitative properties, such as development of diagnostic horizons (Bt, Bk, etc.) and development of soil orders have been assigned general times of formation relative to their strength of development using the developmental indices of Birkeland (1999) (Table 2). Use of qualitative parameters places general time constraints on extent of pedogenic development and geomorphic stability.

Calculations relating paleosol properties to mean annual precipitation (MAP) can also be accomplished for paleosols in the Knudson's Farm section. Ready and Retallack (1995) developed a relationship between MAP (mm) and the molecular ratio of bases to alumina in the Bt horizon (Q) of modern soils, where:

$$\text{MAP (mm)} = -759Q + 1300$$

Qualitative indicators of high MAP (130-250 cm + yr^{-1}) include development of histic epipedon, the presence of gley colors and shallow rooting. Qualitative indicators of mixed, or seasonally variable precipitation can include slickensides, infilled surface cracks, a mixture of shallow and deeply penetrating roots, and argillans.

The integration of stratigraphic, sedimentologic and paleopedologic observations was attempted in order to deduce controls on sediment accumulation and pedogenic change through time. A plot of cumulative deviation of aggradational fluvial cycle thickness was then generated and calibrated to the eustatic curve of Haq et. al., (1988) using the placement of stratigraphic surfaces proposed by Jerzykiewicz (1997). Although fluvial systems are typically complex, accommodation change within the Alberta basin is thought to be controlled by a combination of global eustasy and local tectonism (Catuneanu et. al., 2000). Accordingly, a long-term change in accomodation space should be reflected by systematic shifts in aggradational cycle thickness of sediments during an episode of basin fill (Posamentier and Vail, 1988; Posamentier and Allen,

Table 2. Table of paleosol development

Num.	Development	Description of Development
1	Very Weakly Developed	Root traces, no true A horizon, little or very weak structural development, depositional fabric easily recognizeable.
2	Weakly Developed	True A horizon with rooting, subsurface horizons with evidence of clay traslocation or gley. No true argillic horizon or histic epipedon. May have a cambic endopedon or vertic properties.
3	Moderately Developed	True A, OA, or O horizon with rooting, subsurface horizons with obvious evidence of clay traslocation or gley. True argillic horizon or histic epipedon.
4	Strongly Developed	Thick (60cm+) surficial organic (coal) horizon. May have especially thick (2-3m) subsurface (B) horizons. Obvious zones of eluviation and illuviation.
5	Very Strongly Developed	Unusually thick (3m+) surficial organic (coal) horizon or subsurface (B) horizons. Obvious zones of eluviation and illuviation. Weathering of quartz.

Adapted from Retallack (1988)

1993; Schwans, 1995). Measurement of fining-upward fluvial couplets (single depositional units) were tabulated and an average thickness of 2.3 meters was calculated. Cumulative deviation from this average was calculated by determining the difference in individual cycle thickness from the average and adding that value to the difference determined from the previous deposit. Pedogenic properties that reflect temporal change (drainage, rates of sedimentation, etc.) that may be related to changing base level and tectonism were noted and include: waterlogging, gley colors, and high levels of organic matter accumulation in surface horizons (poor drainage, possible base level high); and clay translocation, presence of eluvial and illuvial horizons, depth of rooting, presence of oxidized color (well drained, possible base level fall) (Table 3). The integration of these techniques provides a base for understanding the composite effects of climate, sedimentation, and base level on the terrestrial sediments.

Table 3. Table of paleosol drainage

Num.	Drainage	Description of Drainage
1	Well Drained	A horizon, no gley colors, deeply penetrating (1m+) roots, argillans.
2	Seasonally Drained	A horizon, deeply penetrating roots, vertic properties including slickensides and surface cracks, evidence of clay translocation (Bt).
3	Wet with Dry History	Organic surface horizon (O or OA), gley colors, deeply penetrating roots, evidence of clay translocation (Bt).
4	Poorly Drained	Thick organic surface horizon (O or OA), gley colors, shallow rooting.

CHAPTER TWO

Depositional Facies

Depositional Facies Descriptions

Depositional facies are defined and interpreted based on the nomenclature of Miall (1996, pages 79 and 131-163). Miall (1996) systematically separates fluvial deposits into architectural elements and their respective facies. The methodology of Miall (1996) allows straightforward interpretation of evolving fluvial styles (Table 4). Initial explanation of relevant architectural elements and associated facies will be followed by description of their vertical distribution through the section. Paleosols will be viewed as facies within this section, and will be more rigorously analyzed in the "Paleosol" and "Paleoenvironmental Reconstruction" sections.

Architectural Element: CH – Channel

Architectural element CH (channel) is defined as "a concave-up lens or sheet of sediment with an erosional base representing the main path of sediment transport in a fluvial system" (Miall, 1985). The shape and scale of channels are highly variable and as a result may actually be broken into separate architectural elements with any combination of facies assemblages (Miall, 1996). In the case of Knudson's Farm, the designation CH was only given to those architectural elements that had visible channelform geometry.

Lithofacies charcteristics of the CH architectural element are unique from unit to unit within the section. Channelform deposits identified in the HSC unit typically have a

Table 4. Facies summary table for deposits at Knudson's Farm (Facies acronyms from Miall, (1996))

	Architectural Element: CH - *Channel*	Architectural Element: SB - *Sandy Bedforms*	Architectural Element: LA - *Lateral Accretion*	Architectural Element: LS - *Laminated Sand Sheet*	Architectural Element: FF - *Overbank Fines*
	Facies: St, Sr, Fl	Facies: Ss, Sh, St, Sr, Sp, Fl	Facies: Sr, Sh, Fl	Facies: Sp, Fl, Sr, P	Facies: Fl, Fsm, C, P
Lithology / Texture	Fine-med. sand, very fine sand, and silt	Fine-med. sand; very fine sand and silt. Minor silt and clay plugs	Fine-very fine sand and silt.	Fine-med. sand and silt.	Dominantly clay, also fine sand and silt
Mechanical Sedimentary Structures	Trough-crossbedding, ripple cross-lamination, fine lamination	Basal scour and fill, planar cross bedding, trough-crossbedding, ripple cross-lamination, horizontal sand lamination, fine lamination	Ripple cross-lamination, horizontal sand lamination, fine lamination	Horizontal sand lamination, fine lamination, minor horizontal sand lamination	Fine lamination to massive silt and mud, coal, carbonaceous mud, pedogenically weathered silts and clays
Fossils	Masticated organic material	Masticated organic material, fragmentary fossilized wood, minor disarticulated macrofaunal remains.	Masticated organic material, fossilized wood in growth position	Masticated organic material, fragmentary fossilized wood, disarticulated macrofaunal remains.	Masticated organic material, root and faunal traces.
Common Stratigraphic Position	Fl channel plug in HSC; Lower Scollard	Mid-upper HSC, T12, Whitemud, Lower Scollard, KT transition zone	Middle and upper T12, Upper Scollard	Lower HSC, lower C11, Intermittantly through T12, near KT transition in Upper and Lower Scollard	Ubiquitous
Associated Pedotypes	Milktoast, Gloom, Doom	Milktoast, Cow1	Gloom, Doom, Oreo	Milktoast, Gloom, Doom, Oreo, Cow 1, Ramp	All
Representative Photographs	Figure 4E	Figure 12	Figure 10A	Figure 14D, 10C	Figure 6

concave-up, lens-type geometry that is incised into adjacent sediments. These deposits are plugged with fine laminated silt and clay (facies fl). Channelforms in the Thompson 12 and lower Scollard Formation have geometries that are difficult to visually constrain. However, basal scour (Ss), uniform paleocurrent direction, and mechanical sedimentary structures that indicate decreasing flow regime upward suggest that these deposits are the result of channel deposition. Mechanical sedimentary structures include planar beds (Sh) and trough crossbeds (St) with pebble lags near the base, trough crossbeds interbedded with planar-tabular beds (Sp) near the middle of the deposits, and current ripples (Sr) interbedded with minor horizontal sand lamina (Sh) at the tops.

Architectural Element: SB – Sandy Bedforms

Sandy bedforms (SB) are representative of "fields of individual migrating fluvial bedforms formed as an aggradational complex" (Miall, 1996). Stacking of varying fluvial bedforms is thought to reflect seasonal changes in discharge within lower-sinuosity paleochannels of a braided fluvial system.

Deposits identified as SB at Knudson's farm also have some characteristics of the CH element, including basal scour and a preferred paleocurrent direction. However, lack of identifiable channelform geometry limits their taxonomic classification to SB, even if the beds may have been deposited in a channelized setting. Typical sedimentary facies in the SB architectural element are planar beds (Sh), trough crossbeds (St) with pebble lags, trough crossbeds interbedded with planar-tabular beds (Sp), current ripples (Sr), and minor horizontal sand and ripple lamina (Fl/Sr). Certain sandy bedforms have paleosol (P) caps, which are indicative of geomorphic stability.

Architectural Element: LA – Lateral Accretion

The lateral accretion (LA) architectural element occurs at a high angle to the channel trend. Lateral accretion deposits typically form the inner bank of a meander bend and prograde toward the channel thalweg (Miall, 1996). LA deposits typically fine upwards, with mechanical sedimentary structures recording a decrease in flow regime with shallowing. LA deposits are also typically inclined towards the direction of accretion. The occurrence of LA architectural elements indicates deposition in a meandering system characterized by a low regional gradient.

Deposits of the LA element are identified in the Knudson's farm as depositionally inclined, accretionary bedsets that both fine upward in grain size, and reduce bedform flow regime upward. The tops of LA deposits are also recognized by root traces, the presence of fossilized trees in growth position, and little to no evidence of pedogenic alteration (indicating sedimentation outpaced pedogenesis). Facies identified in LA elements include: planar-tabular crossbeds (Sp), current rippled sand (Sr), and fine lamina (Fl). The tops of some lateral accretion deposits are capped by paleosols (P) and/or coals (C), which may be indicative of channel migration or abandonment.

Architectural Element: LS – Laminated Sand Sheet

LS (laminated sand sheet) is defined as "a locally extensive blanket of sand deposited during flash flood, typically as crevasse splay" (Miall, 1996). These deposits typically fine upward as current energy wanes and may also include reducing-flow bedforms (Walker and James, 1992). Facies common to LS deposits include current rippled sand (Sr), fine lamina (Fl), minor planar-tabular bedding (Sp), and paleosols (P) at the tops.

The instantaneous, and often catastrophic, nature of LS deposition often leads to the entraining, burial and preservation of plant and animal remains. Additionally, due to the fact that LS deposition regularly results from the breaching of levees, otherwise geomorphically stable surfaces (paleosols) are buried. The position of LS deposits in normally stable areas also leads to pedogenic alteration at their surfaces.

Laminated sand sheet deposits can be recognized in the Knudson's farm section by identifying their characteristic bedforms, thin bedding, a sharp base, and fossilized remains of wood and animals (dinosaurs).

Architectural Element: FF – Overbank/Floodplain Fines

Overbank fines (FF) are "sheet-like deposits of fine-grained sediment deposited in the floodplain of a river system during a flood" (Miall, 1996). Overbank fines typically consist of very fine sand, silt and clay, and may be ripple laminated, horizontally laminated, or massive. Pedogenic alteration is common in overbank fines, and may completely destroy the original depositional fabric. Humification may also occur in floodplain areas when low-lying, frequently inundated, and associated with dense growth of terrestrial plants. Overbank fines make up the majority of architectural elements in the Knudson's farm section. Facies common of FF include: fine lamina (Fl), massive backswamp fines (Fsm), paleosols (P), and coal (C).

Stratigraphic Nomenclature and Unit Description

Lithofacies in the Knudson's Farm section have been stratigraphically divided into separate units based on both the formational nomenclature of Eberth and O'Connell (1995) and on their relationship to the coal seams of Gibson (1977). The base of the

Knudson's Farm section is thought to be approximately 10 meters above the Marker 10 coal seam of Gibson (1977), and the top is directly beneath the Ardley 14 coal seam (Braman, personal communication, 2001). From base to top, the Knudson's Farm section consists of the Horseshoe Canyon Formation, the Whitemud Formation, the Battle Formation, and the lower and upper Scollard Formation (Figure 1). In this study, the Horseshoe Canyon Formation is further subdivided into three distinct units; the lower Horseshoe Canyon (HSC), the Carbon 11 (C11) coal zone, and the Thompson 12 (T12) coal zone. The Battle and Whitemud Formations have not been further subdivided. The Scollard Formation is divided into a lower non-coaly portion and an upper coaly portion using the nomenclature of Eberth and O'Connell (1995). One exception to this nomenclature is the separation between upper and lower members being placed approximately 4 meters beneath the Nevis 13 coal rather than at its base, due to evidence for increasingly poor drainage below the coal. The stratigraphic divisions suggested here are based on a synthesis of depositional and paleopedogenic relationships that are indicative of paleoenvironmental change through time. Additionally, separation of the section into individual units allows for better-constrained description of the evolution of fluvial styles through the section.

Horseshoe Canyon Formation: Lower Horseshoe Canyon (HSC) Unit

The HSC unit described at Knudson's farm consists of twelve, meter to multi-meter thick fining-upward alluvial cycles. The couplets in the HSC unit typically fine up from sand to clay (Figure 3). The lower nine couplets in the HSC unit are fine to very fine grained laminated sands (Sr, Fl) that fine upward into thin, clay-rich paleosols (P), and are interpreted as intermittently stabilized crevasse-splay deposits (Figure 4). Fine-

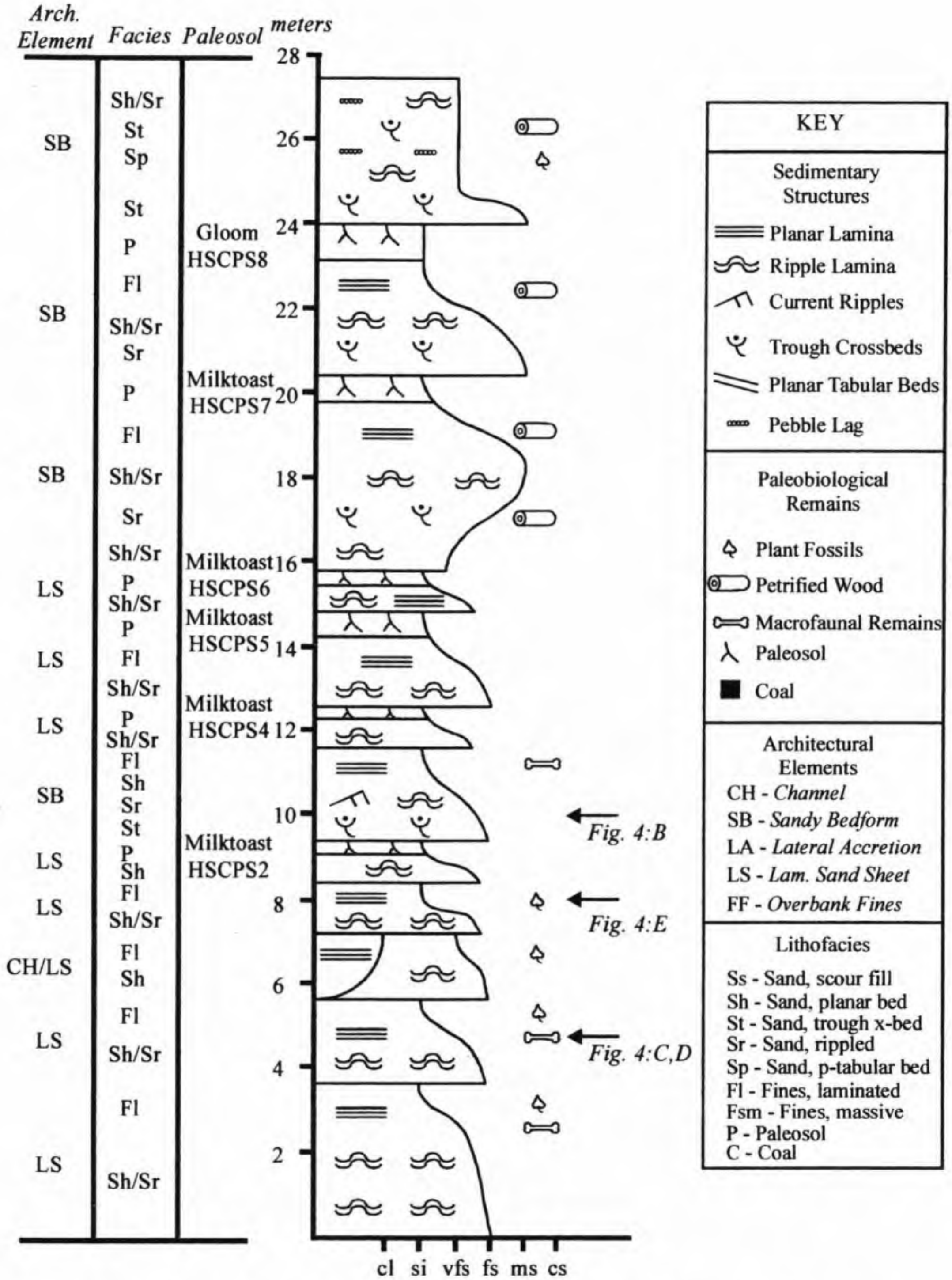

Figure 3. Measured section of Lower Horeseshoe Canyon (HSC) unit.

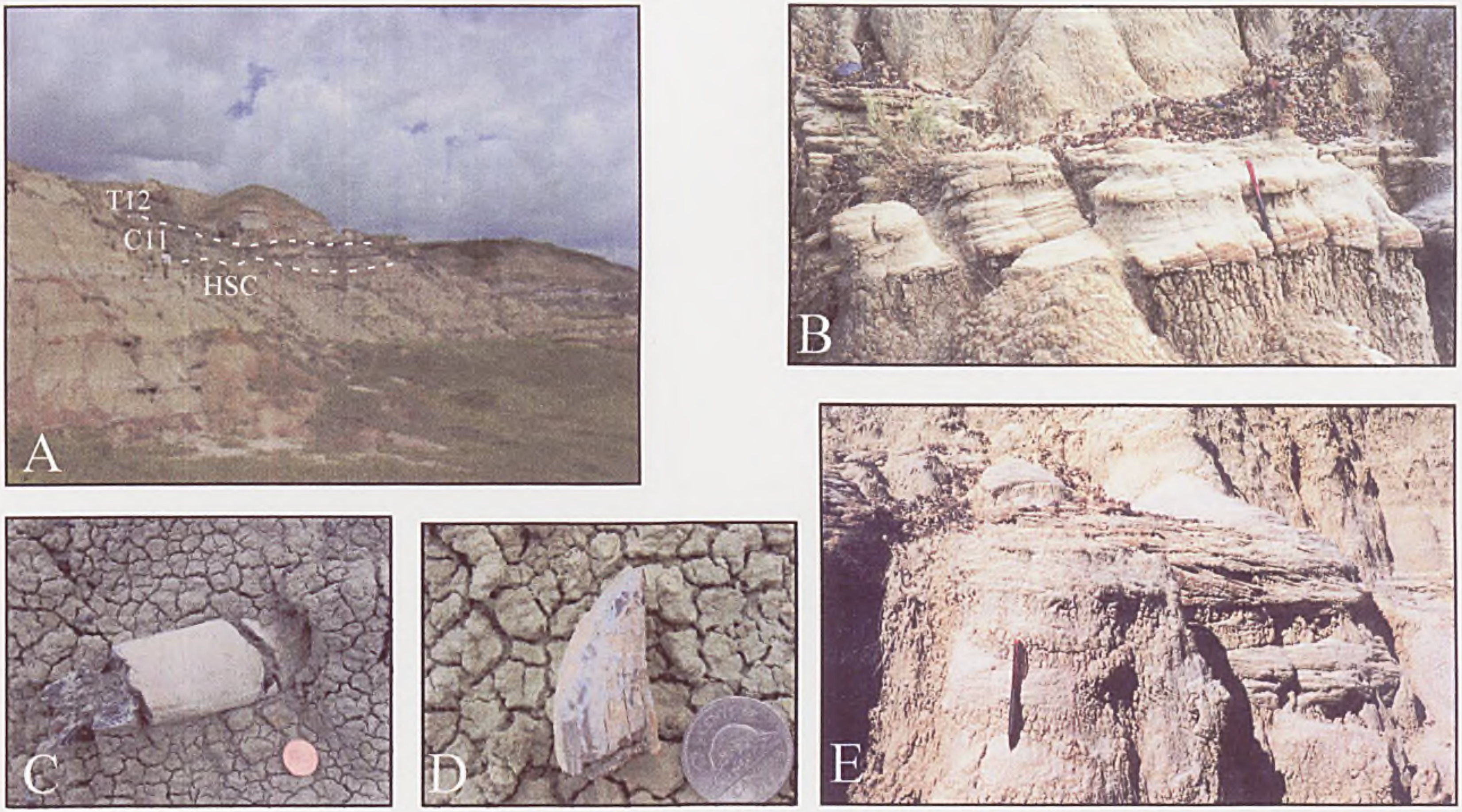

Figure 4. A) View of units in the Horseshoe Canyon Formation: Lower Horseshoe Canyon (HSC), Carbon 11 Coal Zone (C11), and the Thompson 12 Coal Zone (T12). B) Trough crossbeds (St) in HSC couplet 10. C & D) Dinosaur remains from HSC couplet 6. E) Ripples (Sr) in HSC couplet 4.

laminated (Fl), concave-up, lensoid, channelform (CH) bodies incise into some couplets, suggesting that the couplets themselves are not the result of channelized deposition (Figure 4). The channelform source for each crevasse splay could not be identified. Fragmentary remains of terrestrial plants and animals (dinosaurs) are found in the lower, sandier portions of the couplets suggesting rapid deposition. Four of the lower nine couplets show evidence of surficial weathering and pedogenic alteration at their tops and include weakly-developed paleosols of the Milktoast pedotype. The dominance of crevasse splay deposits and weakly-developed paleosols in the basal portion of the HSC suggests frequent flooding, possibly related to heavy rainfall, as well as high sediment supply.

The upper three couplets in the HSC record a transition to increased geomorphic stablity. The basal sediments of the upper three couplets are trough crossbedded (St) medium-grained sand bodies (SB) that fine up into laminated silt and clay (Sr, Fl), with localized basal lags of ironstone pebbles. Only a few paleocurrent measurements could be taken from these deposits, and the general directions of flow were measured at southeast and northeast with equal regularity, possibly as a result of channel sinuosity. Fossilized remains in this interval were dominantly woody material, suggesting that couplet tops were geomorphically stable for periods long enough to allow tree growth, and that subsequent deposition was rapid. Paleosols identified on the tops of the top couplets include a weakly developed Milktoast paleosol and a deeply-rooted, gleyed paleosol of the Gloom pedotype. The occurrence of a paleosol of the moderately-developed Gloom pedotype provides evidence for increasing periods of geomorphic stability between depositional events, as well as an increasingly wet, or poorly-drained environment. The uppermost deposit in the HSC unit is capped by the basal sandstone of the Carbon 11 coal zone. The occurrence of sandy bedforms (SB) at the top of the HSC unit is indicative of increased sedimentation in a braided fluvial system. A substantial increase in fossilized wood fragments in the sandstones and the occurrence of a gleyed paleosol suggests a slight increase in geomorphic stability between depostional events as well as a rising water table through time.

Horseshoe Canyon Formation: Carbon 11 (C11) Coal Zone

The Carbon 11 coal zone is a 9 meter thick unit comprised of fining-upward couplets and paleosols (P) (Figure 5). The couplets in the C11 unit fine up from ripple laminated (Sr) fine grained sand at the base to clay paleosols (P) and coal-capped paleosols (C) at the tops (Figure 6). The basal deposit in the C11 zone is a gray, fine, ripple-laminated (Sr) sandstone (LS) with abundant masticated carbonaceous fragments. This sandstone fines up into a light, olive-gray clay-rich Gloom paleosol (P) with a carbonaceous clay surface horizon. The basal couplet is capped by a second couplet of similar description, but with a 65-centimeter thick coal (C11 coal A) at its top. The presence of this coal not only provides evidence for an elevated water table, but also for prolonged geomorphic stability. The transition from SB elements in the upper HSC to gleyed LS elements in the C11 may indicate a shift from an environment undergoing rapid, regular sedimentation to an increasingly poorly-drained, geomorphically stable, and possibly paludal setting.

Capping C11 coal A is a ripple-laminated (Sr) fine sandstone (LS) that fines upward into a clay paleosol (P). This paleosol (C11PS3), as well as the paleosol above it (C11PS4), both have vertic properties, including large slickensides that are indicative of

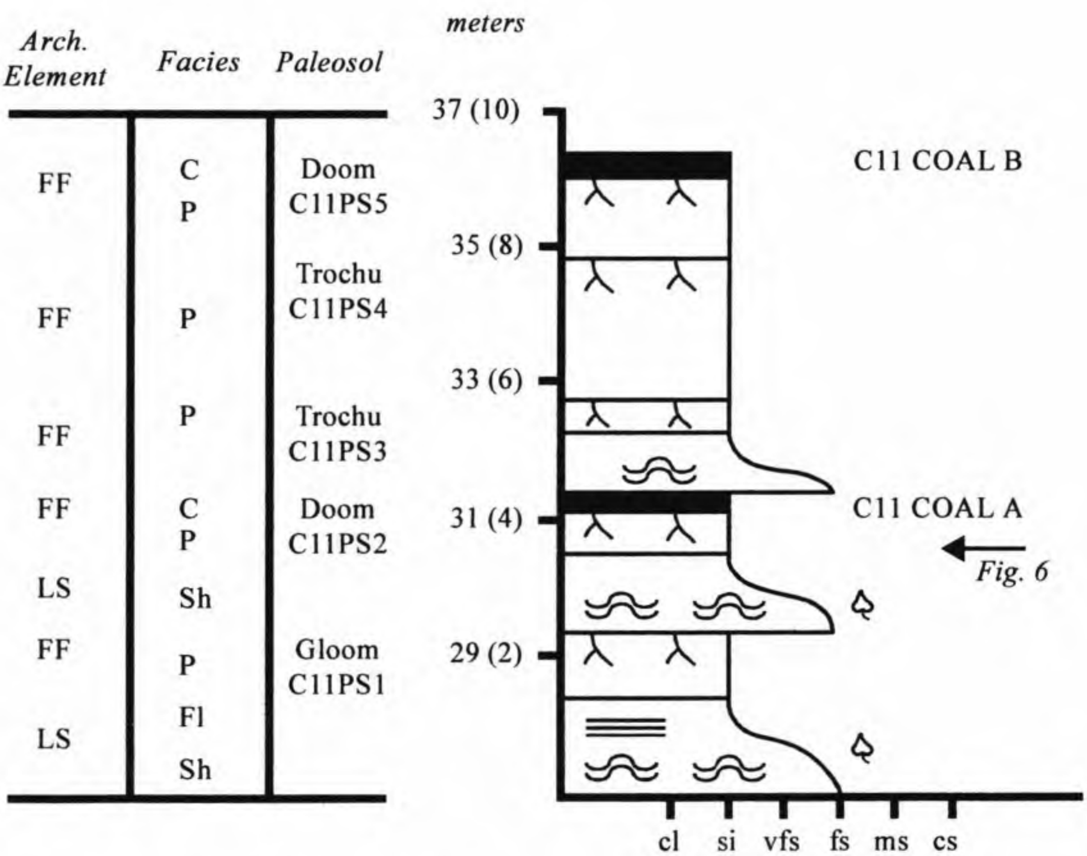

Figure 5. Measured section of Horeseshoe Canyon Carbon 11 (C11) unit.

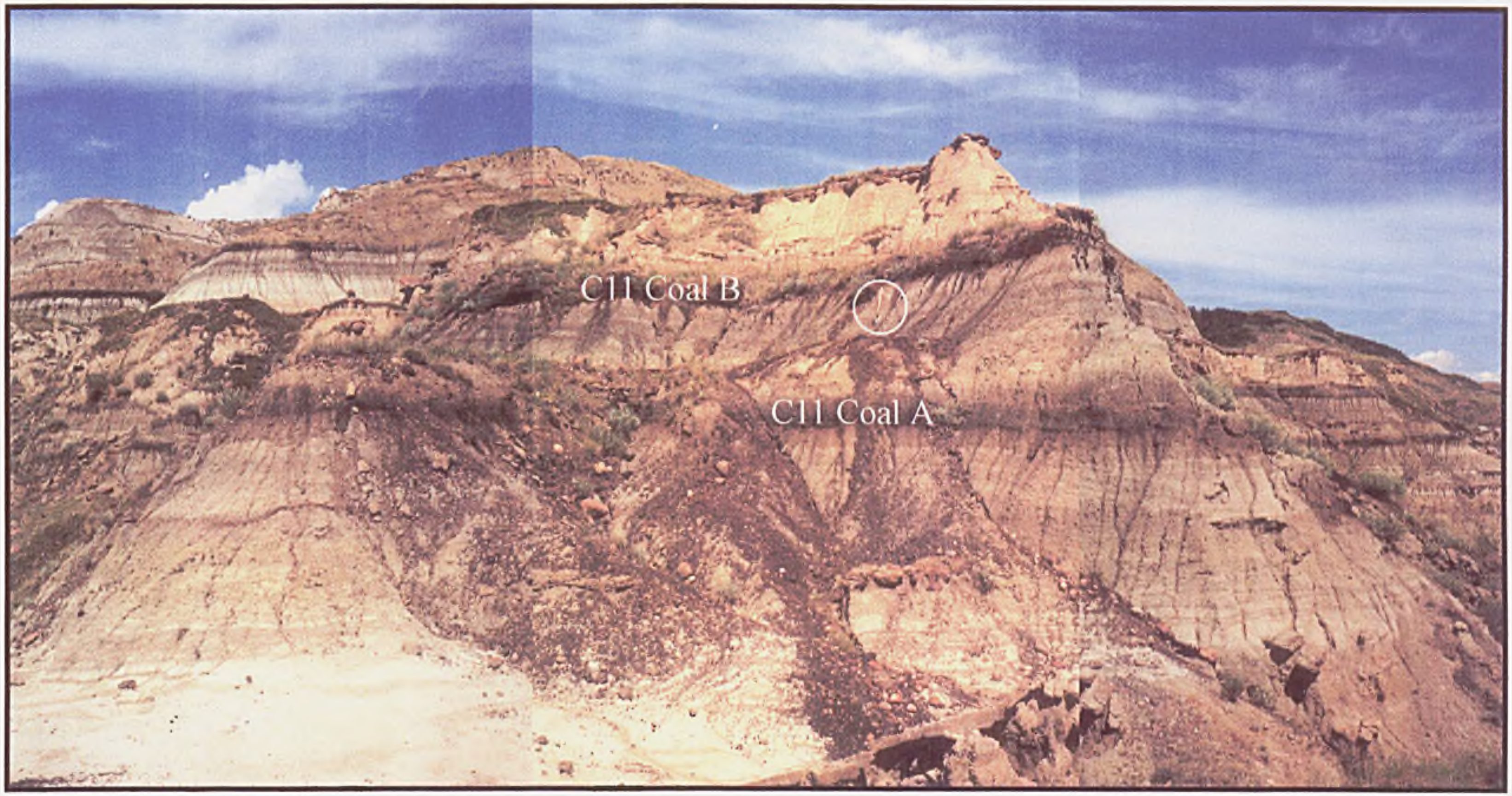

Figure 6. Photopan of the Carbon 11 (C11) Coal Zone showing C11 coal A and C11 coal B. Shovel (circled) is 1.5 meters in length.

shrink/swell clays and pronounced wet/dry seasonality. These Trochu paleosols also exhibit evidence of clay translocation (argillans and sepic fabric), which suggests that periods of free drainage existed at the time of pedogenesis. However, the gray matrix color, lack of pedogenic carbonate, and significant accumulations of organic material at the surface suggest that prolonged periods of groundwater saturation also affected these paleosols. The presence of paleosols with vertic properties does indicate an environmental shift from a poorly-drained, paludal setting to a seasonally-drained setting. The final deposit in the C11 unit is the Carbon 11 "B" coal, which records a return to poorly drained conditions. The Carbon 11 B coal paleosol is morphologically similar to the paleosol containing the C11 A coal. Both are of the Doom pedotype and are indicative of a low-lying, flooded swampland. Both have deeply-penetrating roots (up to 1 meter), that suggest periodic lowering of the water table. The depositional record in the Carbon 11 unit records a shift from an unstable, shifting fluvial environment (top of HSC) to a poorly-drained, geomorphically stable environment in which pedogenic processes predominate.

Horseshoe Canyon Formation: Thompson 12 (T12) Coal Zone

The deposits in the Thompson 12 coal zone record a shift from fluvial aggradation at the base through overbank and accretionary deposition at the top (Figure 7, 8). The basal 9 meters of the Thompson 12 unit is comprised of a sandstone body (SB) that incises into a ripple-laminated (Sr) sandstone (LS), which may have been a remnant of depositional conditions during C11 time. The base of the T12 sandstone body contains planar beds (Sh) with localized sandstone and carbonaceous rip-up clasts. Trough crossbedding (St) dominates the lower and middle sandstone body, and can be recognized

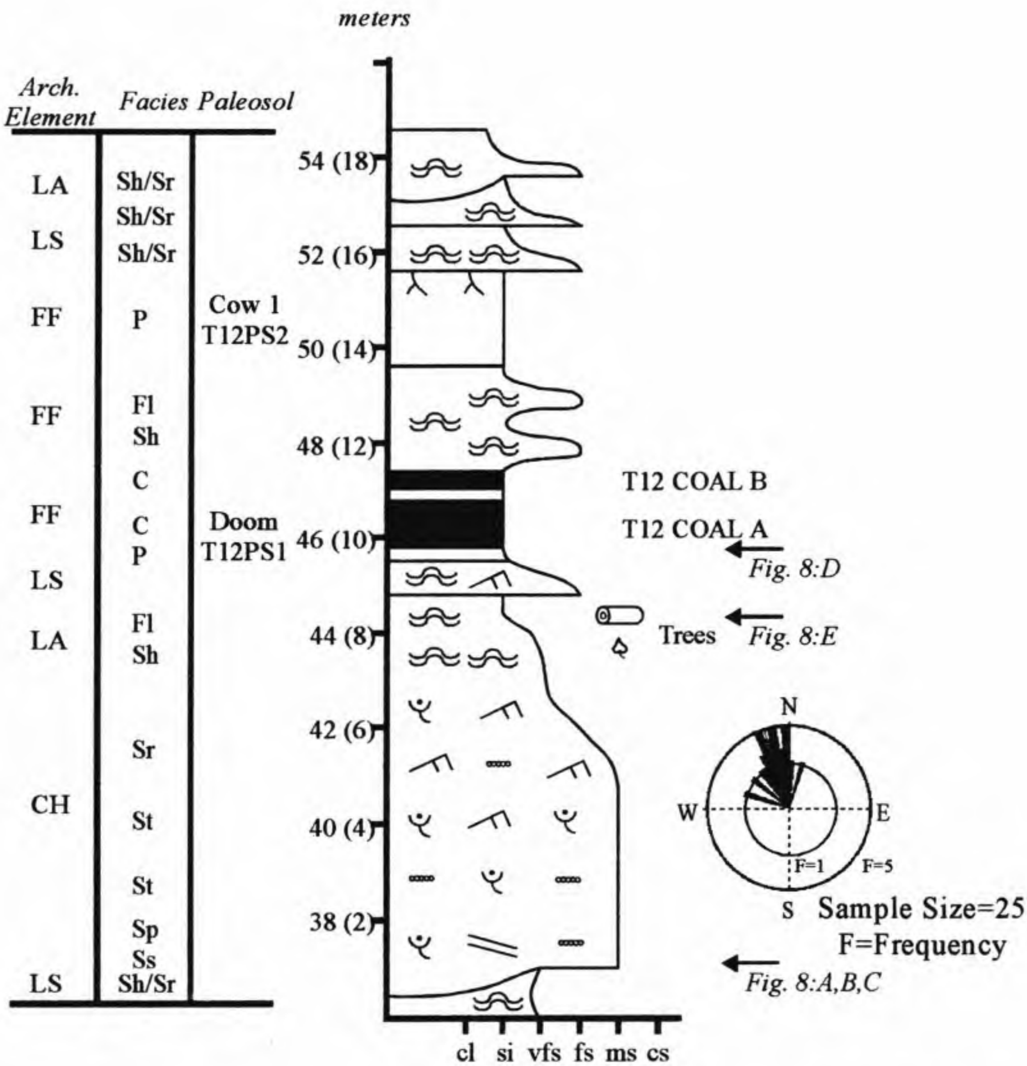

Figure 7. Measured section of Horeseshoe Canyon Thompson 12 (T12) unit.

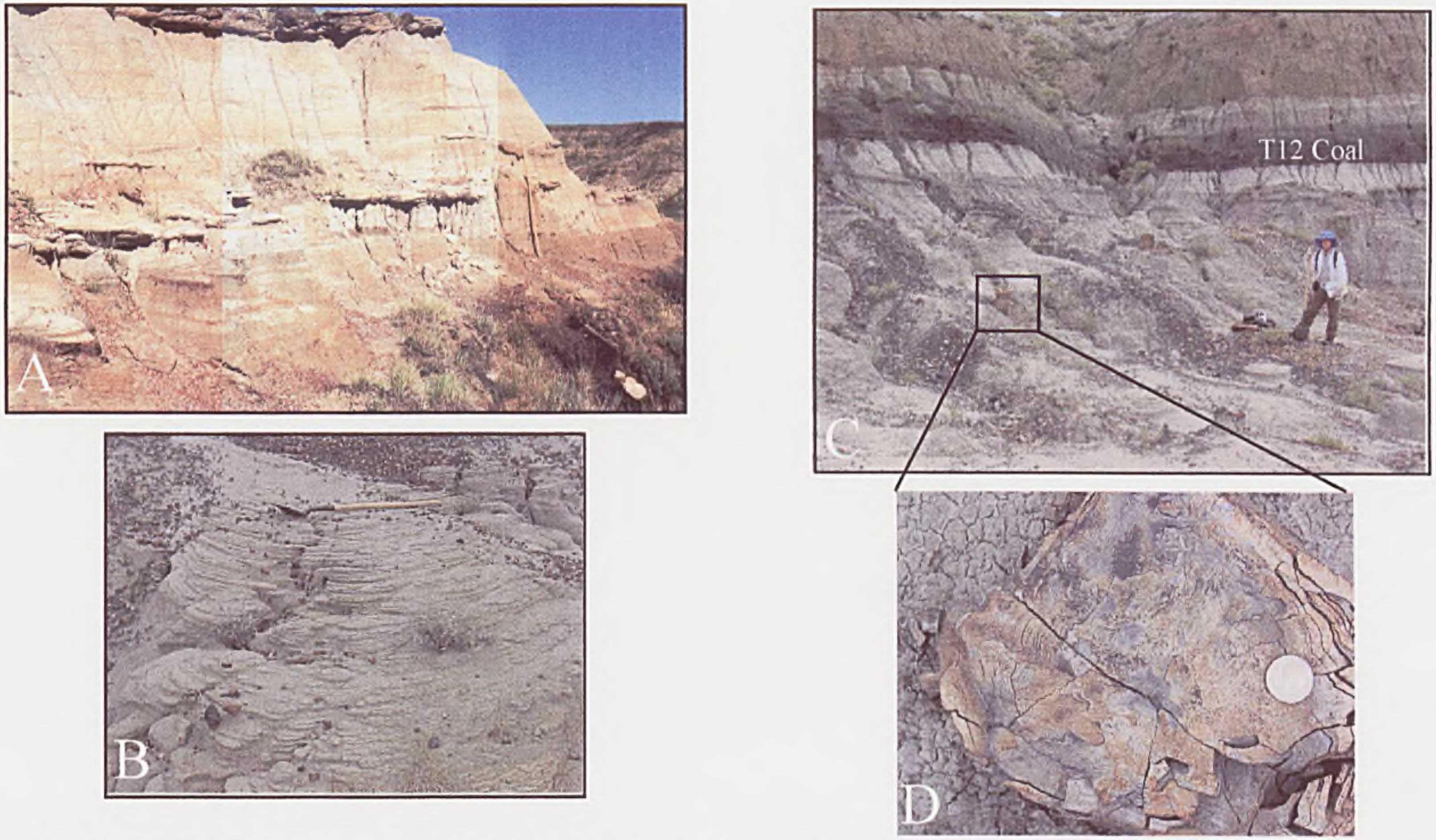

Figure 8. Photographs of the Thompson 12 Coal Zone (T12). A) Photopan of the lower T12 sandstone. Note trough crossbedding (St). Staff is 2 meters long. B) Trough crossbed set indicating a paleocurrent direction of N15W. Shovel is 1.5 meters long. C) Photopan of the middle T12 zone, showing the top of the T12 sand (LA), fossilized trees in growth position, and the Thompson 12 coal seam (C). D) Fossilized tree stump with growth rings.

in areas where the sandstone has been cemented by siderite or where organic material drapes the bedform. Planar-tabular bedsets (Sp) also occur in the middle sandstone, typically at the top of a trough crossbedded set. Paleocurrent measurements indicate a north-northwest transport direction. The typical transport direction for sediments shed from Rocky Mountains is to the east, basinward of the orogenic uplift to the west (Catuneanu et al., 2000). The paleocurrent measurements may reflect increased local sinuosity induced by late-orogenic proximal slope flattening. It may also reflect a change in source area. The basal T12 sand body is likely the result of deposition by amalgamated, aggradational paleochannels, as evidenced by basal scour (Ss) and pebble lags, trough crossbed sets (St) that are capped by planar-tabular sets (Sp), unidirectional paleocurrent orientation, and lack of recognizeable channelforms or accretionary bedforms (Miall, 1985; Eberth and O'Connell, 1995). The upper two meters of the T12 sand body fines into interbedded, ripple laminated silt and very fine sand (Fl, Sr) of a lateral accretion deposit (LA). Well preserved fossilized tree stumps are found in growth position at differing levels in the LA deposit, but no other pedogenic features were recognized. This suggests sustained, limited deposition occurring rapidly enough to inhibit pedogenic alteration (Figure 8). Preserved growth rings in the tree stumps also suggest a seasonal paleoclimate, although quantitative paleoclimatic data is difficult to discern because of the negligible pedogenic alteration of the top of the LA deposit. The basal T12 sand is capped by a meter-thick ripple laminated sand (LS) that is rooted near its top and is, in turn, overlain by the Thompson 12 coal paleosol (C) (T12PS1 paleosol). The T12 coal paleosol differs from underlying C11 coal paleosols because the mineral soil matrix underlying the coal is thinner (only 25-30 cm) and much coarser-textured, and roots only penetrate 20 cm. This suggests a sustained, high water table. The Thompson 12 coal is separated into an upper and lower coal by a thin, laminated carbonaceous mudstone (Fl) that is likely the result of overbank deposition (FF) into a backswamp. Above the T12 coal paleosol are interbedded, ripple- laminated carbonaceous mudstones and very fine sandstones. These deposits are likely overbank fines (FF) of similar origin to the carbonaceous mudstone found within the T12 coal. The second paleosol (P) in the T12 unit (T12PS2) is of the Cow 1 pedotype, and has deeply penetrating roots, argillans on ped faces, and is very thick (3 m) as compared to T12PS1. These morphological characteristics are indicative of pedogenic processes in a humid, well-drained setting that was stable for at least several thousand years (Birkeland, 1999). Above the second T12 paleosol are several lateral accretion (LA) deposits comprised of depositionally-inclined, ripple and fine-laminated (Sr, Fl), silty sandstones. Measurements along the dip of the inclined strata indicate accretion to the southwest (S35W), which may indicate a general paleocurrent direction to the northwest. Southwest accretion is consistent with paleocurrent measurements in the lower T12 sand body.

Deposits in the T12 unit record an evolution in fluvial depositional style from aggradational (braided) at the base to accretionary (meandering) near the top. Bedforms in the basal sand sheet are indicative of being deposited by channels, although the amalgamated, aggradational nature of deposition masks any channelform geometries. The transition to accretionary sedimentation at the top of the T12 SB may indicate increasing channel sinuosity and a corresponding decrease in capacity. Further evidence for a slowdown in sedimentation is the presence of the regionally pervasive T12 coal above the LA deposit. Above the T12 coal zone, there is evidence for improved drainage with Cow 1 paleosol T12PS2. The occurrence of a well-drained paleosol not only indicates improved local drainage conditions from T12PS1 to T12PS2 time, but is also indicative of a time of limited fluvial deposition. Fluvial deposits return at the top of T12PS2 with several lateral accretion deposits that are diagnostic of a meandering fluvial system. These deposits are in turn overlain by the interbedded silty sandstones of the Whitemud Formation.

Whitemud Formation

The Whitemud Formation overlies the Thompson 12 unit, and is approximately 5 meters thick in the Knudson's Farm locality (Figure 9). The base of the Whitemud Formation is comprised of 1 a meter-thick, laminated, very-fine sand and silt (Fl), with common organic fragments draping lamina surfaces (Figure 10). The low-angle, inclined habit of bedforms within the basal Whitemud

suggests lateral accretion (LA). The markedly lighter color in comparison to the oxidized silts and sands of the T12 lateral accretion deposits may suggest post-depositional gleying associated with ponded conditions. Ponding is also suggested by a 20 cm-thick, non-pedogenic, finely laminated carbonaceous shale that caps the basal Whitemud deposit. The overlying Whitemud Formation is approximately 3 meters of ripple-laminated (Sr), depositionally inclined carbonaceous sandy siltstone deposited by lateral accretion. All of the sediments in the upper Whitemud show evidence of reducing conditions, including gray to white sand and matrix colors intermixed with black carbonaceous clasts and detrital drapes on lamina surfaces. The Whitemud Formation is interpreted as deposited by lateral accretion deposits in high-sinuosity, low-competence channels and ponding.

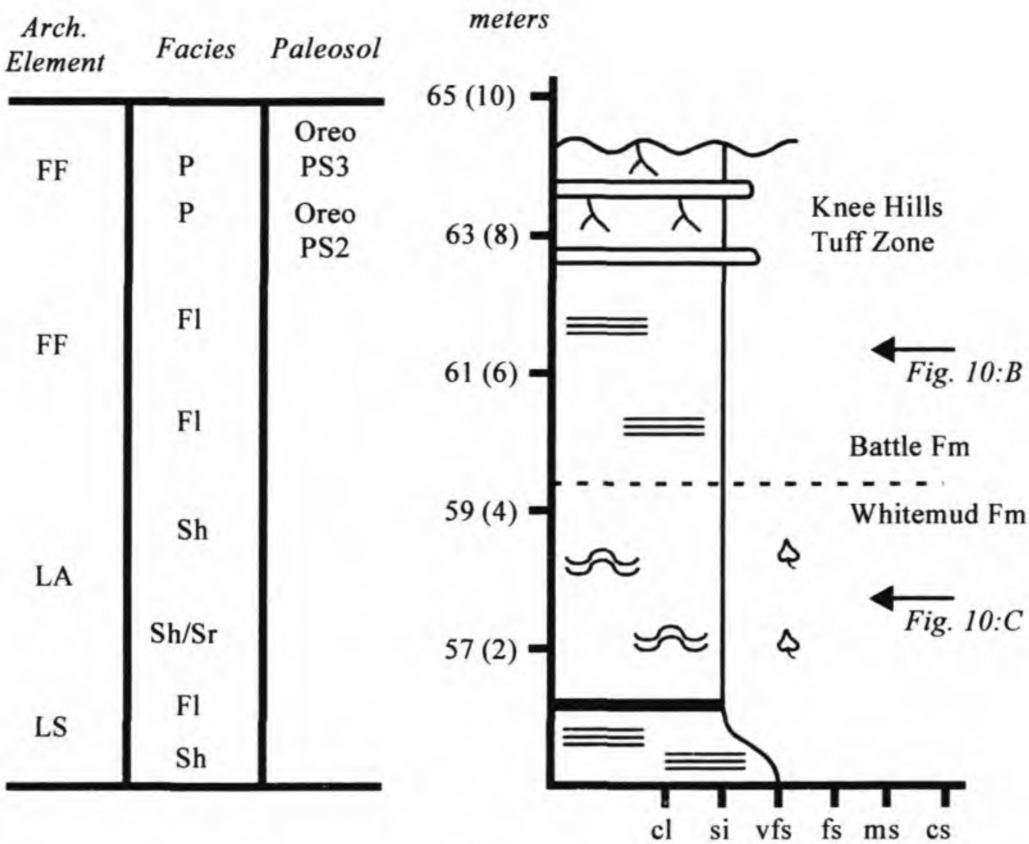

Figure 9. Measured section of Battle and Whitemud formations.

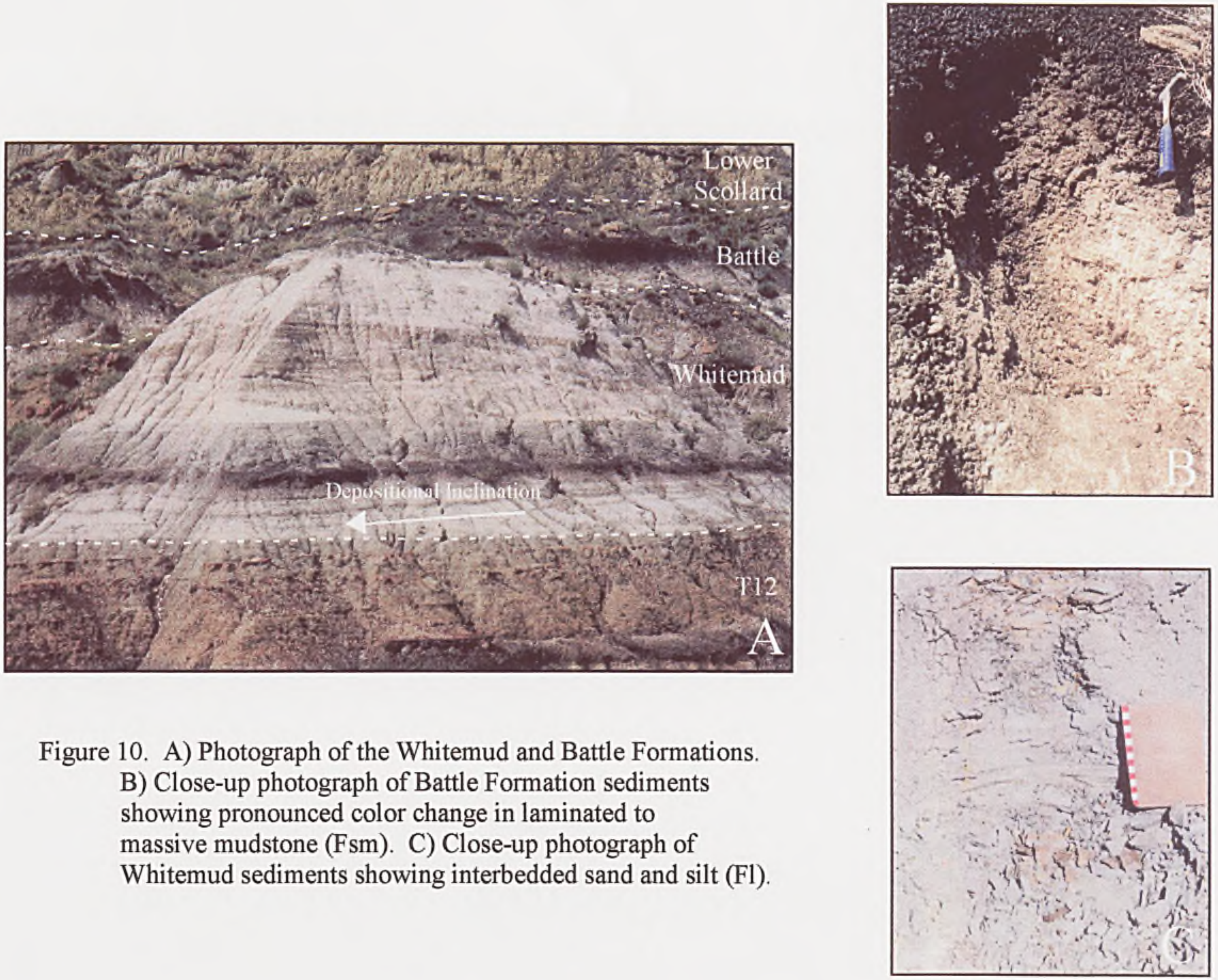

Figure 10. A) Photograph of the Whitemud and Battle Formations. B) Close-up photograph of Battle Formation sediments showing pronounced color change in laminated to massive mudstone (Fsm). C) Close-up photograph of Whitemud sediments showing interbedded sand and silt (Fl).

Battle Formation

The Battle Formation directly overlies the Whitemud Formation and is distinguished by a pronounced color change from light gray at its base to very dark brown at its midpoint (Figure 10). Laminated to massive carbonaceous clayey siltstone (Fl, Fsm) dominates the Battle Formation (Figure 10). Binda (1992) identifies a unique microfossil assemblage in the Battle that is characteristic of lacustrine settings, including 9 species of megaspores resembling *Isotes* and *Selaginalla*, 13 species of Chrysomonad cysts, 9 types of Spongillidae gemmocleres, silicified fungal spores and pollen, and silicified tracheids. Binda (1992) also suggests that the uniform thickness and homogeneity of the massive-to-laminated depositional fabric at several Battle outcrop localities suggests a single, regionally extensive lacustrine or paludal system. Evidence for ponding in the Whitemud Formation, then, may have been a precursor to the more extensive lacustrine environment of the Battle. The top of the Battle Formation is recognized by the thin (1-3 cm), white siliceous beds of the Knee Hills Tuff. Between the two beds of Knee Hills Tuff are two organic-rich paleosols of the Oreo pedotype. The occurrence of paleosols at the top of the Battle Formation may be evidence for drainage of the Battle Lake.

Scollard-Battle Contact

Work by Russell (1983) suggests that an erosional unconformity exists between the top of the Battle Formation and the base of the Scollard Formation. However, the extent of incision represented by this unconformity has not been quantitatively established (Russell, 1983; Eberth and O'Connell, 1995). Gibson (1977) places the Scollard-Battle contact at the point where the Knee Hills Tuff contacts the base of the first Scollard sandstone. However, several paleosols occur between these two depositional units, the uppermost of which has been variably truncated by the Scollard-Battle unconformity. These paleosols are not accounted for in the formational nomenclature of Gibson (1977). It is probable that these intermediate paleosols represent a locally uneroded record of geomorphic stability during the retreat of the "Battle Lake".

Scollard Formation: Lower Scollard

The Lower Scollard Formation is characterized by channel/sand body (CH/SB) sheets and stacked paleosols (P) (Figure 11). The pervasive basal Scollard sand body has basal scour-and-fill bedforms (Ss), is fine-grained, and dominated by trough crossbedded (St) and planar-tabular (Sp) bedsets (Figure 12). These bedforms are easily observed in areas of siderite cementation, but difficult to recognize in uncemented portions of the unit. Lower Scollard paleocurrents generally indicate southeasterly transport due to uplift and shedding from the orogen to the west. Lower Scollard sand bodies are overlain by increasingly-thick paleosols. Two paleosols overlie the basal Scollard sandstone, and are moderately-developed, well-drained paleosols of the Cow 1 pedotype. The Scollard Tuff, a regionally extensive marker bed thought to be of volcanic origin occurs between the two paleosols. An overlying sand body is morphologically similar to the basal Scollard sand body (albeit half as thick), with mechanical sedimentary structures that include trough crossbeds (St) and planar-tabular bedsets (Sp). Paleocurrent measurements from trough crossbeds indicate consistent paleoflow to the southeast. The second Lower Scollard sandstone is also capped by two moderately-developed, well-drained of the Cow 1 paleosols. The basal two sand bodies in the Lower Scollard were likely the result of

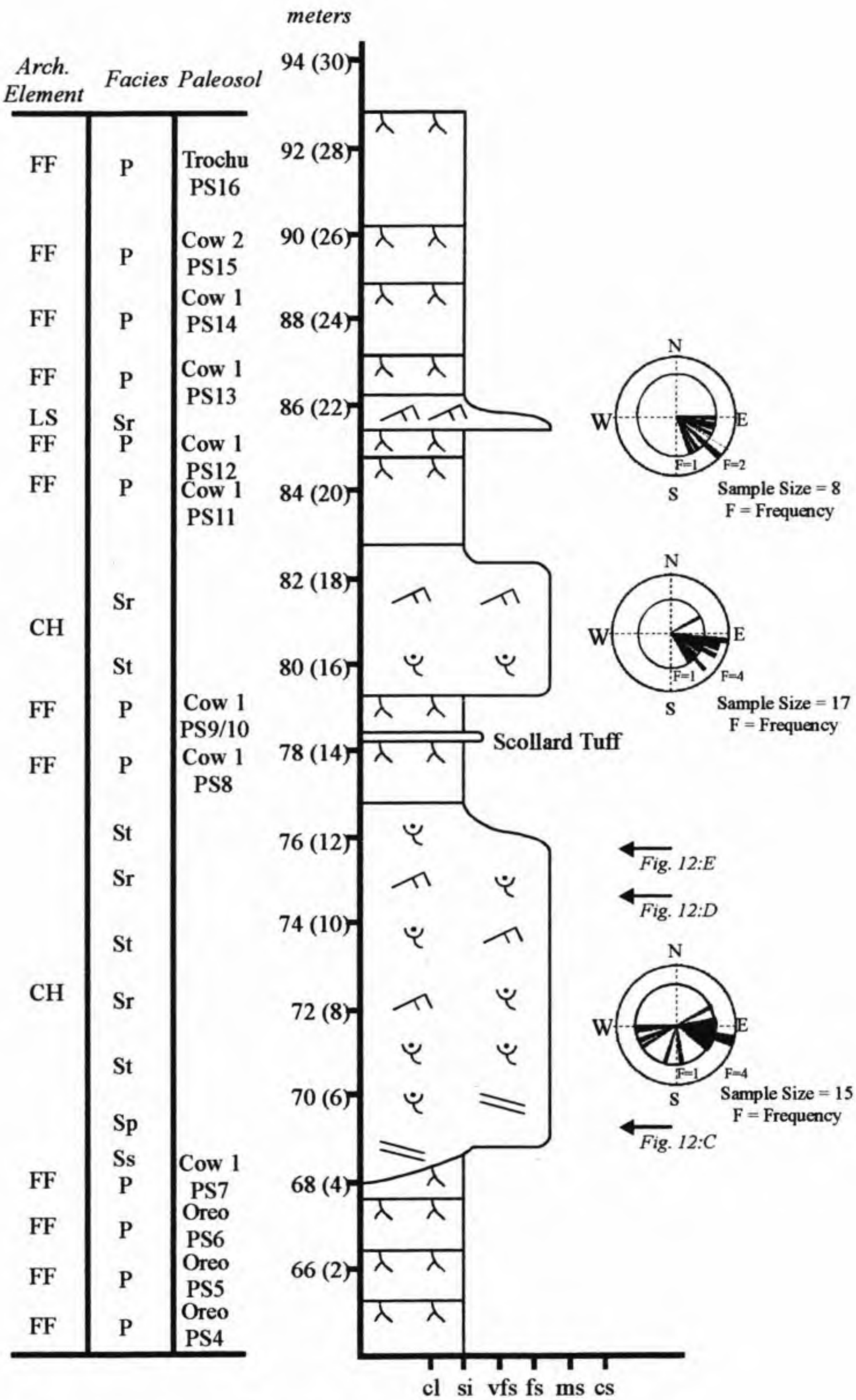

Figure 11. Measured section of Lower Scollard Formation.

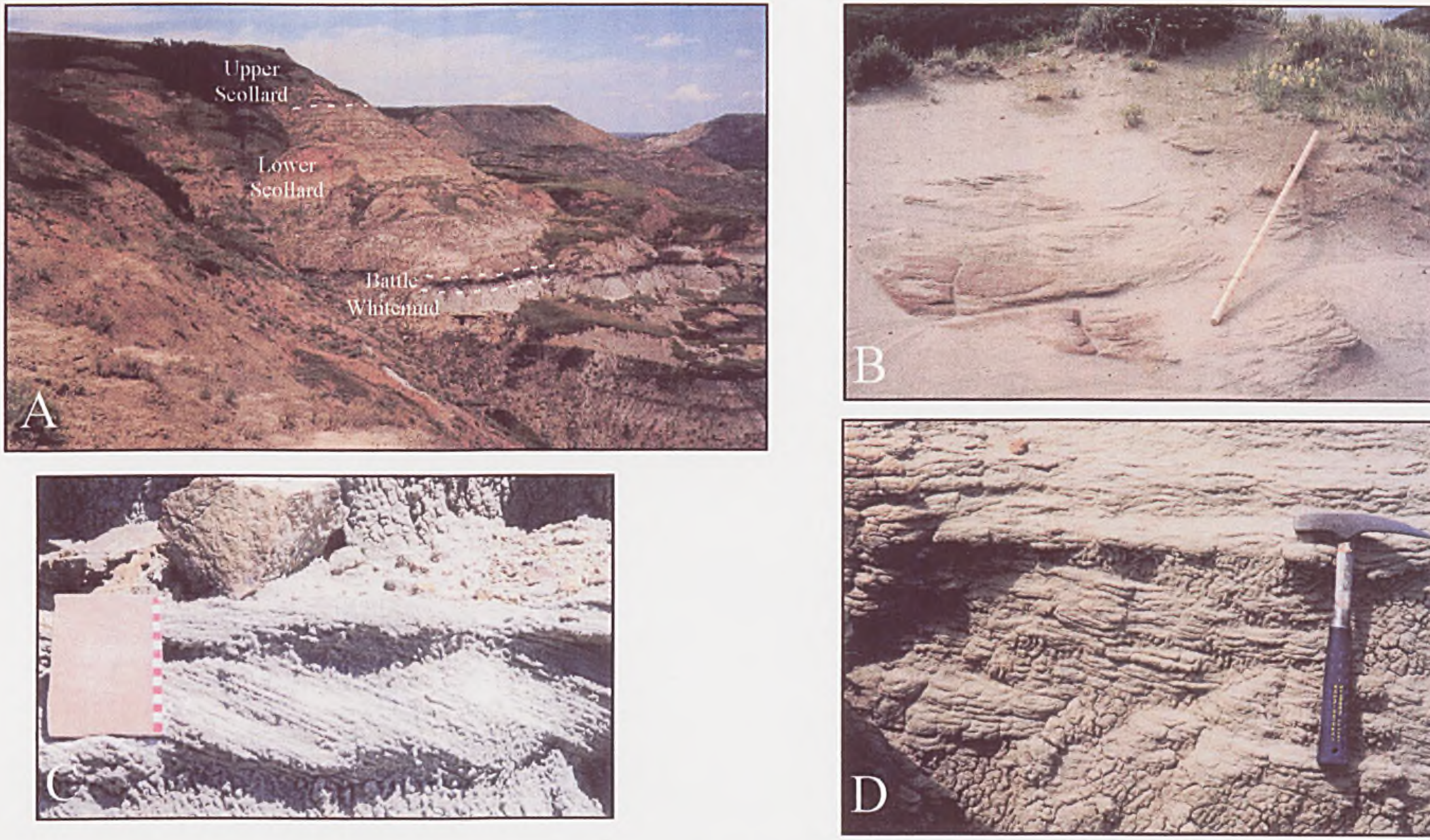

Figure 12. Lower Scollard deposits. A) Photograph showing the stratigraphic location and thickness of the Lower Scollard. B) Trough crossbeds (St) in the Lower Scollard, oriented to the southeast. C) Planar-tabular (Sp) crossbeds in a Lower Scollard sandstone. D) Ripple sets (Sr) in a Lower Scollard sandstone.

deposition by aggradational paleochannels (similar to the T12 sand). Basal scour (Ss) and pebble lags, trough crossbed sets (St), planar-tabular sets (Sp), preferred southeasterly paleocurrent direction, and the lack of recognizeable channel or accretionary bedforms suggest that these sand bodies were deposited in an accretionary, possibly braided fluvial complex.

The remainder of the sandstones in the Lower Scollard are thin (≤1 m) laminated sand sheets (LS), likely deposited as crevasse-splays. These sandstones contain abundant planar-tabular (Sp) bedding and ripple lamina (Sr), as well as minor trough crossbedding (St). Paleosols occurring between sandstones in the Lower Scollard are generally moderately-developed, well-drained soils that formed in humid climates. Paleosols 8 through 15 are all from the Cow 1 pedotype. Paleosols 16 through 25 are mixed, with examples from the Cow 1, Cow 2, Ramp, Trochu, and Milktoast pedotypes present. The paleosols are all distinctly clay-rich, and tend to have sandy parent material, suggesting that pedogenesis occurred on clay-rich overbank parent material that caps a fining-upward alluvial cycle. Increasing paleosol maturity near the top of the Lower Scollard indicates a general increase in time between depositional events.

Depositional processes that accounted for the Lower Scollard were bimodal, within a transition from channelized fluvial sand bodies at the base, and crevasse-splay and overbank-dominated sedimentation near the top. Paleoenvironmental indicators from paleosols interbedded with lower sands are similar to those found in the overbank-dominated interval, suggesting limited paleoclimatic change through time.

Scollard Formation: Upper Scollard

Separation of the Scollard into upper and lower units is based on the occurrence of regionally extensive coal seams within the Upper Scollard that are not present lower in the section (Eberth and O'Connell, 1995) (Figure 13). The Upper Scollard records a shift in fluvial depositional style from aggradational (SB, braided) to accretionary (LA, meandering) (Figure 14). Sandstones in the lower portion of the Upper Scollard are typically thin (≅1 meter), fine-grained, inclined, ripple-laminated (Sr) sands deposited as a lateral accretion set. Minor trough crossbedding (St) with detrital carbonaceous draping is recognized within the lower portion of some sands (Figure 14). These sandstones typically fine upwards and are capped by gleyed, organic-rich paleosols. Sandstones in the upper portion of the Upper Scollard are generally thicker (3 to 6 meters), but are morphologically similar and reflect similar depositional style. Local siderite cementation of sandstone accentuates ripple and fine lamination (Sr, Fl) (Figure 14). Thin, gleyed paleosols (P) occur at the tops of the deposits, but are less mature than sand-capping paleosols within the lower portion of the Upper Scollard.

Paleosols in the Upper Scollard have characteristics of soils formed in poorly-drained, reducing environments. Recognition of this has led to the placement of the boundary between the Lower and Upper Scollard at the base of paleosol PS27, approximately 5 meters below the KT boundary coal paleosol (PS28) (Figure 13). Paleosol PS27 is the type paleosol of the Oreo pedotype, and has characteristics indicative of both waterlogged and well-drained conditions. The presence of a Oreo paleosol at the boundary between the Lower and Upper Scollard is likely due to increased rates of precipitation, and/or increasingly poor drainage. The basal Upper Scollard

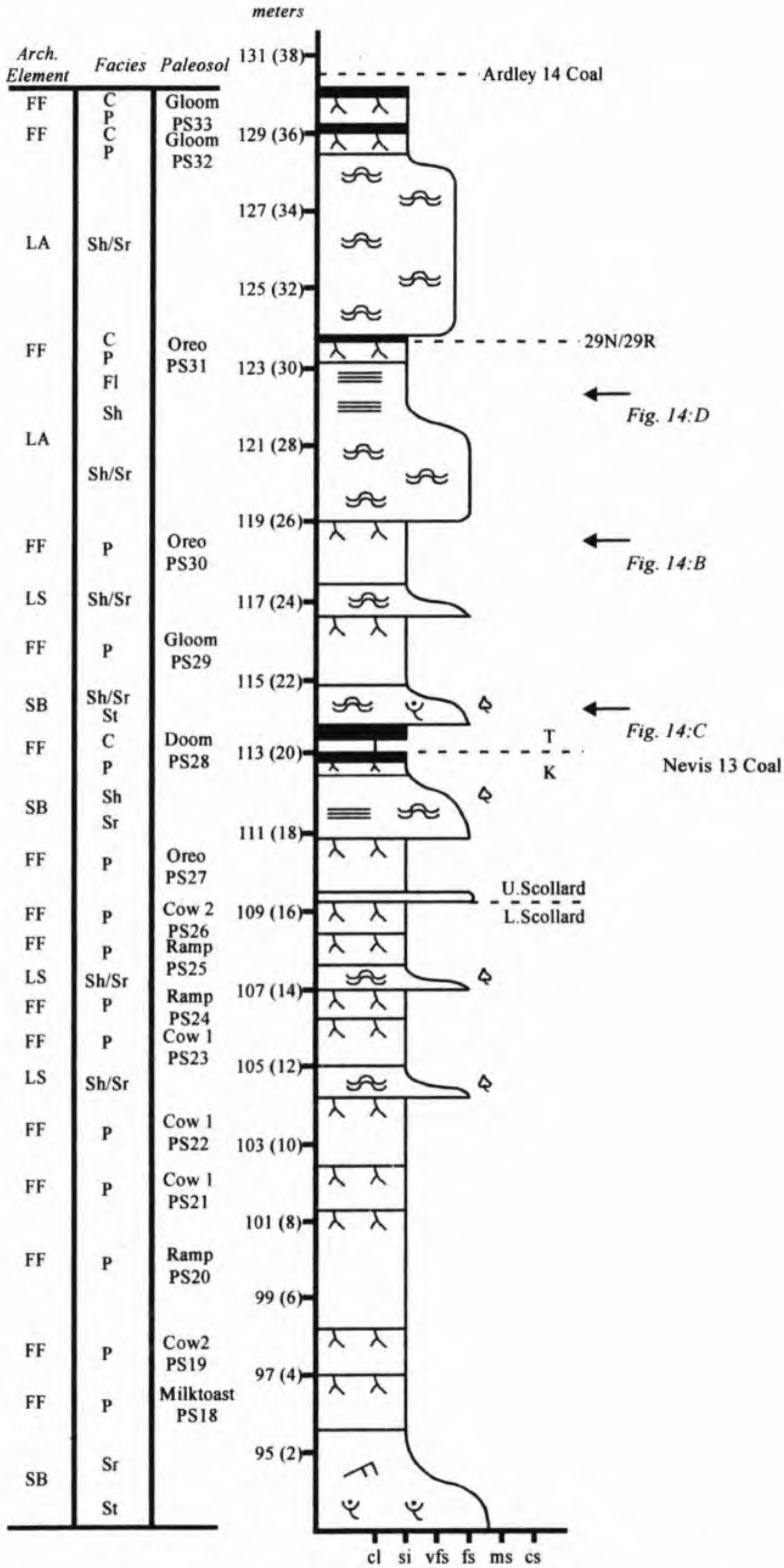

Figure 13. Measured section of Upper Scollard Formation.

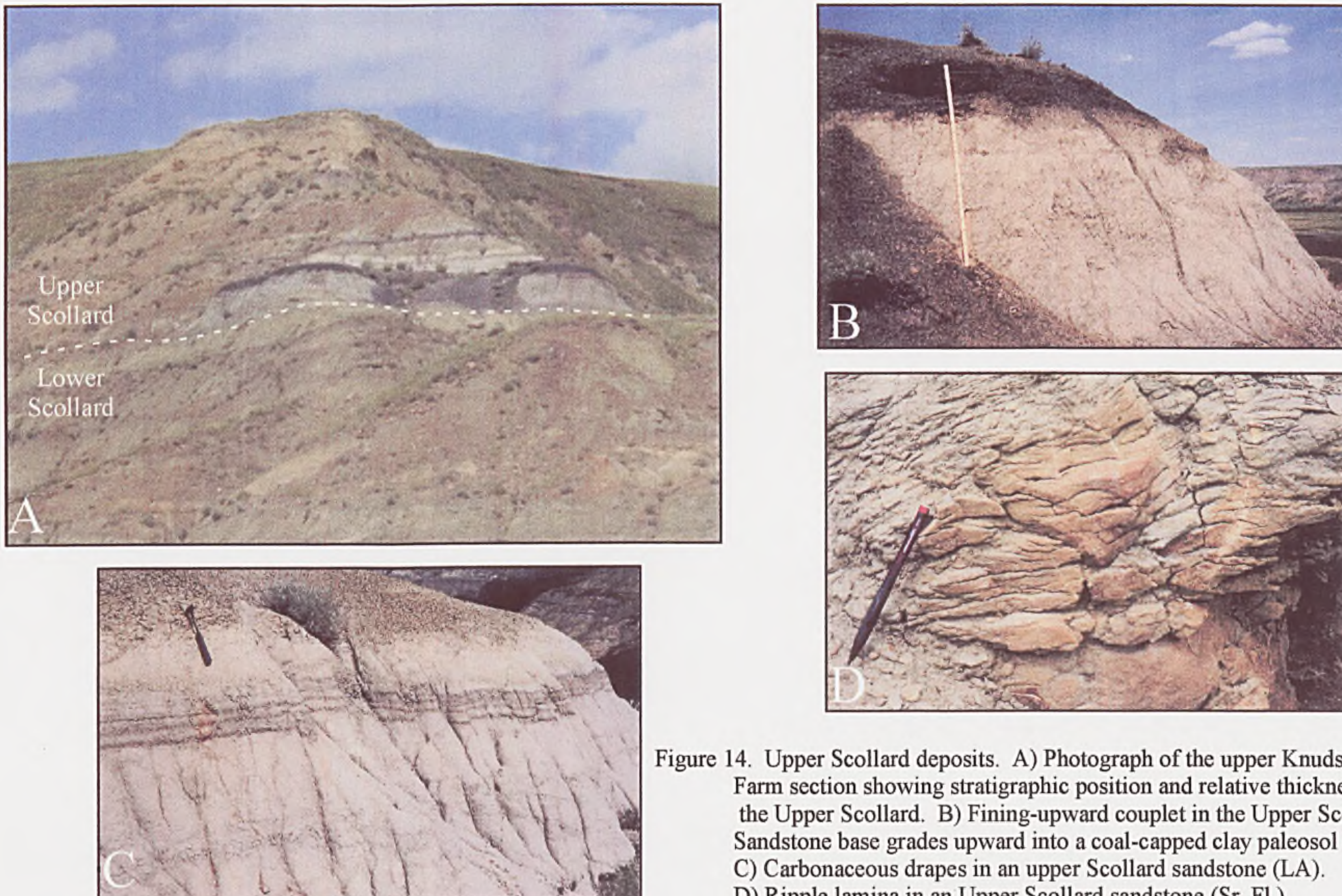

Figure 14. Upper Scollard deposits. A) Photograph of the upper Knudson's Farm section showing stratigraphic position and relative thickness of the Upper Scollard. B) Fining-upward couplet in the Upper Scollard. Sandstone base grades upward into a coal-capped clay paleosol (PS28). C) Carbonaceous drapes in an upper Scollard sandstone (LA). D) Ripple lamina in an Upper Scollard sandstone (Sr, Fl,).

sandstone overlies PS27, and fines upward at its top into the Nevis 13 KT boundary coal paleosol (PS28). The KT boundary paleosol is the type paleosol for the Doom pedotype and is recognized regionally as the Nevis 13 coal. The KT boundary clay is a 3 cm thick, salmon-colored clay, and located within the middle of the coal seam. Paleosol PS29 overlies the PS28 zone, and like PS28, formed at the top of a thin sand sheet. Paleosol PS29 is the type paleosol of the Gloom pedotype. PS29 is gleyed and has a coal surface horizon indicative of 1,400 to 2,800 years of geomorphic stability in a regularly inundated, reducing environment (Retallack et al., 1996). The remaining paleosols, PS30 through PS33 are also gleyed and have pronounced accumulations of organic material at their surfaces. The uppermost paleosols, PS31 through PS33 are all thin (<1 m) and do not contain the thick coal surface horizons characteristic of the better-developed organic paleosols in the section. This may be due to an increased sedimentation rate, pedogenic immaturity, or drainage conditions were not favorable to the preservation of large amounts of plant material. The Ardley 14 coal seam (not preserved at the Knudson's Farm) is roughly equivalent with the top of the Upper Scollard Formation. The Upper Scollard records a change in fluvial style from aggradational deposits in the Lower Scollard, to accretionary deposits in the Upper Scollard. The evolution of fluvial style is corroborated by increasingly poor drainage within the Upper Scollard (coals and gley), and may be related to a decrease in regional dip and/or a cooler, wetter climate.

CHAPTER THREE

Paleosols

Paleclimatic Implications of Paleosols

Analysis of evolving fluvial styles can yield appreciable insight into sedimentation rates, accommodation space, and general paleoclimatic conditions (rainfall, glaciations, etc.) related to discharge and sediment load. However, morphological properties preserved in paleosols can be analyzed in order to deduce quantifiable paleoclimatic conditions. Certain properties, such as coal formation or rooting depth are related to specific paleoenvironmental parameters such as mean annual precipitation (MAP) and drainage, while other properties, such as degree of pedogenic carbonate development and morphology of redoximorphic features leave more room for interpretation of paleopedogenic conditions.

A general model by Jenny (1941), (expanded on by Birkeland, 1999) of modern soils in the mid-continental United States found that the dividing line of calcic and non-calcic soils occurs where MAP is roughly 125-150 cm, with free pedogenic carbonate forming in the drier soils. Models that relate the depth to calcic horizon (Bk) to MAP also suggest that free pedogenic carbonate is rare in soil with MAP > 100 cm (Retallack, 1994). While factors such as soil drainage, leaching, temperature, and amount of available calcium in the parent material affect the occurrence of carbonate in soils, the 125-150 cm MAP of Birkeland (1999) serves as a reasonable baseline from which to interpret soil precipitation regime. Other methods, such as the relationship between MAP and the ratio of bases to alumina in the Bt horizon (inverse relationship), and the thickness of organic surface horizons can further constrain the MAP in non-calcareous paleosols (Ready and Retallack, 1995; Retallack, 1996).

The state of molecular iron in a paleosol can also be diagnostic of paleoenvironmental conditions. Paleosols with a history of prolonged waterlogging typically have a drab, blue-to-gray gleyed color as a result of iron being reduced to the ferrous state by anaerobic microbes (Retallack, 2001). Gleyed paleosols typically also have organic-rich surface horizons and evidence of biological communities that are typically found in paludal settings. Conversely, paleosols that are well drained often experience reddening due to the oxidation of iron-bearing minerals (Retallack, 2001). Soils that are oxidized typically have deeply penetrating roots, evidence of clay formation and translocation, and thinner organic surface horizons than gleyed soils. In the case of Knudson's Farm paleosols, pedogenic gley and oxidation, as well as diagenetic oxidation (related to dehydration of iron hydroxides) are observed. The morphologies are distinguished by comparing the presence of iron oxides to other indicators of the environment of pedogenesis, including matrix colors and degree of organic matter accumulation in the surface horizon. For example, iron oxide films on fracture planes in a coal seam were described as diagenetic, whereas iron oxide hypocoats (within a single paleosol) on peds of soils with thin surface horizons, deeply penetrating roots, and argillans were considered to be pedogenic. Diagenesis may have distorted the accuracy of oxide description, however, oxide descriptions were compared with ancillary evidence of drainage and paleoclimate before conclusions were made.

Pedotypes

As previously stated, use of the pedotype method is one of the most efficient ways to generate paleoclimatic interpretations from a large number of paleosols within a single interval. A *pedotype* is defined as a group of paleosols with such distinct descriptive and morphological similarities (i.e., horizonation, color, texture, translocation, etc.), that they can be referenced by a representative profile. In this study, representative profiles are used to generate paleopedogenic parameters for each pedotype, including paleoclimatic implications, duration of surficial exposure, biological influences, geochemical trends, and mass flux of mobile constituents. Key morphological features of pedotypes have been condensed into a pedotype summary table for Knudson's farm paleosols (Table 1). Data and descriptions of representative profiles have been recorded in appendices A through H.

Horseshoe Canyon Formation: Lower Horseshoe Canyon (HSC) Unit

The limited development of paleosols in the lower HSC unit makes a reliable interpretation of paleoclimate difficult. Limited horizonation, clay translocation, rooting, or structural development suggests that the Milktoast paleosols in the lower HSC were geomorphically stable for only a few hundred years (Figure 15; Appendix A) (Birkeland, 1999). However, the occurrence of weak ferriargillans observed in thin section, as well as sepic fabric does provide evidence for pedogenesis in a seasonal, well-drained setting (Figure 15). The absence of pedogenic carbonate in HSC paleosols may be related to pedogenic immaturity, but lack of any pedogenic carbonate, even in better-developed paleosols, is suggestive of a humid paleoclimate and MAP of 125-150 cm (Birkeland,

Figure15. Photographs of Milktoast type paleosol (HSCPS7) and associated features.
A) Typical profile of a Milktoast paleosol with horizon designations.
B) Photomicrograph of an oxide ped coating from the A horizon. Field of view is 3.3 mm. C) Photomicrograph of mosepic porphyroskelic microfabric in the Bw horizon, indicative of seasonality. Field of view is 1.3 mm.
D) Photomicrograph of iron reduction along a void in the C horizon. Probable evidence for colonization by plants. Deep rooting indicates seasonally fluctuating water table. Field of view is 3.3 mm.

1999). Additionally, the presence of dinosaur remains in HSC sandstones suggests rapid rates of sedimentation in between periods of pedogenic stabilization.

Whereas the lower HSC is dominated by immature paleosols, the upper HSC unit does have a gleyed, organic rich paleosol (HSCPS8) of the Gloom pedotype, indicating a mixed history of free drainage (argillans, sepic fabric), and prolonged periods of inundation (gley) and organic material accumulation (Figure 16; Appendix B). The presence of a paleosol of the Gloom pedotype near the top of the HSC section may represent increasing MAP and/or a restriction of free drainage prior to the formation of the Carbon 11 coal zone.

Fossilized plant and animal remains are common in the HSC. Fossilized remains include disarticulated bones from dinosaurs and fragments of wood, some of which have seasonal growth rings preserved. This suggests that sediments were deposited rapidly, such that remains were buried and preserved. An increasing proportion of fossilized wood to animal remains near the top of the HSC unit provides evidence for an increasingly wet, geomorphically stable environment.

Horseshoe Canyon Formation: Carbon 11 (C11) Coal Zone

Paleosols within the Carbon 11 coal zone all have morphological characteristics suggesting pedogenesis in inundated, slightly-seasonal conditions. The basal paleosol (C11PS1) in the Carbon 11 coal zone is a better-developed example paleosol of the Gloom pedotype than in the upper HSC unit. As with the underlying HSCPS8, the first C11PS1 has morphological characteristics suggesting a humid climate with high rates of precipitation and variable drainage. High concentrations of organic matter in the surface

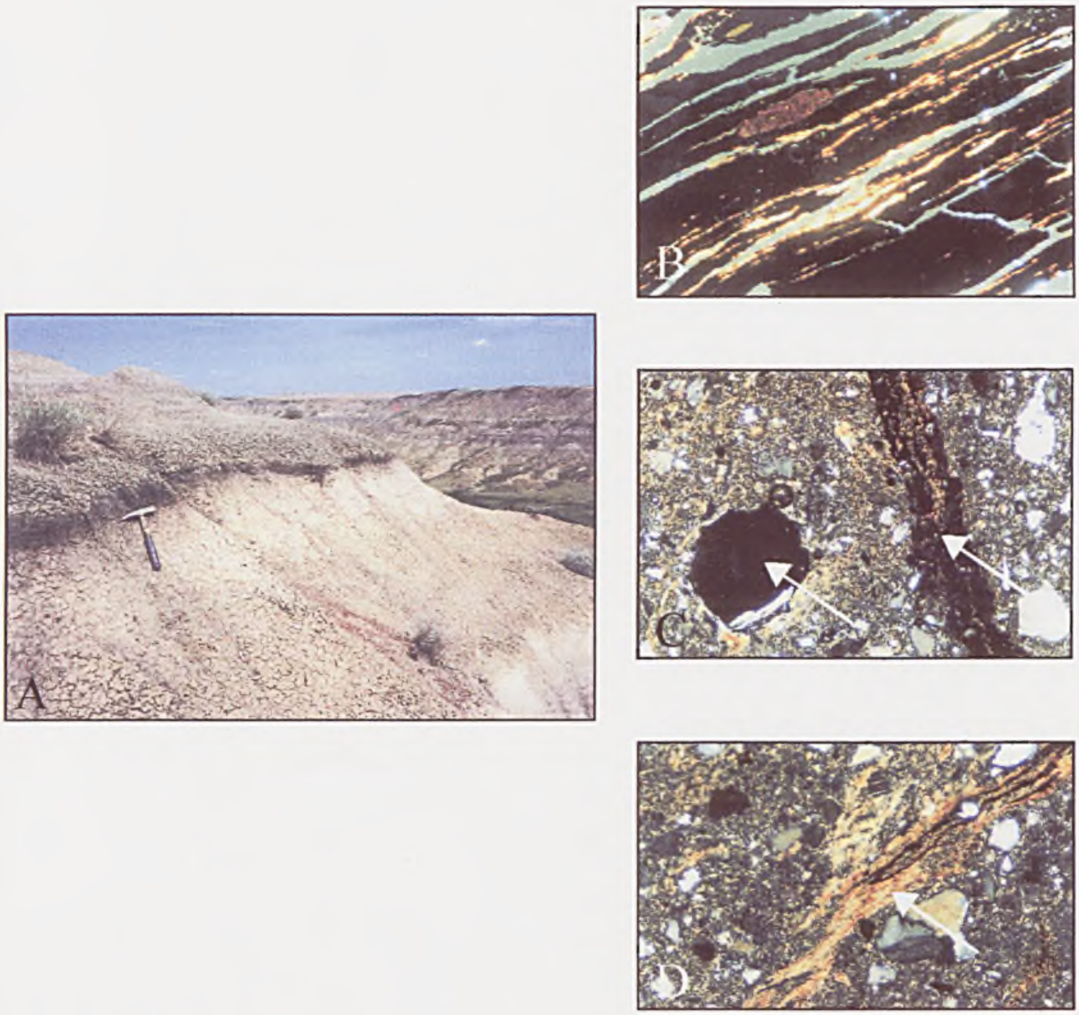

Figure 16. Photographs of Gloom type paleosol (PS29) and associated features. A) Typical Gloom paleosol with thin coal surface horizon. B) Photomicrograph of coal with organic traces and clay present. From the OA horizon of PS29. Field of view is 3.3 mm. C) Photomicrograph showing insepic microfabric (possibly indicating periods of wet and dry), preserved root trace, and a void with an argillan along the wall (indicating periods of free drainage) from the Bg2 horizon. Field of view is 1.3mm. D) Photomicrograph of an argillan along a root wall from the Bg3 horizon. Indicative of periods of free drainage and clay translocation. Field of view is 1.3 mm.

horizon, as well as subsurface gley are indicative of pedogenesis in poorly drained conditions (Retallack, 2001). The presence of root traces that penetrate to the depth of pedogenic parent material, however, suggest a periodic drop in the water table to at least 60 cm through some portion of the year.

Lengthening periods of inundation and increased geomorphic stabiliy were the likely cause for the formation for the first Carbon 11 coal, here called "C11 coal A". Assuming a conservative amount of compaction has occurred (0.1 times original thickness), and using the peat accumulation rate of 0.5-1.0 mm yr^{-1}, a reasonable range for the time of geomorphic stability of this surface is 6,500-13,000 years (Retallack et al., 1996). The presence of a thick, well developed coal is indicative a high water table, poor drainage, and very high (250 cm+) mean annual precipitation during the formation of the Carbon 11 A coal (Retallack, 2001).

Capping the first Carbon 11 coal are two related paleosols with vertic properties, both of the Trochu pedotype (Figure 17; appendix C). The presence of large slickensides is diagnostic of pronounced wet/dry seasonality during pedogenesis (Wilding and Puentes, 1988). The paleosols also exhibit evidence of clay translocation and deep (approximately 1 meter) rooting, which suggests periods of free drainage at the time of pedogenesis. However, the dominance of a gray matrix color, a lack of pedogenic carbonate, and significant accumulations of organic material in the surface horizons suggest that periods of sustained groundwater inundation also affected these paleosols. The wet/dry seasonality recorded by the two vertisols in the Carbon 11 unit may have been a function of seasonal inundation and drainage.

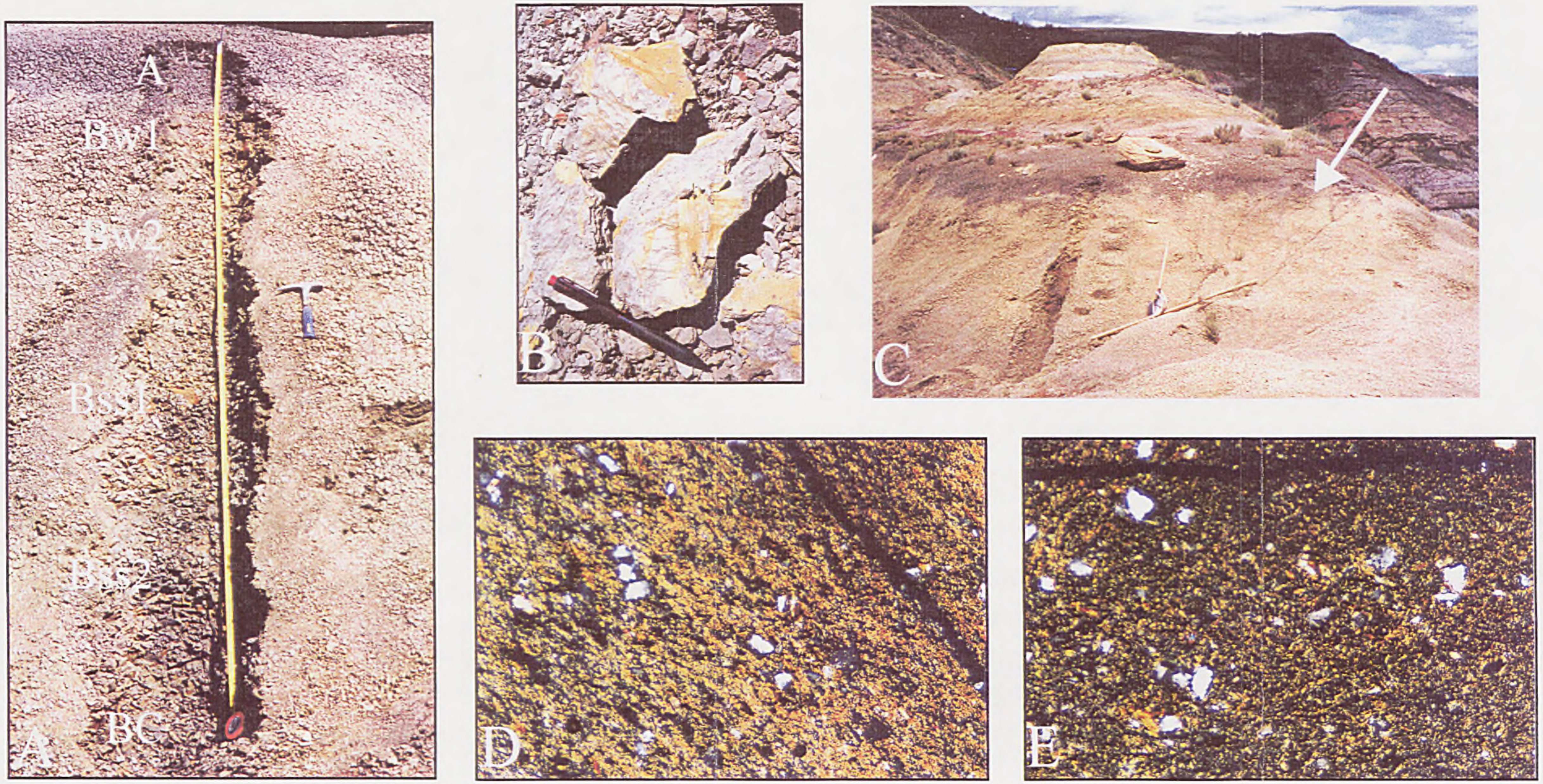

Figure 17. Photographs of Trochu type paleosol (PS16) and associated features. A) Typical profile of a Trochu paleosol with horizon designations. B) Grooved, shiny ped faces of slickensides from the Bss1 horizon, indicative of seasonality and the presence of shrink-swell clays. C) Photograph of PS16 showing sawtooth-pattern of infilled dry season cracks at the A-Bw1 horizon contact. D&E) Photomicrographs of mosepic microfabric in the Bss2 horizon. Extinction angle of oriented clay is approximately 50 degrees. Oriented clay is also indicative of wet/dry seasonality, and suggests the presence of shrink/swell clays. Field of view is 1.3mm.

The Carbon 11 B coal paleosol is morphologically similar to the paleosol containing the C11 A coal. Both are of the Doom pedotype and are indicative of a low-lying, flooded swampland. Assuming the same compaction and peat accumulation rates as with the C11 A coal, the C11 B coal paleosol likely underwent active pedogenesis for a period between 7,800 and 15,600 years (Retallack et al., 1996). The occurrence of a well developed coal seam is indicative of a high water table, poor drainage, and very high (250 cm+) MAP (Retallack, 2001).

Deposits in the C11 unit record a period of increased geomorphic stability relative to the underlying HSC unit. The morphology of carbon 11 coal zone paleosols suggests that the environment of paleo-pedogenesis represented by the unit was a regionally extensive, flat, low-lying, poorly-drained swampland adjacent to areas of fluvial sedimentation.

Horseshoe Canyon Formation: Thompson 12 (T12) Coal Zone

Paleoclimatic interpretation through the entire Thompson 12 coal zone is somewhat problematic because there are comparatively fewer paleosols per unit thickness than in other portions of the section. Fluvial deposits, including SB, LA, and FF dominate the lithology of the sediments. These deposits aid in determining the geographic position of paleosols within the fluvial system, but do not contain a large amount of information concerning paleoclimate. The first recognized zone of pedogenesis in the Thompson 12 zone is the lateral accretion deposit capping the T12 sand body. This zone is recognized by fossilized tree stumps with seasonal growth rings preserved at the top of the deposit (Figure 8). Excavation around two of the stumps did not reveal root traces. While the lack of root traces may suggest that the stumps were transported as fragments, the vertical orientation of all observed stumps suggests that the trees were preserved in situ. Pedogenic alteration of the parent material is negligible, with no rooting, horizonation, or structural development recognized, which is likely because of limited weathering of a temporarily-stabilized point bar.

The second Thompson 12 paleosol (T12PS1), the Thompson 12 coal, caps a sand deposit overlying the stabilized point bar. The Thompson 12 coal is morphologically distinct from the underlying C11 coals because the solum underlying the T12 coal is thinner (only 25-30 cm), texturally coarser, and has roots that penetrate 20 cm. These characteristics are indicative of a water table that was high year-round with little fluctuation such that water was readily available to plants near the surface. A thin laminated carbonaceous mudstone (Fl) occurs in the middle of the Thompson 12 coal seam, likely the result of overbank deposition into a backswamp. Assuming the same compaction and peat accumulation rates as with the C11 coals, the T12 coal paleosol was likely stable for a period between 10,000 and 20,000 years (Retallack et al., 1996).

Near the top of the Thompson 12 coal zone is the third pedogenic zone (T12PS2) of the T12 unit. T12PS2 is of the Cow 1 pedotype and exhibits evidence of a seasonally well-drained setting, including deeply penetrating roots, and argillans on ped faces (Figure 18; appendix D). Using the Bt alumina ratio equation of Ready and Retallack (1995) general MAP of Cow 1 paleosols is approximately 73 cm. While the lack of pedogenic carbonate suggests a MAP of at least 100 cm, pedogenesis in a cool, humid climate with limited evaporation would have prevented the formation of pedogenic carbonate.

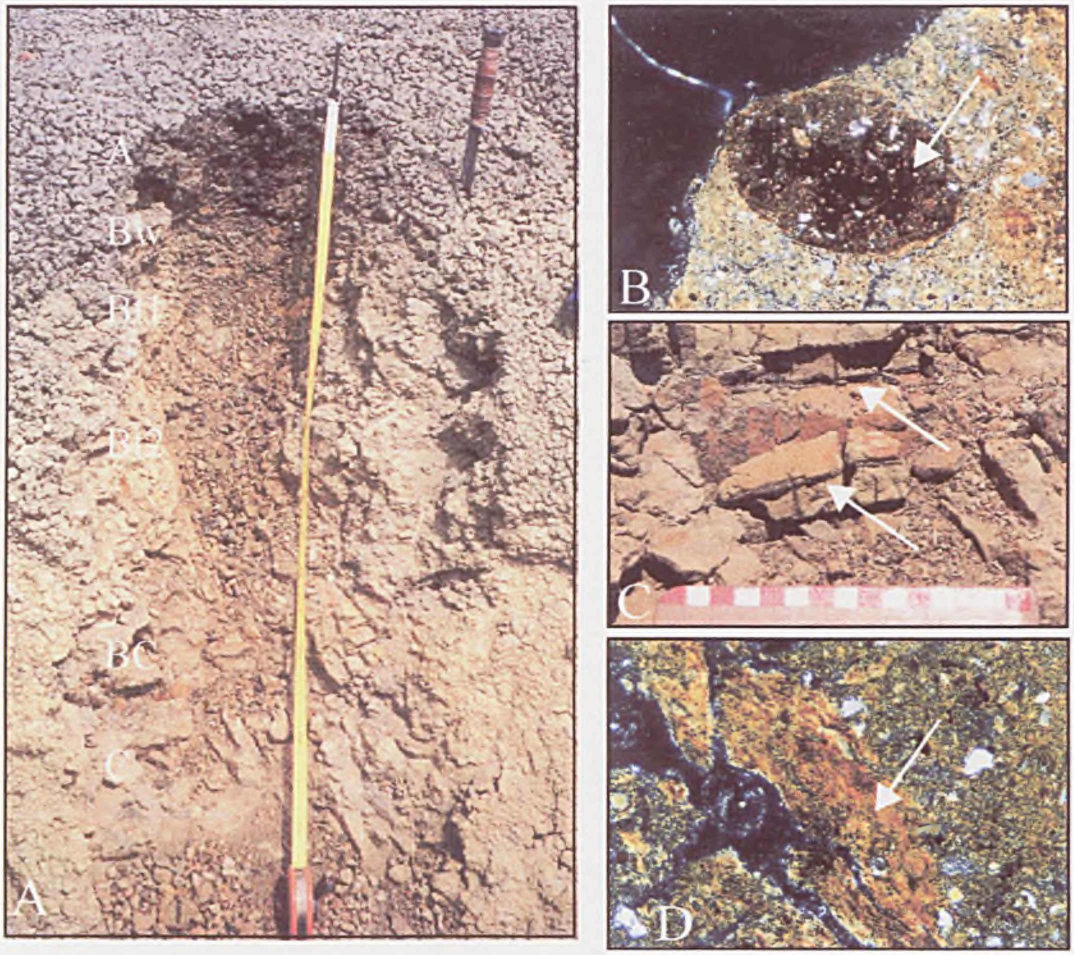

Figure 18. Photographs of Cow 1 type paleosol and associated features. A) Typical profile of a Cow 1 paleosol with horizon designations. B) Microscopic organic-enriched pellet from the A horizon. Field of view is 3.3 mm. C) Root traces from the Bw horizon. D) Photomicrograph of an argillan along a void wall from the Bt2 horizon, indicative of clay illuviation. Field of view is 1.3 mm.

It is difficult to determine whether paleosols in the T12 unit record a changing of paleoclimatic regime, or if they record differing drainage conditions. The Thompson 12 coal records a prolonged period of poorly drained conditions possibly in swampland, in a humid climate with MAP though to be 250cm+ yearly. Above the T12 coal zone, there is evidence for improved drainage in a humid climate with Cow 1 paleosol T12PS2. Indications of a humid paleoclimate suggest the possiblity that free drainage may have allowed for the formation of T12PS2 rather then a true climatic shift.

Whitemud Formation

Paleoclimatic interpretation of the Whitemud Formation is problematic due to a lack of paleosols. However, sedimentologic criteria can give a general sense of paleoclimate during the deposition of the Whitemud. The light gray to white color of Whitemud deposits may represent iron reduction and gley due to high water table, possibly related to post depositional ponding. Preservation of masticated organic material as drapes along bedding planes is also indicative of high levels syndepositional organic material production. Production and preservation of high levels of organic material do suggest a warm, humid climate with areas of sustained waterlogging.

Other paleoenvironmental studies of the Whitemud Formation support the conclusion that deposition occurred in a subtropical-type environment. Palynological work by Nambudiri and Binda (1991) suggests that the Whitemud was deposited by meandering streams in a subtropical to warm temperate climate. Additionally, isotopic studies of pedogenic sphaerosiderite by Ludvigson et al., (1998) on the time-equivalent Whitemud formation in Saskachewan modeled a mean annual temperature range of 15-23°C. While sphaerosiderite was not found in Knudson's Farm Whitemud deposits, sediment gley and preservation of organic material is consistent with hydric conditions necessary for sphaerosiderite formation. Observations of Whitemud deposits at Knudson's farm are consistent with the paleoenvironmental parameters determined by these studies.

Battle Formation

The base of the Battle Formation is composed of laminated to massive silty mudstone that is not pedogenically altered. These sediments contain abundant fragmentary organic material, which is indicative of high levels of organic material production contemporary with deposition. Binda (1992) suggests that Battle sediments were deposited within a regional lake or swamp. The conclusions of Binda (1992) are consistent with observations made in this study. Paleosols capping the Battle formation are of the Oreo pedotype (PS2, PS3) and are interbedded with the Knee Hills siliceous tuff beds. The PS2 and PS3 paleosols are both thin, and have characteristics of an environment that was variably flooded and drained (Figure 19; appendix E). Both PS2 and PS3 have subsurface gley and significant organic matter accumulation in the surface horizon as well as evidence for clay illuviation in subsurface horizons. Additionally, fine rooting throughout the profile and sepic microfabric are indicative of variable drainage conditions, possibly related to gradual retreat of the Battle lake. Calculated MAP using the equation of Ready and Retallack (1995) indicates MAP of Oreo paleosols is approximately 72 cm yr^{-1}. Strong evidence for aquic conditions combined with evidence of only 72 cm yr^{-1} suggests that poor drainage was more likely the cause of hydric paleosol morphology than was climate.

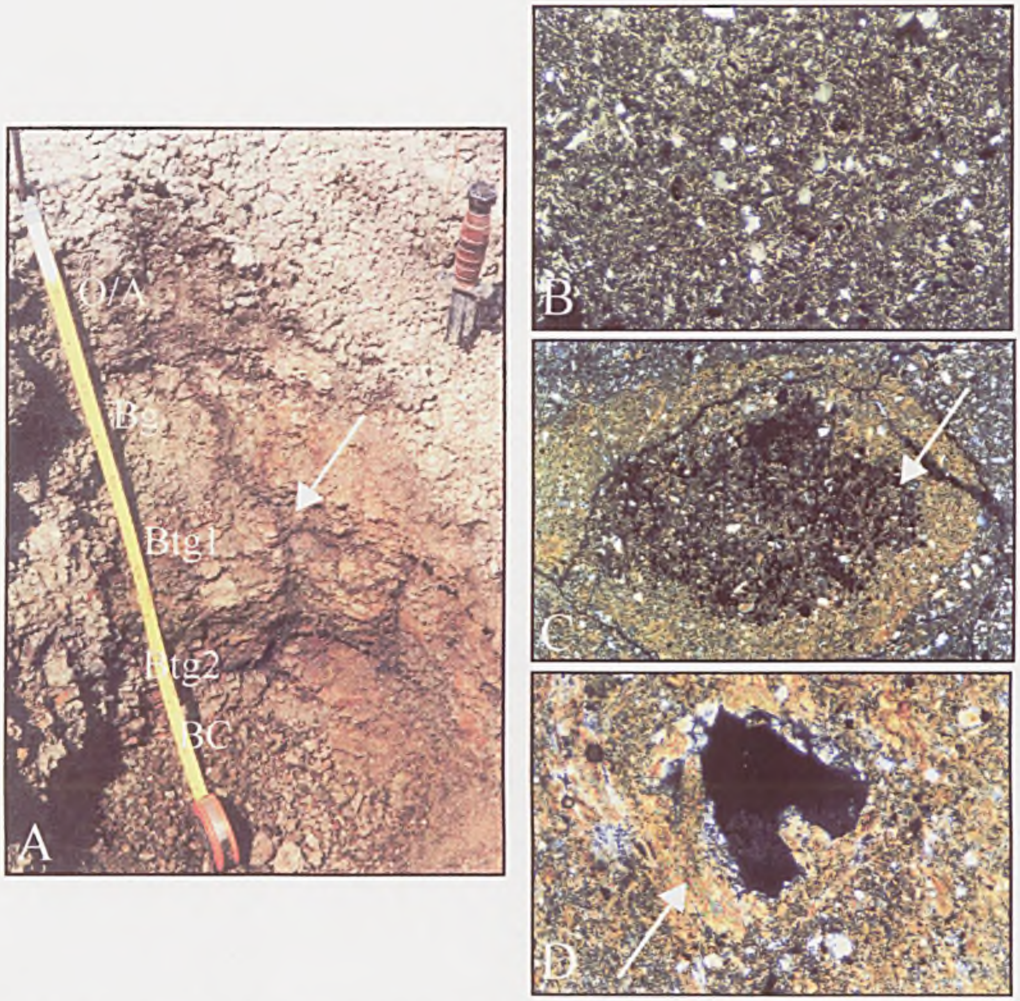

Figure 19. Photographs of Oreo type paleosol (PS27) and associated features. A) Typical profile of an Oreo paleosol with horizon designations. Large infilled biological traces highlighted with arrow. B) Photomicrograph of abundant organic fragments and skelesepic/lattisepic microfabric in the A horizon. Field of view is 1.3 mm. C) Cross section through an organic trace from the Bg horizon. Note oriented clay rim, likely a result of clay illuviation from the O/A horizon. Field of view is 3.3 mm. D) Photomicrograph of an argillan along a void wall from the Btg1 horizon, a result of clay illuviation. Field of view is 1.3 mm.

Scollard-Battle Contact

The paleosols of the Scollard-Battle 'transition' (PS4, PS5, and PS6) are are of the same pedotype (Oreo) as underlying paleosols capping the Battle Formation, but are thicker and more mature. As with other Oreo paleosols, the morphological characteristics of PS4, PS5, and PS6 include subsurface gley and significant organic matter accumulation in the surface horizon. These characteristics suggest prolonged periods of inundation by water. Illuvial clay coats on peds, and root traces that penetrate to over 1 meter in depth are evidence of periodic drainage. Application of the MAP equation of Ready and Retallack (1995) to the Oreo type paleosol indicates MAP of approximately 72 cm yr^{-1}. Whereas the lower 3 paleosols in the Scollard-Battle transition do not record a significantly different paleoclimate from the paleosols of the Battle Formation, their increased profile and horizon thicknesses do suggest increased duration of landscape stability (Birkeland, 1999).

The uppermost paleosol in the Battle-Scollard contact interval (PS7) is truncated by the first major Scollard sand sheet, and subsequently, has only subsurface horizons preserved. While truncation does not allow for complete profile description and interpretation, the subsurface horizons of PS7 share many morphological characteristics with soils that formed in the Lower Scollard: clay films on peds, lack of pedogenic carbonate, and colors that suggest oxidizing condition. The occurrence of a better-drained paleosol at the top of the Battle-Scollard contact may be evidence of a shift to a somewhat drier climate or of improved drainage as the retreat of the Battle Lake was reaching completion and deposition of the Scollard Formation was initiated.

Scollard Formation: Lower Scollard

Homogeneity of morphological features in paleosols of the lower Scollard Formation are indicative of improved drainage conditions (as compared to Battle paleosols) and relative paleoclimatic stability. Paleosols PS8 through PS15 are all from the Cow 1 pedotype and have been identified as moderately developed, well-drained, non-calcareous Inceptisols indicative of well drained, seasonally moist conditions. Common masepic and lattisepic plasma fabric indicates moderate wet/dry seasonality, and the presence of illuvial clay films indicates that the paleosols did have periods of free drainage (Retallack, 2001). The Presence of Bt horizons in Cow 1 paleosols allows for the use of the MAP equation of Ready and Retallack (1995), and indicates that MAP was approximately 73 cm yr^{-1}. Additionally, the presence of clay films and the lack of pedogenic carbonate in palesols PS8 through PS15 suggest that they formed in a humid climate with wet/dry seasonality in well-drained conditions.

Paleosols in the upper portion of the Lower Scollard have morphological features that are indicative of longer durations of surficial exposure and of more pronounced seasonality. Paleosols 16 through 25 include Cow 1, Cow 2, Ramp, Trochu and Milktoast pedotypes. Cow 1 and Cow 2 paleosols are morphologically similar to one another in that neither have pedogenic carbonate, and both have sepic fabric and prominent argillans. The equation of Ready and Retallack (1995) indicates a similar MAP (approximately 73 cm) and drainage conditions in both pedotypes. The taxonomic difference between Cow 1 and Cow 2 pedotypes is the presence of an argillic horizon in the Cow 2, which is likely due to longer exposure time (1,000-2,000 years). (Figure 20; appendix F).

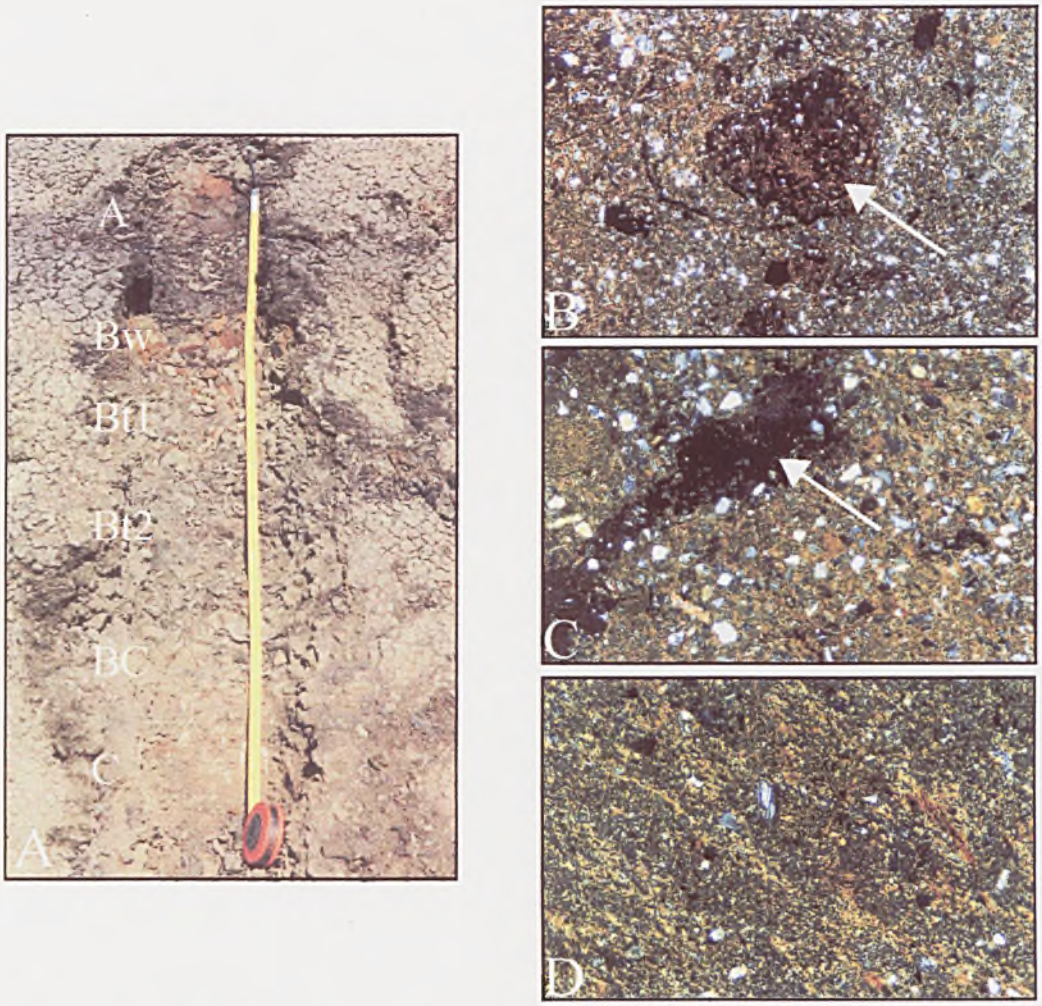

Figure 20. Photographs of Cow 2 type paleosol and associated features. A) Typical profile of a Cow 2 paleosol with horizon designations. B) Photomicrograph of an organic fragment from the A horizon. Field of view is 3.3 mm. C) Photomicrograph of a void from the Bw horizon, possibly associated with rooting. Field of view is 3.3 mm. D) Photomicrograph of clay increase (as compared to Bw) and mosepic porphyroskelic microfabric from the Bt1 horizon. Field of view is 1.3 mm.

Paleosols of the Ramp and Trochu pedotypes also occur in the upper portion of the Lower Scollard (Figure 21; appendix G). Climatically-influenced morphological features in Ramp and Trochu pedotypes are also very similar. Vertic properties, including slickensides, strong sepic fabric, and infilled cracks indicate pronounced wet/dry seasonality in both Ramp and Trochu paleosols (Wilding and Puentes, 1988; Retallack, 2001). A lack of pedogenic carbonate in both paleosols also suggests that MAP was between 125 and 150 cm yr^{-1} (Birkeland, 1999). However, other indicators of increased rainfall, including subsurface gley, and an increase in organic material in surface horizons are not present. It is more likely that Ramp and Trochu paleosols record a paleoclimate with a similar MAP as Cow 1 and Cow 2 paleosols, but with more pronounced seasonality. Ramp and Trochu pedotypes differ in their morphological features that relate to duration of pedogenesis. Trochu paleosols possess developmental features such as ferriargillans and deep (over 1 m), well-developed root and biological traces that suggest longer exposure history (500-1,000 years) than Ramp paleosols (Retallack, 2001).

Although the paleosols in the lower Scollard Formation have morphological distinctions, the paleoclimatic conditions implied by their morphologies are similar. In general, Paleosols in the Lower Scollard formation appear to have formed in an environment too humid for pedogenic carbonate formation, with probable MAP between 70 and 125 cm. Argillans indicate that drainage was sufficient for carbonate removal and clay illuviation in the profile, and vertic properties indicate that there was some measure of wet/dry seasonality during pedogenesis.

Figure 21. Photographs of Ramp type paleosol (PS25) and associated features. A) Typical profile of a Ramp paleosol with horizon designations. B) Root traces from the Bss1 horizon. C) Carbonized root trace and clinobimasepic microfabric in Bss1 horizon. Strong clay orientation is related to the formation of slickensides. Field of view is 3.3 mm. D) Photomicrograph of clinobimasepic microfabric in the Bss3 horizon. Extinction angle between oriented clay is 55 degrees. Field of view is 3.3 mm.

Scollard Formation: Upper Scollard

Paleosols in the Upper Scollard formation record a dramatic morphological shift to a wetter environment from the better-drained environment of the lower Scollard. The stratigraphic location of the climatic shift occurs at PS27, the type palsosol of the Oreo pedotype. Paleosols of the Oreo pedotype are well developed aquic alfisols that show evidence of both subsurface gley and heavy accumulation of organic material at the surface. Oreo paleosols also have morphological elements indicative of well-drained conditions, including argillans along voids and ped faces, sepic fabric, and roots that penetrate into subsurface horizons (up to 50cm) (Retallack, 2001). The equation of Ready and Retallack (1995) indicates a MAP of 72 cm for the PS27, which seems low for a paleosol with properties reflecting hydric conditons. It is possible that PS27 records the shift from well-drained conditions in the lower Scollard to poorly-drained conditions in the upper Scollard, rather than an increase in mean annual precipitation.

The KT boundary paleosol (PS28), directly overlies PS27, and is capped by the regionally pervasive Nevis 13 coal. The development of a thick coal indicates that drainage became increasingly poor and/or mean annual precipitation increased dramatically between the formation of PS27 and PS28. It should be noted that the shift from better-drained paleosols in the lower Scollard to poorly drained paleosols in the upper Scollard: 1) occurs prior to the KT boundary claystone, 2) is recorded in PS27, indicating a gradual environmental shift, and 3) that changes in paleosol morphology in the upper Scollard are matched by changes in fluvial style from braided (SB dominated in lower Scollard) to meandering (LA dominated in upper Scollard). A tectonically-influenced flattening of the depositional profile may have caused shift in from a braided to a meandering fluvial style.

The KT boundary at Knudson's Farm has been studied extensively using geochemical, palynological, and petrographic techniques to interpret the climatic effects of a bolide impact. Sweet and Braman (1992) recognize composite "ejecta" and "fireball" layers and associated iridium spike and shocked quartz at Knudson's farm. Sweet (2001) suggests that the initial ejecta layer is associated with fireball irradiance (a thermal pulse accompanied by strong winds), which resulted in the destruction of the forest canopy and the extinctions of a wide range of plant and animal species. Argillaceous coal directly above the ejecta layer is cited as evidence for post-impact aerosolic debris that blocked solar radiation for up to 10 years, causing global cooling (Sweet, 2001). The cooling trend was eventually reversed as impact dust settled and pre-impact greenhouse conditions returned over a period of 500-10,000 years (Sweet, 2001).

Pedological observations made at Knudson's farm may validate Sweet's (2001) conclusions. The KT boundary occurs in the O horizon of the Nevis 13 coal paleosol (PS28), in lower portion of the upper Scollard Formation (Figure 22, appendix H). The occurrence of the boundary claystone in the middle of the otherwise homogeneous Nevis 13 coal seam suggests rapid return to pre-impact conditions. Both pre-impact and post-impact environments produced significant amounts of vascular plant material in a poorly-drained setting, eventually leading to coal formation. Assuming a conservative amount of compaction has occurred, a reasonable range for the time of formation is between 1,100 and 2,200 years for the pre-impact O horizon, and between 1,700 and 3,400 years

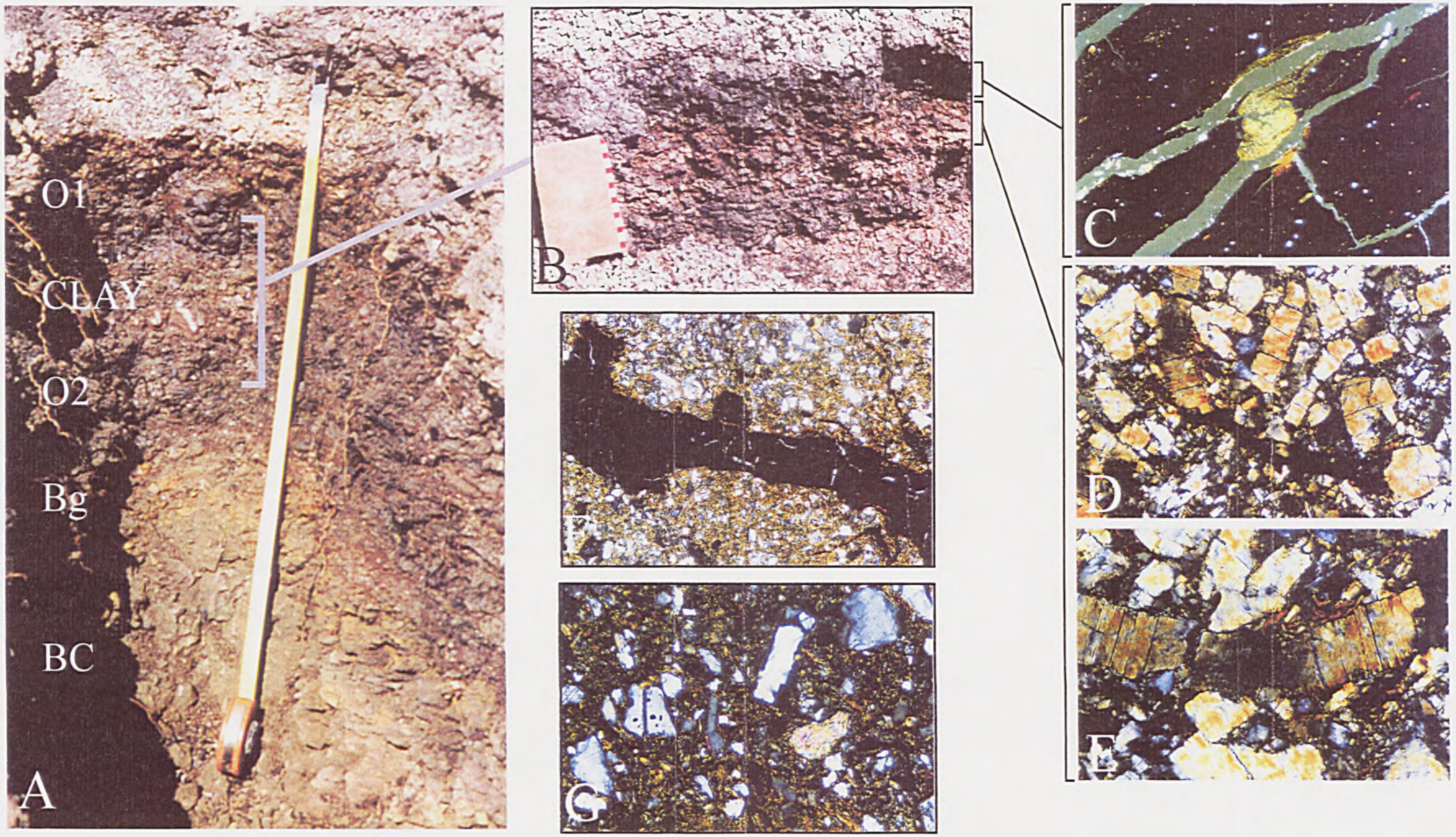

Figure 22. Photographs of the Doom type paleosol (PS28) and associated features. A) Profile of the PS28 coal paleosol with horizon designations. B) Close-up view of KT boundary clay layer between the O horizons of the Nevis 13 coal seam (Braman, personal communication, 2001). C) Photomicrograph of Nevis 13 coal from the O1 horizon. Field of view is 3.3 mm. D&E) Photomicrographs of boundary clay, identified as vermicular kaolinite (L.P. Wilding, personal communication, 2002). Photomicrograph E highlights the sweeping extinction found in each kaolinite book. Field of view is 1.3mm (D) and .66 mm (E). F) Photomicrograph of a carbonized root trace from the Bg horizon. Field of view is 3.3 mm. G) Photomicrograph of primary mineral grains and rock fragments from the upper BC horizon. Field of view is 1.3 mm.

for the post-impact O horizon (Retallack et al., 1996). The presence of a thick, well-developed coal paleosol (PS28) is indicative of a humid climate with a MAP of 250 cm+ (Retallack, 2001).

Paleosol PS29, the type paleosol of the Gloom pedotype, overlies PS28, and has morphological characteristics of a soil formed in a poorly drained setting. Sepic fabric and weak argillans indicate moderate wet/dry seasonality possibly produced by periodic drainage (Retallack, 2001). The coaly surface horizon of PS29 indicates 130-250 cm MAP (Retallack, 2001). The remainder of the paleosols in the Upper Scollard are of the Oreo and Gloom pedotypes and have morphologies and environmental implications similar to PS27 and PS29. The similarity of paleosols in the Upper Scollard indicates that the environment of pedogenesis was probably humid, that MAP was generally between 150 and 250 cm, and that drainage was generally poor.

While it is certainly possible that indicators of hydric conditions preserved in upper Scollard paleosols were generated by, and/or modified by, an increasingly wet climate, the probable influence of foreland tectonism on paleosol morphology must be considered. The effects of tectonically induced restriction of free drainage on paleosols (gley, coal formation) are similar to the effects of increasingly cooler and wetter paleoclimate on paleosols. As a result, calibration of evolving paleosol morphology to coeval tectonism must be considered before conclusions regarding paleoclimate can be made with confidence.

CHAPTER FOUR

Paleoenvironmental Reconstruction

Paleoclimatic Overview

The succession of paleosols in the Knudson's Farm section indicates a Late Cretaceous to early Tertiary history of humid climatic conditions punctuated by variations in mean annual precipitation and drainage. The lack of pedogenic carbonate, weakly-developed argillans, well-developed coals and gley features are all evidence of humid paleoclimate in aquic and/or udic moisture regimes (Soil Survey Staff, 1998; Birkeland, 1999). The occurrence of coal-bearing intervals (e.g. Knudson's farm) in central Alberta and time-equivalent caliche-bearing intervals in south-central Alberta, however suggests regional climatic variance (Jerzykiewicz and Sweet, 1988). Whereas a rain shadow effect from the Rocky Mountains during the latest Cretaceous and earliest Tertiary may have limited precipitation in southern Alberta (an effect that persists to the present) the interaction of westerlies and polar air masses moving parallel to the mountain front within central Alberta produced significant amounts of precipitation (Jerzykiewicz and Sweet, 1988). Correlation of time-equivalent strata by Jerzykiewicz and Sweet (1988) indicates that coeval wetting/cooling and drying/heating trends can be recognized in both caliche and coal-bearing facies. The time-equivalence of climatic shifts in both caliche-bearing and coal-bearing regimes suggests a regional control on climate. Comparison of wetting/drying events to sea level change indicates that drier facies within both southern and central Alberta occur during lowstands in sea level (shoreline distal), and that more humid facies occur during highstand (shoreline proximal) (Jerzykiewicz and Sweet, 1988). The seemingly coincidental relationship between orographic and base level to climate must be investigated further in order to constrain the true impacts of inputs on paleoclimate.

Numerous studies indicate that base level influences landscape stability and fluvial aggradation and degradation (Posamentier and Vail, 1988; Miall, 1992; Schumm, 1993; Zaitlin et al., 1994; Shanley and McCabe, 1994; Miall, 1996; Blum and Tornqvist, 2000). In general, rising base level coincides with thick fluvial aggradational cycles as accommodation space is generated (Posamentier and Vail, 1988; Kraus, 1988; Schumm, 1993; Blum and Tornqvist). Conversely, falling base level leads to fluvial incision and entrenchment, amalgamated channel deposits, and prolonged exposure of overbank deposits (Posamentier and Vail, 1988; Schumm, 1993; McCarthy et al., 1999; Blum and Tornqvist, 2000). Although this model provides a theoretical template for the relationship between base level and fluvial style, it places no limits on the extent of updip (landward) influence that base level may have of fluvial systems. Studies of sedimentation in the Mississippi River by Fisk (1944) suggest that eustasy influences sedimentation upwards of 1,000 km inland. More recent studies rebuff this claim and set general constraints to 100-150 km (Blum and Tornqvist, 2000), but a standard definition for the placement of this distance has not yet been determined. Blum and Tornqvist (2000) further suggest that eustatic influence on fluvial depositional systems varies from tens of kilometers for systems with steep gradients and low sediment supplies, to many hundreds of kilometers for systems with low gradients and high sediment supplies. Lerbekmo et al., (1992) suggests that base level change and terrestrial sedimentation in central Alberta are related. Lerbekmo et al. (1992) indicates that the regression of the Cannonball seaway may have led to time-equivalent Paskapoo unconformity (mid-Paleocene hiatus stratigraphically above the Knudson's farm section) (Figure 1). This work suggests that base level might have had effect on sedimentation at Knudson's Farm section, even as shoreline was located 750-1,000 km to the southeast (Eberth and O'Connell, 1995). While this distance to paleoshoreline is at this distal end of the landward influence of base level change, the occurrence of a regionally ubiquitous unconformity that is time-correlative with maximum regression suggests that a relationship between base level change and fluvial sedimentation did exist (Lerbekmo et al., 1992).

Tectonically-driven inputs may mute the influence of base level in terrestrial depositional systems (Miall, 1996). Catuneau et al., (1997, 2000) indicate that the evolution of fluvial style and base level within the Alberta basin was driven by foreland basin uplift and subsidence. Based upon the correlation of over 400 well logs across the Alberta foreland basin, Catuneanu et al., (1997) suggests a reciprocal stratal architecture of coeval transgressions and regressions at opposite sides of the basin induced by the back-and-forth uplift and subsidence on a flexural hinge that separates the basin into proximal (orogen) and distal (craton) sides. According to Catuneanu et al., (1997, 1999, 2000), times of orogenic loading cause subsidence (accommodation increase) adjacent to the proximal side of the hinge, and foreland bulge uplift (accommodation decrease) on the distal side of the hinge (Figure 2). Conversely, orogenic quiescence and erosion decrease the lithostatic load on the proximal side of the flexural hinge, which results in isostatic rebound (proximal side uplift) (Catuneanu et al., 2000) (Figure 2). Additionally, Posamentier and Allen (1993) suggest the possibility of proximal side "backward rotation" (flattening) during periods of extended quiescence and rebound.

The timing and duration of periods of orogenic loading and quiescence is key to interpreting the duration of sedimentation and geomorphic stability of lithologic units at Knudson's Farm. Studies by Catuneanu et al. (1997, 1999, 2000) suggest that transgressive sequences dominate the distal reaches of the basin. If this is true, then the reciprocal model suggests proximal transgressive events (orogenic loading) punctuated longer periods of regression (orogenic slowing and quiescence) (Catuneanu et al., 1997, 1999, 2000). Studies of stratigraphic relationships in the Alberta basin by Catuneanu et al. (1999, 2000) indicate that two loading/quiescence cycles occurred from the beginning of the Maastrichtian through the early Paleocene. As a result, evidence of two successive periods of loading and quiescence are observed at Knudson's Farm. By correlating time-stratigraphic surfaces, the first cycle begins with an orogenic loading phase at the base of the Horseshoe Canyon Formation (HSC), and ends with orogenic quiescence at the top of the Battle Formation. The second cycle begins at the base of the Lower Scollard, but is not completely preserved through an orogenic quiescence phase in the Upper Scollard..

As related to the study interval, the Knudson's Farm locality is located within a proximal-side position relative to the hingeline (Figure 2). During orogenic uplift and loading, subsidence generates increased regional slopes and accommodation space in both the marine and nonmarine realms. Increased sediment supply from orogenic uplift quickly fills terrestrial accommodation space, and is evidenced by high net to gross, and architectural elements reflecting fluvial aggradation (SB, vertically stacked CH and LS.) in response to accommodation filling. Stacked LS and SB in the HSC, as well as stacked

SB in the Lower Scollard record periods of orogenic loading and shedding (Figures 3 and 11). Additionally, paleosols found in this interval are immature, as high rates of sedimentation prevent prolonged geomorphic stability. This is reflected by the presence of immature entisols and inceptisols in the HSC and lower Scollard (Figures 15 and 18). As orogenic loading and subsidence slow, the depositional profile may begin to flatten causing rivers to become more sinuous as the depostional profile flattens and sediment supply decreases. An increase in accretionary bedforms (LA, FF) accompanies a slowing of orogenesis, and can be observed in both the C11 and upper T12 of cycle 1, and in the upper Scollard in cycle 2. Paleosols become more mature and/or numerous during this interval as the landscape begins to stabilize. This is evidenced by the vertisols and histosols occurring in the C11 and the vertisols and alfisols occurring in the upper portion of the Lower Scollard. During orogenic quiescence, the depositonal profile flattens to its greatest degree, which is likely due to backward rotation of the proximal foreslope (Posamentier and Allen, 1993; Schwans, 1995). The fluvial response to extreme flattening of the depositional profile is reflected in and increase in accretionary elements (LA, FF) and possible lacustrine or paludal sedimentation. These types of deposits can be observed in the Whitemud and Battle Formations (top of cycle 1) and in the upper Scollard (near the top of cycle 2). If paleosols are found in this setting, they may show evidence of hydric conditions due to poor drainage of a flat regional slope. Paleosols capping the both the Battle Formation and the Upper Scollard all show evidence of having undergone pedogenesis in water-saturated conditions (Figures 16 and 22). A correlation fluvial deposits and paleosol morphology within the section may serve as a test of this model. Additionally, a test of accommodation change can be made by comparing a plot of cumulative deviation of aggradational cycle thickness at Knudson's farm to a plot of relative paleoshoreline position generated by the combined work of Gill and Cobban (1973), Cherven and Jacob (1985) and Catuneanu et al., (1997).

Assessment of Paleoenvironmental Change

Using paleosols to reconstruct paleoclimatic variability across the KT boundary is complicated by the composite effects of climate, drainage, and duration of exposure as modulated by Laramide orogenesis and eustasy. A comparison of sedimentologic and paleopedologic observations within the Knudson's farm section allows discrimination of the tectono-eustatic events that influenced both deposition and pedogenesis (Figure 23).

Early Maastrichtian (early)– Horseshoe Canyon Formation (HSC, C11, T12)

Catuneanu et al., (2000) describe the early Maastrichtian time as a period of orogenic loading in the Alberta basin (Figure 23). Initiation orogenic loading results in the deposition of large amounts of orogenic sediment into subsidence-generated accommodation space. Lithofacies in the HSC support this model. Fluvial deposits consist of crevasse splay laminated sand (LS) near the base that thicken up section into amalgamated sand bodies (SB) near the top. This suggests a sediment load increase that possibly exceeded fluvial capacity. Possible additional evidence for high rates of sedimentation in the HSC is the presence of fossilized dinosaur remains, suggesting that sedimentation was rapid enough to preserve organic material. Paleosol evidence also supports the idea of relatively rapid, sustained sedimentation. Immature paleosols of the Milktoast pedotype dominate the HSC. These paleosols reflect only a few hundred years

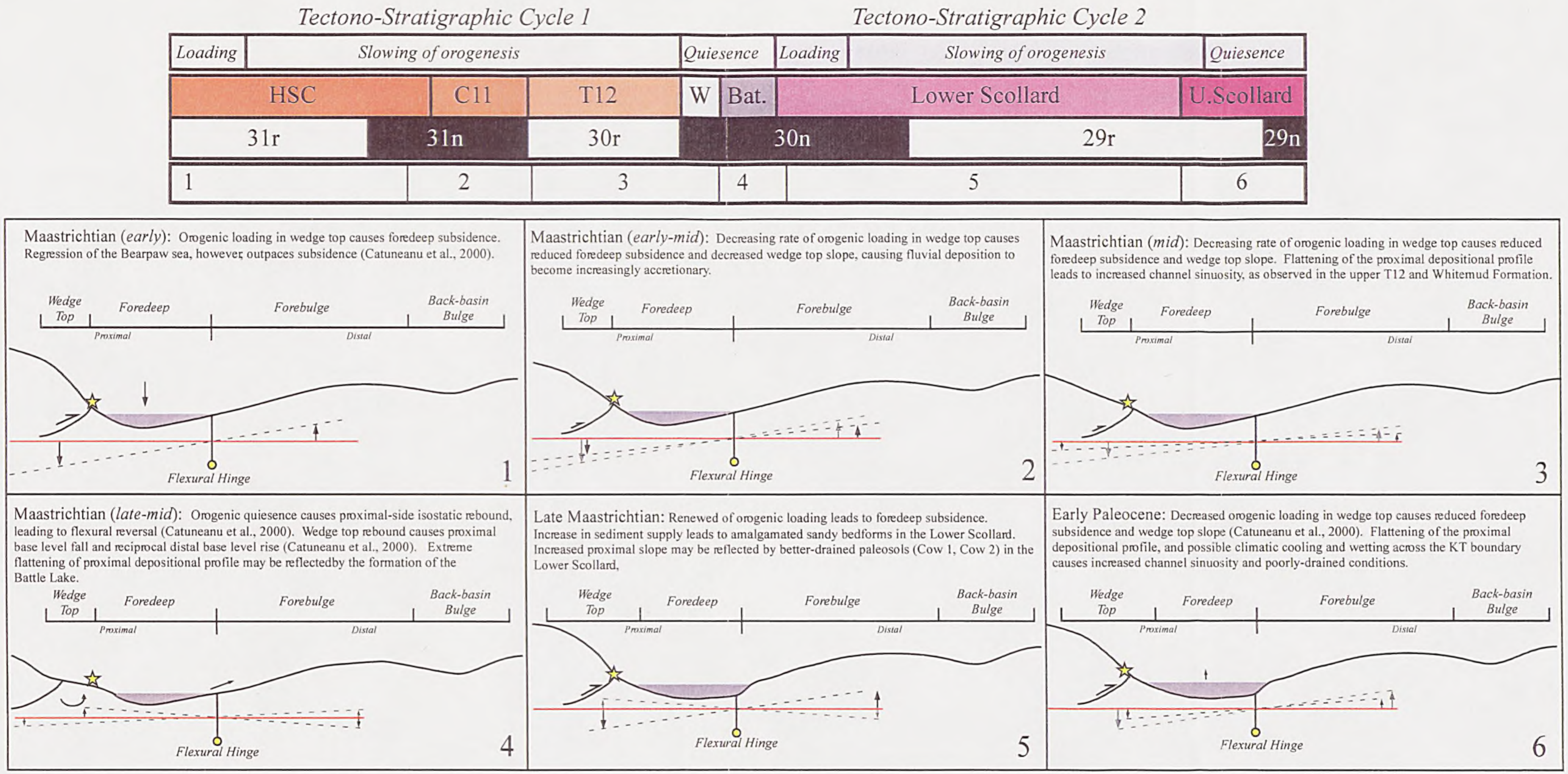

Figures based on field observations compared to tectonic model of Catuneanu et. al., 2000

☆ *Location of Knudson's farm*
- - - *Ongoing subsidence/uplift*
- - - *Previous subsidence/uplift*
▢ *Accomodation*

Figure 23. Depositional model for the Alberta foreland basin as proposed by Catuneanu et. al. (1997, 2000). Notes based on field observations at Knudson's Farm accompany each numbered cell. Figures adapted from Posamentier and Allen (1993), and Catuneanu et al., (1997, 2000). Time stratigraphic position for each cell is provided (top) for correlation to tectono-stratigraphic cycles illustrated in Figure 24.

of geomorphic stability between episodes of deposition. During the deposition of the upper portion of the HSC, distance from Knudson's farm to paleoshoreline decreased from approximately 300 km to 150 km (Catuneanu et al., 1997). Catuneanu et al., (2000) suggest that maximum shoreline transgression is time-correlative with the depostion of the upper HSC. This late HSC transgression (and resultant increase in accommodation) may have led to the occurrence of a more poorly-drained "Gloom" paleosol. Additionally, a plot of cumulative deviation of aggradational cycle thickness in the uppermost HSC indicates an increase in accommodation-controlled sedimetation at the top of the HSC, possibly caused by transgression (Figure24).

The transition from the HSC to the Carbon 11 zone took place during a period of shoreline retreat that outpaced orogenically-induced subsidence (Catuneanu et al., 2000). Shoreline retreat combined with decreased rates of subsidence may have caused a rapid decrease in accommodation space. Sedimentary features within the C11 zone are consistent with this model. Fluvial deposits at the base of the Carbon 11 zone record a progressive loss of architectural elements more commonly associatied with fluvial amalgamation (Miall, 1996). Architectural elements change dramatically over a few meters, from SB in the upper HSC, to LS and FF in the middle C11. Additionally, fluvial aggradational cycle thickness decreases in the lower to mid C11, likely reflecting a decrease in accommodation space as shoreline retreated (Figure 24). Paleosol morphology within the Carbon 11 is also consistent with a decrease in regional slope and sedimentation (Figure 23). Paleosols within the Carbon 11 zone have morphological characteristics suggesting pedogenesis on inundated to slightly seasonal conditions: subsurface gley and large concentrations of organic matter in the surface horizons.

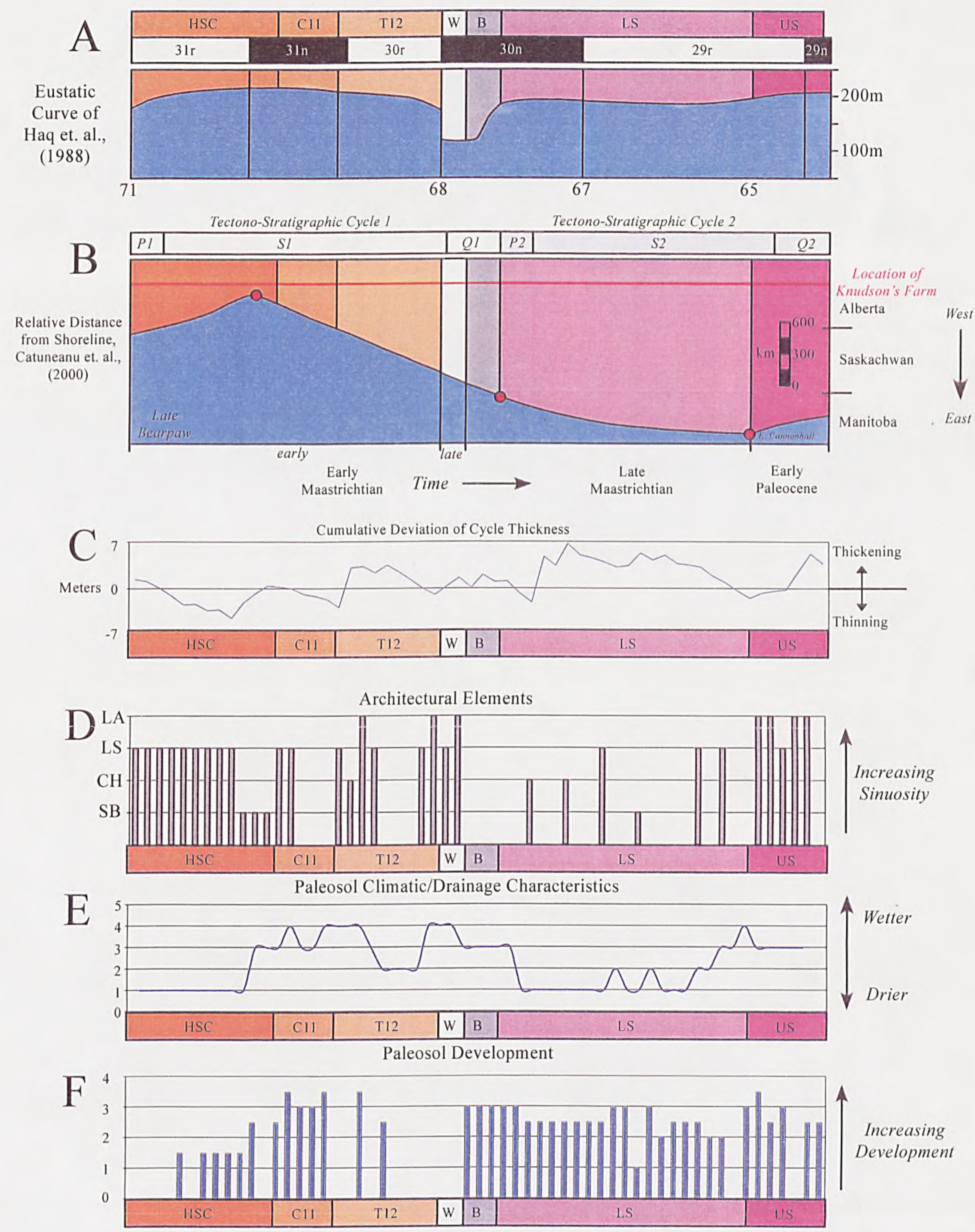

Figure 24. Synthesis of stratigraphic, lithologic, tectono-eustatic, and pedogenic parameters affecting Late Cretaceous and earliest Tertiary strata at the Knudson's Farm locality. All plots are time correlative. A) Global eustatic curve of Haq et al., (1988) matched to polarity chrons established for the locality by Lerbekmo (in press). B) Plot of relative shoreline distance from the Knudson's farm locality (Catuneanu et al., 2000). Two orogenically-driven, second-order pulses are labeled "Tectono-Stratigraphic Cycle 1" and "Tectono-Stratigraphic Cycle 2" (Catuneanu et al., 2000). Periods of orogenic loading are labeled "P", periods of slowing of orogenic loading are labeled "S", and periods of orogenic quiesence are labeled "Q" (Catuneanu et al., 1997; Cherven and Jacob, 1985; Gill and Cobban, 1973). C) Cumulative deviation of fluvial aggradational cycle thickness at the Knudson's Farm locality. Increases in cycle thickness reflect proximal side accomodation fill associated with orogenic shedding. D) Plot of fluvial architectural elements that occur at Knudson's Farm. Notice that paleochannel sinuosity increases as the system moves toward orogenic quiesence. E) Relative soil drainage for paleosols at Knudson's Farm. Paleosol drainage becomes increasingly poor as the system moves towards orogenic quiesence and paleochannels become increasingly sinuous. Refer to Tables 3 and 4 for explanation of data points. F) Relative paleosol development through the Knudson's Farm section. Note a general trend of increasing paleosol maturity during episodes of orogenic quiesence.

Deposits and paleosols in the Thompson 12 coal zone may also reflect the tectono-eustatic model of Catuneanu et al., (1997, 2000). Deposition of the basal T12 sandstone (SB) may have been the result of aggradational filling associated with a third-order rise in base level (Catuneanu et al., 2000). Accommodation filling, subsequent shoreline retreat, and flattening of the depositional profile related to slowing of orogen-induced subsidence is recorded by evolution of fluvial styles from amalgamated (SB) at the base of the T12 sandstone to accretionary (LA) deposits at the top. Continued flattening of the depositional profile and increasingly poor drainage may have aided in producing environmental conditions favoring coal formation. This is likely recorded by the T12 coal, which caps the LA deposits at the top of the T12 sandstone. Additional evidence for decreased depositional gradient includes accretion deposits (LA) in the upper T12, indicating increased channel sinuosity relative to SB deposits in the lower T12. An anomaly in the succession of lithologic units in the T12 is the second T12 paleosol (T12PS2). T12PS2 has morphological characteristics that suggest it formed in either a better-drained environment than the T12 coal, or in a climate with a lower MAP. It is possible that channel migration allowed for the formation of T12PS2 in a better-drained setting than the T12PS1 coal paleosol. If this is the case, then T12 PS2 (of the Cow 1 pedotype) may be a more accurate representation of paleoclimate during late T12 time.

Early Maastricatian (late)– Whitemud/Battle Formations

Fluvial and lacustrine deposits of the Whitemud and Battle Formations may have formed as a result of flattening, and possible backtilting of the proximal depositional profile associated with orogenic unloading and proximal-side rebound (Catuneanu et al.,

2000) (Figure 23). The Whitemud likely accumulated in highly sinuous meandering streams, as indicated by depositionally inclined, ripple laminated carbonaceous sandy siltstone (LA, Sr) and laminated very fine sand and silt (Fl). Laminated carbonaceous claystone interbedded with LA deposits in the Whitemud indicates episodes of reduced flow and high organic productivity. The most extreme result of topographic flattening may have been the creation of local curved ponds, swamps, and regional lakes (e.g., "Battle Lake" of Binda (1992)). Multiple exposures of the Battle Formation (including the exposure at Knudson's Farm) include massive to slightly laminated carbonaceous mudstone that includes a lacustrine microfossil assemblage (Binda, 1992). The presence of poorly-drained paleosols in the upper Battle indicates retreat of the Battle Lake prior to the deposition of the Scollard Formation. Drainage of the Battle Lake may relate to the initiation of orogenic loading and proximal side tilt associated with tectono-stratigraphic cycle 2 (Figure 23). Paleosols become increasingly better-drained approaching the Battle-Scollard contact, and may be evidence of improving regional drainage related to increasing regional slope (Catuneanu et al., 2000).

Late Maastrichtian – Lower Scollard Formation

The tectono-eustatic model of Catuneanu et al., (2000) suggests that the Lower Scollard Formation was deposited during a second phase of orogenic loading and foredeep subsidence (Figure 23). Basal Scollard sand bodies (SB) were deposited as an amalgamated, braided fluvial system, as indicated by basal scour, multistory channels, and dominance of trough and planar tabular (St, Sp) bedforms. Weakly-developed Cow 1 paleosols occur in the basal portion of the Lower Scollard. Paleosols are immature, but well drained, and may reflect improved drainage resulting from steepened depositional slope related to orogenic uplift. Increased subsidence and orogenic shedding may be indicated by the increased aggradational cycle thickness at the base of the Lower Scollard (Figure 24).

The increased number and maturity of paleosols within the upper portion of the Lower Scollard may reflect decreased subsidence and orogenic loading or climate change independent of tectonic influence. Reduced rates of sedimentation and increased geomorophic stability likely account for increasing paleosol maturity upwards in the Lower Scollard. A decrease in precipitation is indicated by the well-drained, seasonal morphological features (decreased organic matter accumulation in the surface horizon, ferriargillans, oxidized matrix color, sepic fabric, and slickensides) found in the Cow 1, Cow 2, Trochu and Ramp paleosols that occur in the upper portion of the Lower Scollard.

Early Paleocene – Upper Scollard Formation

The accretionary, meandering fluvial style and poorly-drained, gleyed, and coal-capped paleosols of the Upper Scollard may reflect post-orogenic proximal-side rebound and associated reduction in depositional slope (Catuneanu et. al, 2000) (Figure 23). The Upper Scollard includes horizontal-inclined, rippled and finely laminated (Sr, Fl), lateral accretion (LA) deposits. The abundance of accretionary bedforms is indicative increased channel sinuousity. Eberth and O'Connell (1995) conclude that fluvial deposits in the Upper Scollard deposited by higher sinuosity fluvial systems the Lower Scollard. Increased paleochannel sinuosity may be related to a reduction in regional slope associated with foredeep rebound (Figure 23). Decreased slope and free drainage may also be reflected by the occurrence of poorly drained paleosols of the Gloom, Doom, and Oreo pedotypes in the Upper Scollard.

CHAPTER FIVE

Conclusions

Analysis of Late Cretaceous and earliest Tertiary depositional and pedogenic lithofacies at Knudson's Farm reveals the following:

1) Paleoclimatic indicators in paleosols indicate a humid climate throughout the section, with a minimum range of precipitation of 70-125 cm yr^{-1} in alfisols (Cow 2 pedotype) and a maximum range of 250 cm yr^{-1}+ in histosols (Doom pedotype). General ranges of precipitation per paleosol-bearing lithostratigraphic unit are: HSC – 125-150 cm yr^{-1}; C11 – 150-250 cm yr^{-1}; T12 – 75-250 cm yr^{-1}; Battle - 70-200 cm yr^{-1}; Lower Scollard – 70-150 cm yr^{-1}; Upper Scollard – 150-250 cm yr^{-1}.
2) It is unclear whether paleosol morphology reflects climatic variability, changes in drainage, or a combination of the two.
3) Regular variability in the distribution of lithofacies may be indicative of some extrinsic control on sedimentation. The depositional history records cyclical evolution from amalgamated, multi-story, braided sand bodies to accretionary, single-story, overbank prone meandering deposits. The Horseshoe Canyon Formation consists of stacked crevasse splay (HSC) and amalgamated sandy bedforms (lower T12) that grade upwards into accretionary (LA) deposits (upper T12 and Whitemud Formation). The Scollard Formation records amalgamated SB at its base and single-story LA at its top.

4) The distribution of paleosols throughout the section is also cyclical. Immature, well-drained paleosols occur with braided deposits, whereas mature, poorly-drained paleosols occur with meandering deposits. Mature, well-drained paleosols occur during periods of reduced sedimentation. Stacked, amalgamated deposits in the lower Horseshoe Canyon Formation (HSC) include weakly developed entisols and inceptisols, whereas accretionary deposits upsection (T12) contain well-developed histosols. Paleosols formed in between stories of SB in the Lower Scollard Formation include weakly developed inceptisols that grade into alfisols and vertisols up section as sedimentation wanes. The Upper Scollard Formation includes well developed Histosols that form caps on LA deposits.
5) The sedimentary cyclicity observed at Knudson's Farm corroborates the tectono-stratigraphic model of Catuneanu et al. (1997, 1999, 2000). Pulses of orogenic loading and subsidence produce increased sediment supply and accommodation, which is reflected by amalgamated fluvial deposits (SB) and immature paleosols. As orogenesis slows, the proportion of paleosols to fluvial deposts increases, and paleosols become more mature. Finally, as orogenic quiescence ensues, flattening of the depositional profile leads to increased channel sinuosity (LA) and poorly drained paleosols.

APPENDICES

APPENDIX A

Milktoast Pedotype

HSCPS7 Type Clay Paleosol for Milktoast Pedotype

A 0-14 cm; pale olive (5Y 6/3) clay; moderate fine subangular blocky structure; common prominent yellowish brown (10YR 5/8) iron oxide stains; few fine black (N 2.5/) root traces; non-calcareous; porphyroskelic argillasepic/insepic microfabric; few root traces and biocasts/pellets; iron reductions along void walls; abrupt smooth boundary. (Sand (S)/Silt (Si)/Clay (C) – 17/37.6/45.3)

Bw 14-30 cm; pale olive (5Y 6/3) clay; moderate fine subangular blocky structure; common prominent yellowish brown (10YR 5/8) iron oxide stains; very few fine black (N 2.5/) root traces; non-calcareous; porphyroskelic insepic microfabric, few root traces and biocasts/pellets; few ferriargillans along void walls; clear smooth boundary (S/Si/C – 26.3/32/41.6)

C 30- 41 cm; pale olive (5Y 6/3) clay; weak coarse subangular blocky to massive structure; common prominent yellowish brown (10YR 5/8) iron oxide stains; non-calcareous; agglomeroplasmic masepic microfabric; few ferriargillans and iron reductions along void walls. (S/Si/C – 40.3/19.3/40.3)

Taxonomic Classification of Type Paleosol HSCPS7:
Epipedon:

Ochric
- Fails to meet definition for any other epipedon.

Endopedon:

Cambic
- Texture of vf sand, loamy vf sand, or finer
- Soil structure, roots
- Evidence of alteration in the form of:
    - o Higher clay content in Bw than underlying horizons
- No argillic, kandic, oxic, or spodic horizon
- No cementation or induration
- A lower depth of 25 cm or more from the mineral soil surface

Order:

Inceptisol (Cambic Horizion)
- Udept – Udic moisture regime (assumed from lack of carbonate)
- Dystrudept- Meets no great group definition
- Either:
    - o Lithic Dystrudept- Lithic contact (sandy parent material) within 50 cm of soil surface
    - o Lamellic Dystrudept – Lamellae within 200 cm of soil surface.

Paleosols in the Milktoast Pedotype:
HSCPS1 – A-Bw-C
HSCPS2 – A-Bw1-Bw2-C
HSCPS4 – A-Bw-C
HSCPS5 – A-C
HSCPS6 – A-Bw-C
HSCPS7 – A-Bw-C

Characteristics of paleosols in the Milktoast pedotype:

Paleosols in the Milktoast pedotype are weakly developed and occur at the tops of fining-upward fluvial deposits in the Horseshoe Canyon formation (Figures 4, 15). Milktoast paleosols are weakly developed Inceptisols or Entisols (Soil Survey Staff, 1996). The relatively weak development of Milktoast paleosols make determination of paleoclimatic processes difficult.

Geochemistry (absolute values by Retallack, 1997, p. 14):

- Clay Formation: Elemental ratio indicates little or no clay formation has taken place in Milktoast paleosols. However, slight depletion in aluminum and potassium relative to parent material (mass transport function) may provide ancillary evidence for slight lessivage in better-developed Milktoast paleosols.
- Calcification: Elemental ratio indicates little or no calcification has taken place in Milktoast paleosols. Slight depletion in calcium relative to parent material (mass transport function) provides evidence for slight carbonate removal Milktoast paleosols.
- Weathering: A relative depth trend indicates a decrease in soluble products of hydrolytic weathering (CaO, MgO, K_2O, Na_2O) with depth, indicating that the surface of Milktoast paleosols were weakly weathered. Absolute values of weathering ratios also indicate little weathering has taken place in Milktoast paleosols.
- Salinization- Absolute values for salinization are inordinantly large for all paleosols that were investigated. This may be due to excess sodium in feldspar being mistakenly counted as pedogenic Na_2O in the weathering ratio. The mass transport function indicates that sodium has been leached from upper horizons relative to the parent material, as would be expected in a seasonally wet soil.
- Oxidation- The molecular weathering ratio for ferric iron indicates a slightly higher proportion of oxidized iron in the horizons above the parent material. The mass transport function also indicates that there is more iron in upper horizons than in the parent material. While this may be a function of oxidation of iron during dry season in the surface horizons, it may also be true that there is a greater density of iron-rich clays in the surface horizons due to the preservation of depositional upward-fining.
- Leaching- Low value of Ba.Sr ratio indicates little leaching,
- Organic Carbon- Organic carbon levels peak in the surface horizon of the Milktoast pedotype, although the absolute value of organic carbon does not indicate a significant accumulation of organic material.

Paleoclimatic implications:

- No pedogenic carbonate, either because of lack of development or because of MAP of at least 125-150 cm (Birkeland, 1999).
- Sepic fabric and iron depletions indicate moderate wet/dry seasonality.
- Weak argillans indicate periodic drainage and/or seasonality (Retallack, 2001)

Paleobiology:

- Fossilized wood and dinosaur remains are pervasive, indicating rapid deposition of fluvial sediments.
- Fine roots penetrate 15-30 cm, indicating seasonably variable water table. While this may seem shallow, the soils are not well developed, and only approximately 15-30 cm thick.

Paleotopography:

- Sandy stream and levee deposits on a relatively flat alluvial plain (Eberth and O'Connell, 1995).

Parent Material:

- Silt and clay capping fining-upward alluvial deposits.

Time for Formation:

- 100-500 years, estimated from preservation of fining-upward texture, relative lack of color development and development of cambic horizon and microscopic ferriargillans in better-developed examples (Birkeland, 1999).

Raw chemical data for Milktoast Pedotype (HSCPS7)

SAMPLE DESCRIPTION	Ag ppm	Al %	As ppm	Ba ppm	Be ppm	Bi ppm	Ca %	Cd ppm	Co ppm	Cr ppm	Cu ppm	Fe %	K %	Mg %	Mn ppm	Mo ppm	Na %	Ni ppm	P ppm	Pb ppm	S %	Sb ppm	Sr ppm	Ti %	V ppm	W ppm	Zn ppm	SiO2 % fusion
HSCPS7A	<0.5	6.27	<5	790	1	2	0.79	<0.5	10	90	28	3.17	1.64	0.82	545	<1	1.59	27	480	22	0.03	<5	211	0.34	136	<10	74	61.6
HSCPS7Bw	<0.5	6.26	<5	690	1	<2	0.7	<0.5	7	64	23	2.63	1.53	0.62	115	1	1.6	20	390	18	0.02	5	218	0.28	87	<10	66	69.1
HSCPS7C	<0.5	6.76	<5	840	1	<2	0.76	<0.5	8	72	19	2.48	1.59	0.56	125	<1	1.79	23	340	20	0.04	<5	269	0.27	70	<10	58	66.9

HSCPS7 Major Elements, Oxide Mass

Depth (cm)	Al_2O_3	CaO	Fe_2O_3	K2O	MgO	Na2O	SiO_2	TiO
0	11.85	1.1	4.54	1.98	1.36	2.14	61.6	0.45
20	11.83	0.98	3.76	1.84	1.03	2.16	69.1	0.37
40	12.78	1.06	3.55	1.92	0.93	2.41	66.9	0.36

Organic Carbon

Depth	OC %
0	0.4
10	0.39
20	0.28
30	0.23
40	0.2

Strain

Depth	BD	Strain
0	1.93	-0.14
20	2.12	-0.049
40	2.09	0

Elemental Ratios

Depth (cm)	Al_2O_3/SiO_2	$CaO+MgO/Al_2O_3$	$CaO+MgO+K_2O+NaO/Al_2O_3$	Na_2O/K_2O	Fe_2O_3/SiO_2	Ba/Sr
0	0.113	0.466	0.948	1.67	0.027	2.39
20	0.101	0.37	0.845	1.75	0.021	2.02
40	0.113	0.336	0.808	1.95	0.02	1.99

Mass Transport

Depth (cm)	Al	Ca	Fe	K	Mg	Na	SiO_2	Ti
0	-0.26	-0.17	0.015	-0.18	0.163	-0.29	-0.27	0.00006
20	-0.107	-0.112	0.023	-0.072	0.068	-0.14	-0.004	0.0004
40	0	0	0	0	0	0	0	0

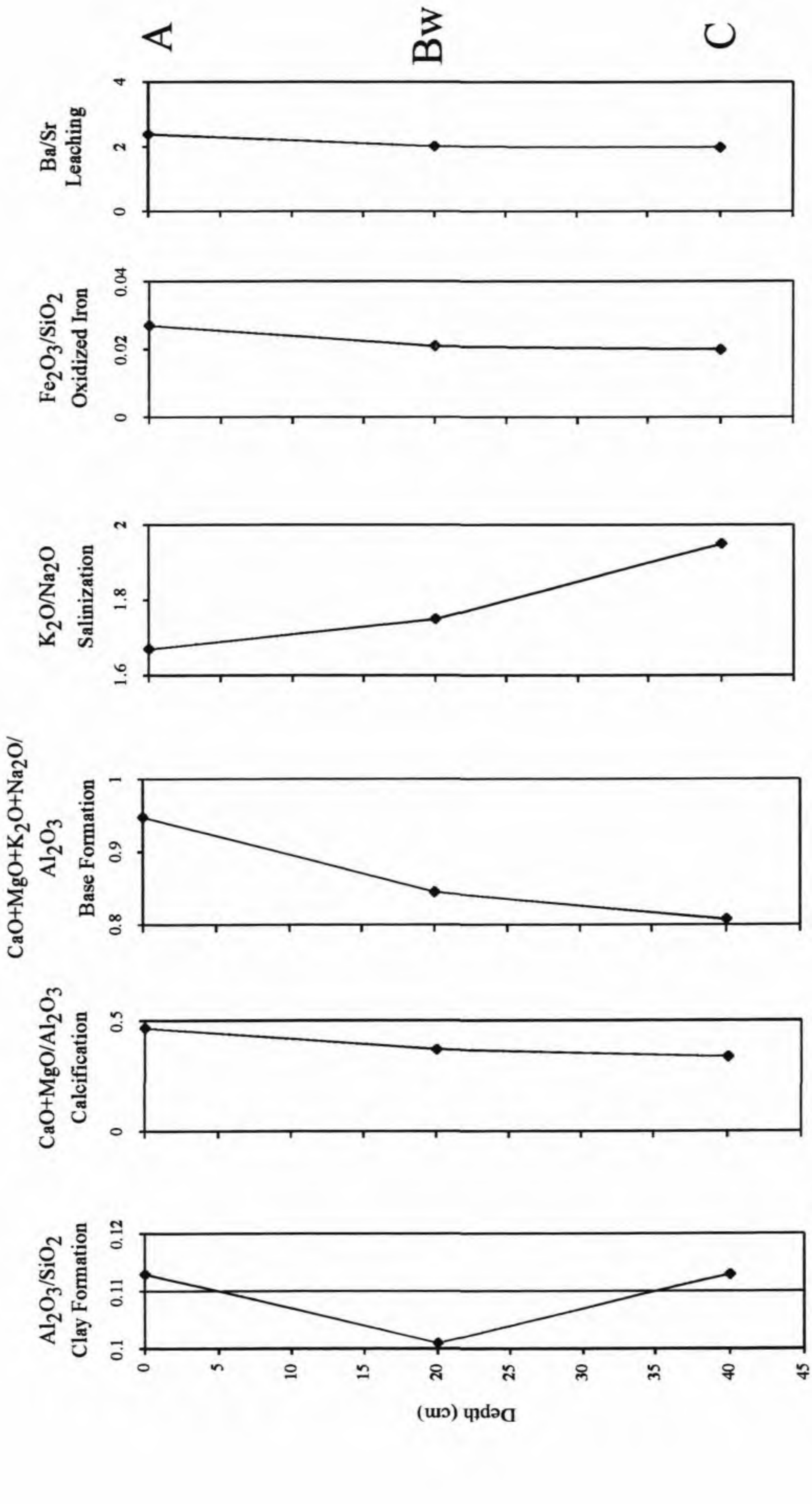

A
Bw
C
Ba/Sr
Leaching
0
2
4
Fe_2O_3/SiO_2
Oxidized Iron
0
0.02
0.04
K_2O/Na_2O
Salinization
1.6
1.8
2
$CaO+MgO+K_2O+Na_2O/$
Al_2O_3
Base Formation
0.8
0.9
1
$CaO+MgO/Al_2O_3$
Calcification
0
0.5
Al_2O_3/SiO_2
Clay Formation
0.1
0.11
0.12
0
5
10
15
20
25
30
35
40
45
Depth (cm)

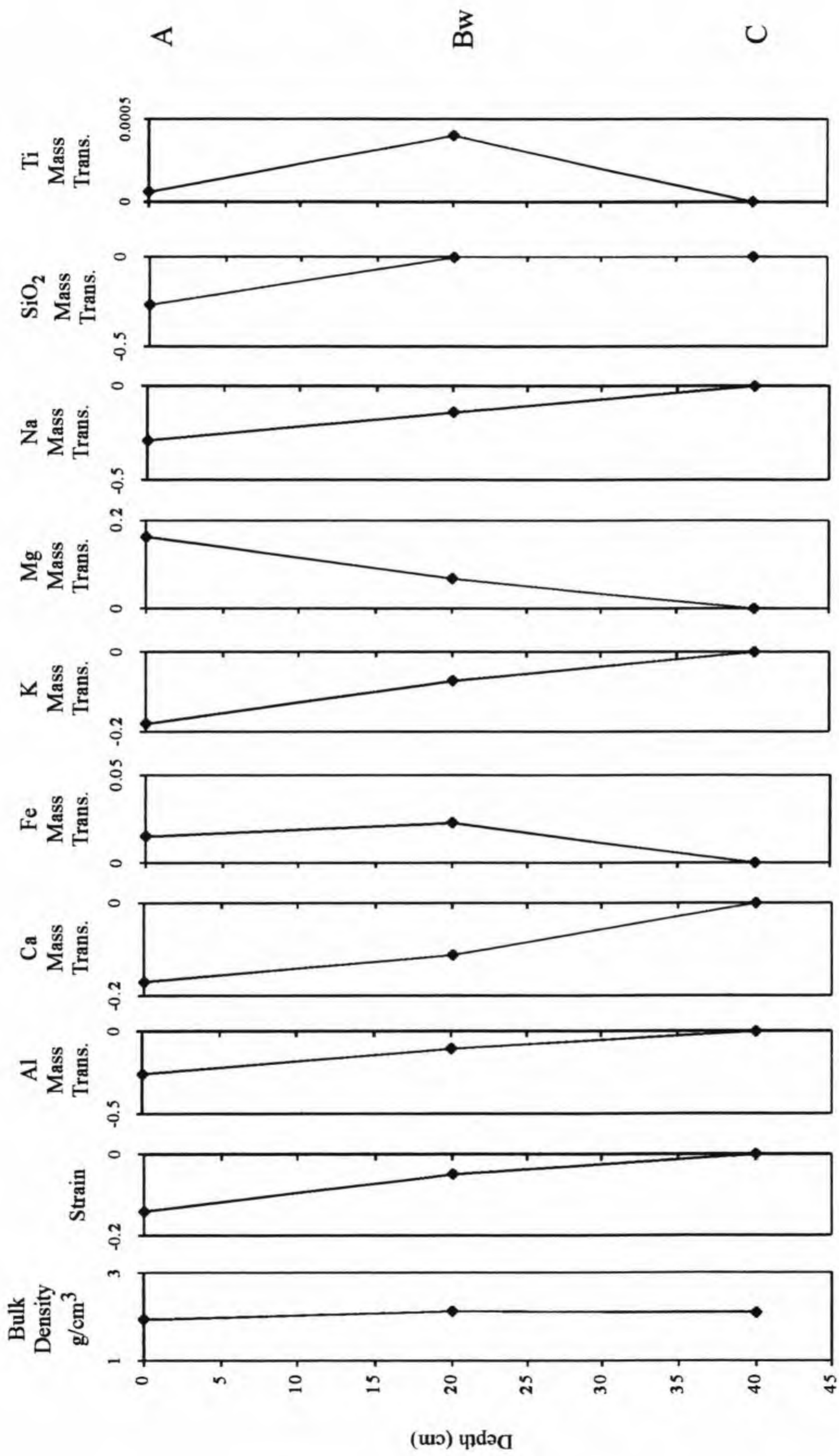
A
Bw
C
Ti Mass Trans.
0
0.0005
SiO2 Mass Trans.
-0.5
0
Na Mass Trans.
-0.5
0
Mg Mass Trans.
0
0.2
K Mass Trans.
-0.2
0
Fe Mass Trans.
0
0.05
Ca Mass Trans.
-0.2
0
Al Mass Trans.
-0.5
0
Strain
-0.2
0
Bulk Density g/cm3
1
3
0
5
10
15
20
25
30
35
40
45
Depth (cm)

APPENDIX B

Gloom Pedotype

PS29, Type Coal Paleosol for Gloom Pedotype

O 0-14 cm; black (N 2.5/) coal; strong thin platy structure; non-calcareous; few fine black (N 2.5/) root traces and biocasts; clear smooth boundary.

Bg1 14-32 cm; light olive gray (5Y 6/2) clay; moderate medium subangular blocky structure; very few fine prominent strong brown (7.5YR 5/8) iron oxide masses; non-calcareous; common fine black (N 2.5/) root traces and biocasts; agglomeroplasmic masepic microfabric; common root traces and biocasts/pellets; iron reductions along pores; Mn nodules present; few argillans along voids; clear smooth boundary (S/Si/C – 33.0/21.0/46.0).

Bg2 32-50 cm; light gray (5Y 7/1) clay; moderate medium subangular blocky structure; common prominent strong brown (7.5YR 5/8) iron oxide stains and masses; non-calcareous; common fine black (N 2.5/) root traces and biocasts, agglomeroplasmic masepic microfabric; common root traces and biocasts/pellets, iron reductions along pores, few argillans along voids; clear smooth boundary (S/Si/C – 33.6/23.6/44.3).

Bg3 50-60 cm; light gray (5Y 7/2) clay; moderate medium subangular blocky structure; common prominent strong brown (7.5YR 5/8) iron oxide stains and masses; non-calcareous; few fine black (N 2.5/) root traces and biocasts; agglomeroplasmic masepic/lattisepic microfabric; iron reductions along pores; few argillans along voids; clear smooth boundary (S/Si/C – 29.6/20/50.3).

C 60+ cm; light gray (5Y 7/2) clay loam; moderate medium subangular blocky structure; non-calcareous; agglomeroplasmic (to intertextic) argillasepic microfabric, grains long-axis parallel. (S/Si/C – 40.3/19.6/40).

USDA Taxonomic Classification for Type Paleosol PS29
Epipedon:

Ochric

- Fails to meet definition for any other epipedon.

Endopedon:

Cambic

- Texture of very fine sand, loamy very fing sand, or finer
- Soil structure
- Alteration in the form of:
    - o Evidence of aquic conditions, 50% of chroma is 2 or less, redox features present.
- No argillic, kandic, oxic, or spodic horizon
- No cementation or induration

A lower depth of 25 cm or more from the mineral soil surface

Order: Histosol (reconstructed O horizon thickness >60 cm)

- Hemist- meets no other definition for suborders
- Haplohemist- meets no other great group definition

Paleosols in the Gloom Pedotype:
HSCPS8 – A-Bg1-Bg2-C
C11PS1 – A1-A2-Bg1-Bg2-BC-C
PS29 – OA-Bg1-Bg2-BC
PS32C – OA-Bg1-Bg2-BC

Characteristics of paleosols in the Gloom pedotype:

Paleosols in the Gloom pedotype are moderately developed histosols that occur at intervals of transition from well-drained paleosols to poorly drained paleosols. Gloom paleosols do show evidence of pre-inundation or periodic drainage, including weak argillans along voids and roots that penetrate into subsurface horizons (50cm+). However, the dominant features of Gloom paleosols are gleyed subsurface horizons and thin surficial horizons that contain nearly 40% organic carbon, possibly representing compressed histic epipedons.

Geochemistry (absolute values by Retallack, 1997):

- Clay Formation: Weathering ratio indicates that very little clay formation has taken place in Gloom paleosols. Use of the mass transport function for mobile constituents associated with clays (potassium and aluminum) indicates that mobile constituents have been lost from upper horizons relative to the parent material. This may be evidence for pre-inundation or periodic lessivage.
- Calcification: Absolute values indicate very little calcification has taken place in Gloom paleosols. Both the calcification weathering ratio and mass transport function indicate that the largest amounts of calcium are found in the organic surface horizon.
- Weathering: Soluble products of hydrolytic weathering occur in the greatest abundance in the surface horizon of the type Gloom paleosol. This may be due to weathering during periodic drops in the water table. However, absolute values of weathering ratios indicate little weathering has taken place in Gloom paleosols.
- Salinization- Absolute values for salinization are inordinantly large for all paleosols that were investigated. This may be due to excess sodium weathering from feldspar in surface horizons being mistakenly counted as Na_2O in the weathering ratio. The mass transport function indicates that sodium has been leached from upper horizons relative to the parent material, as would be expected in a seasonally wet soil.
- Oxidation- The molecular weathering ratio for ferric iron indicates the greatest amount of iron oxide occurs in the surface horizon of Gloom paleosols. However, the mass transport function indicates that iron has been depleted from upper horizons relative to the parent material, which would be expected for a soil in reducing conditions.

- Leaching- Ba/Sr ration indicates increased leaching with depth. In an absolute sense, leaching is moderate.
- Organic Carbon- Organic carbon levels peak in the surface horizon of the type Gloom paleosol, with the absolute value of organic carbon indicating a significant accumulation of organic material (in excess of 40% organic carbon), to the point of being considered coaly. Input of organic matter is the probable cause of positive strain (dilation) in the surface horizons.

Paleoclimatic Implications:

- Coaly surface horizon indicates 130-250 cm MAP (Retallack, 2001).
- Sepic fabric indicates moderate wet/dry seasonality possibly previous to inundation and accumulation of surficial organic layer.
- Weak argillans indicate periodic drainage and/or seasonality (Retallack, 2001).

Paleobiology:

- Fine roots penetrate nearly 50 cm (up to 75% of soil thickness) into Gloom paleosols, indicating either wet/dry seasonality or a pre-inundation history.

Paleotopography:

- Flat, seasonally flooded overbank plain.

Parent Material:

- Clay-rich overbank/floodplain sediments.

Time for Formation:

- 1400-2800 years, assuming coal compaction of 0.1 times former thickness and peat accumulation of 0.5-1.0 mm/yr (Retallack, 1997). Development of cambic horizon and microscopic ferriargillans (Birkeland, 1999). Paleosols with thinner coal surface horizon may be younger.

Raw chemical data for Gloom pedotype (PS29)

SAMPLE DESCRIPTION	Ag ppm	Al %	As ppm	Ba ppm	Be ppm	Bi ppm	Ca %	Cd ppm	Co ppm	Cr ppm	Cu ppm	Fe %	K %	Mg %	Mn ppm	Mo ppm	Na %	Ni ppm	P ppm	Pb ppm	S %	Sb ppm	Sr ppm	Ti %	V ppm	W ppm	Zn ppm	SiO_2 % fusion
PS29OA	<0.5	1.55	<5	430	3	<2	0.43	<0.5	3	16	10	0.63	0.2	0.13	35	3	0.44	11	40	8	0.12	15	160	0.1	38	<10	18	19
PS29Bg1	<0.5	6.49	<5	760	0.5	2	0.32	<0.5	4	84	13	1.52	1.11	0.33	55	1	0.9	11	50	26	0.03	<5	135	0.37	48	<10	26	67
PS29Bg2	<0.5	6.34	<5	970	0.5	<2	0.32	<0.5	3	70	8	1.76	1.25	0.37	50	<1	0.98	11	10	18	0.03	5	165	0.31	48	<10	24	68.2
PS29Bg3	<0.5	6.31	<5	870	0.5	<2	0.4	<0.5	3	88	8	1.83	1.37	0.4	50	<1	1.16	9	<10	20	0.03	5	155	0.31	53	<10	24	67.4
PS29C	<0.5	6.16	<5	1870	0.5	<2	0.58	<0.5	3	73	9	2.14	1.32	0.42	45	<1	1.28	8	10	16	0.06	<5	224	0.26	64	<10	38	62.5

Major Elements Oxide Mass

Depth (cm)	Al2O3	CaO	Fe_2O_3	K_2O	MgO	Na_2O	SiO_2	TiO
0	2.93	0.6	0.9	0.24	0.22	0.59	19	0.13
20	12.27	0.45	2.17	1.34	0.55	1.21	67	0.49
40	11.98	0.45	2.52	1.51	0.61	1.32	68.2	0.41
50	11.93	0.56	2.62	1.65	0.66	1.56	67.4	0.41
80	11.64	0.81	3.06	1.59	0.7	1.73	62.5	0.35

Organic Carbon

Depth (cm)	OC %
0	38.9
10	6.77
20	0.59
30	0.52
40	0.3
50	0.33
60	0.23
70	0.25
80	0.25

Strain

Depth	BD	Strain
0	1.3	2.84
20	2.02	-0.33
40	2.06	-0.22
50	2.02	-0.2
80	1.92	0

Elemental Ratios

Depth (cm)	Al_2O_3/SiO_2	$CaO+MgO/Al_2O_3$	$CaO+MgO+K_2O+NaO/Al_2O_3$	Na_2O/K_2O	Fe_2O_3/SiO_2	Ba/Sr
0	0.09	0.55	1	3.33	0.019	1.71
20	0.108	0.18	0.47	1.43	0.013	3.6
40	0.104	0.197	0.51	1.31	0.014	3.76
50	0.104	0.222	0.59	1.39	0.014	3.58
80	0.11	0.272	0.67	1.65	0.018	5.47

Mass Transport

Depth (cm)	Al	Ca	Fe	K	Mg	Na	SiO_2	Ti
0	-0.346	0.93	-0.23	-0.61	-0.195	-0.11	-0.21	0
20	-0.257	-0.61	-0.499	-0.41	-0.45	-0.5	-0.24	0.003
40	-0.139	-0.54	-0.31	-0.21	-0.26	-0.36	-0.087	-0.002
50	-0.138	-0.42	-0.28	-0.13	-0.2	-0.24	-0.092	0.0035
80	0	0	0	0	0	0	0	0

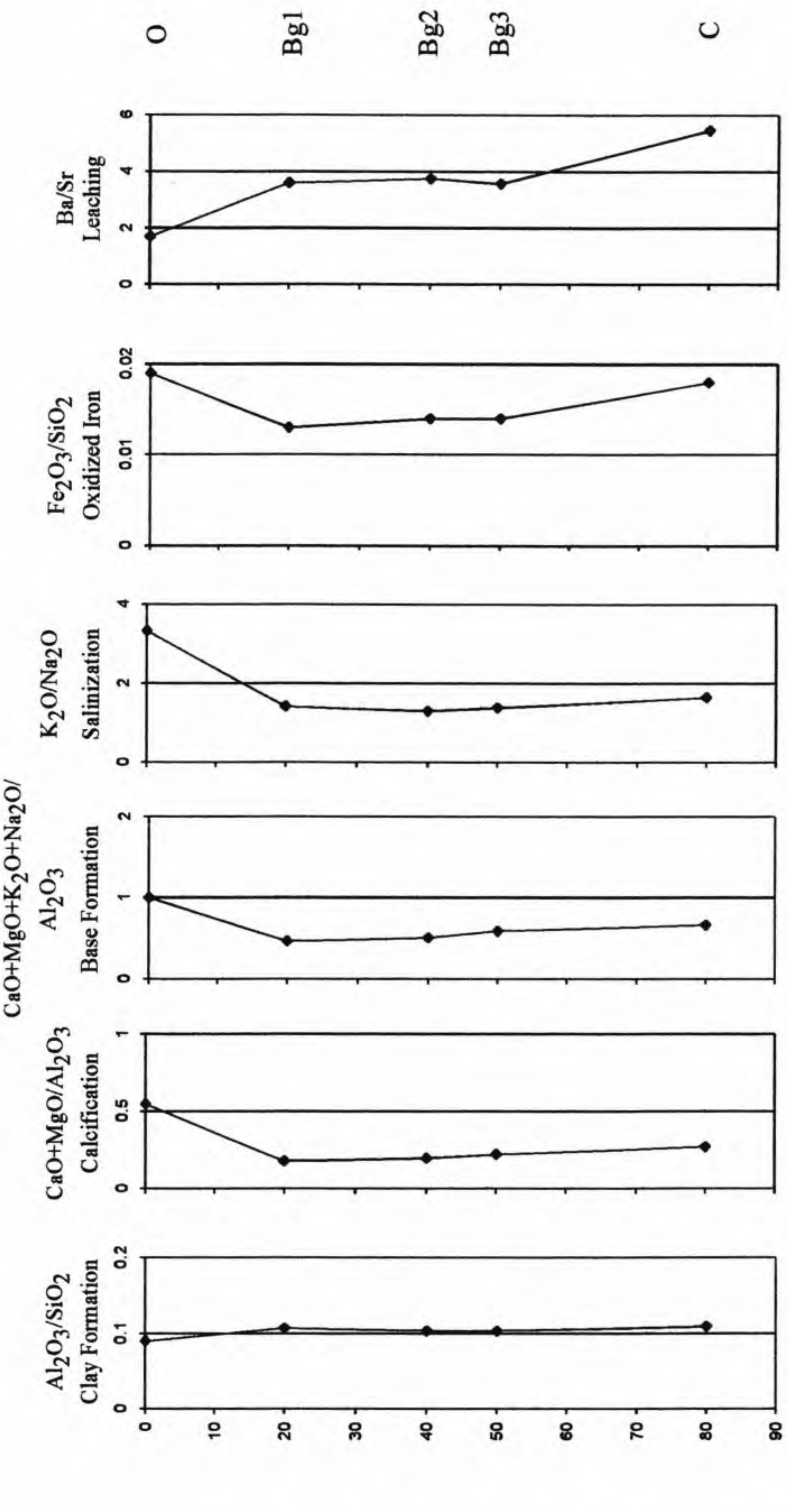
O
Bg1
Bg2
Bg3
C
Ba/Sr
Leaching
Fe_2O_3/SiO_2
Oxidized Iron
K_2O/Na_2O
Salinization
$CaO+MgO+K_2O+Na_2O/$
Al_2O_3
Base Formation
$CaO+MgO/Al_2O_3$
Calcification
Al_2O_3/SiO_2
Clay Formation
0 10 20 30 40 50 60 70 80 90

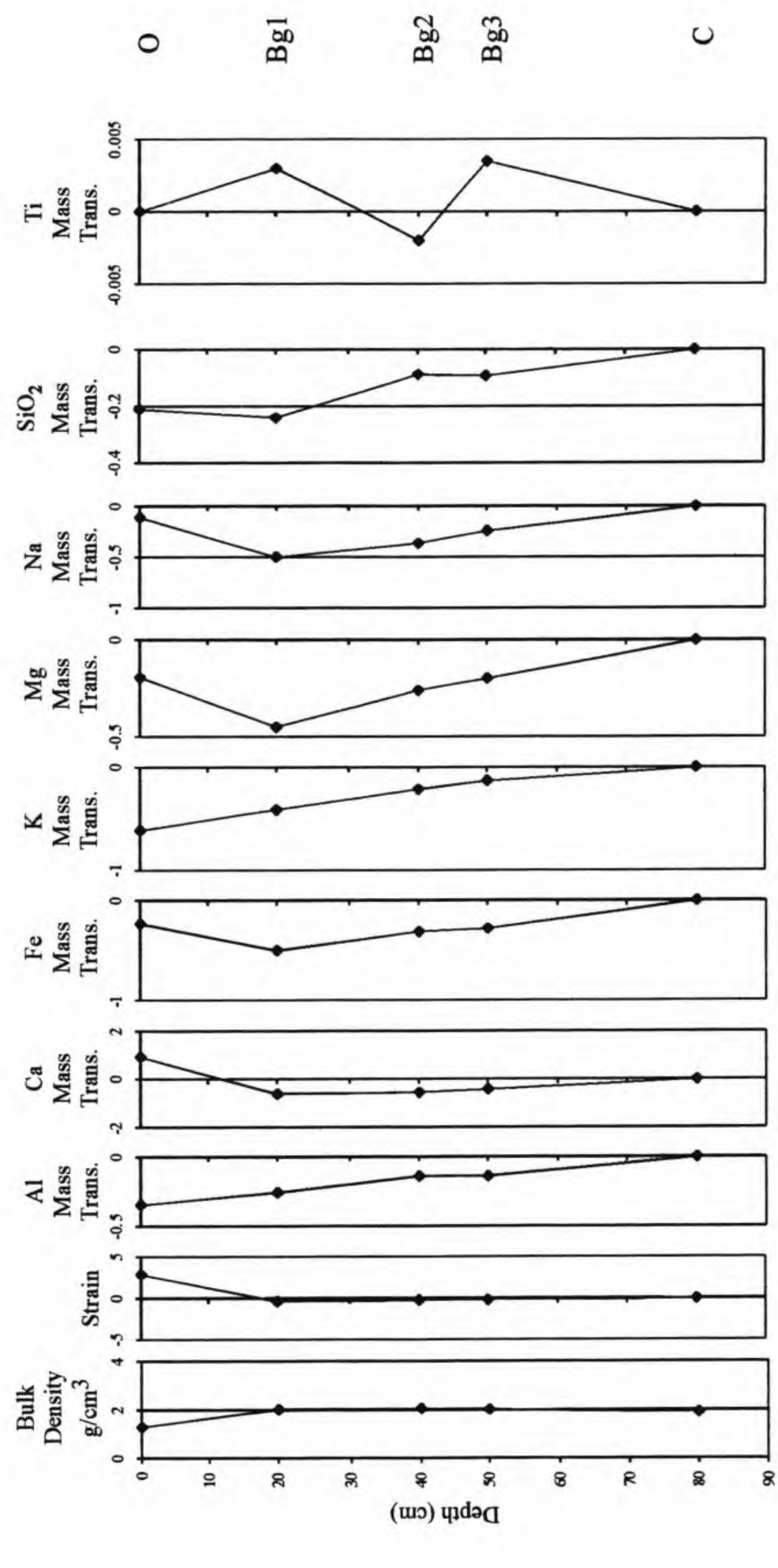

O
Bg1
Bg2
Bg3
C
Ti Mass Trans.
0.005
0
-0.005
SiO2 Mass Trans.
0
-0.2
-0.4
Na Mass Trans.
0
-0.5
-1
Mg Mass Trans.
0
-0.5
K Mass Trans.
0
-1
Fe Mass Trans.
0
-1
Ca Mass Trans.
2
0
-2
Al Mass Trans.
0
-0.5
Strain
5
0
-5
Bulk Density g/cm3
4
2
0
0 10 20 30 40 50 60 70 80 90
Depth (cm)

APPENDIX C

Trochu Pedotype

PS16 Type Clay Paleosol for Trochu Pedotype

A 0-30 cm; very dark gray (5Y 3/1) clay; strong thin platy structure; few prominent yellowish red (5YR 4/6) iron oxide stains; few fine black (N 2.5/) root traces and biocasts; non-calcareous; porphyroskelic insepic/skelesepic microfabric with masepic zones; common root traces and biocasts/pellets; iron depletions along channels; abrupt smooth boundary (S/Si/C – 11/27.6/61.3).

Bw1 30-50 cm; olive (5Y 5/4) clay; moderate fine angular blocky structure; few prominent yellowish red (5YR 5/8) iron oxide stains; few fine black (N 2.5/) root traces and biocasts; non-calcareous; porphyroskelic insepic/skelesepic microfabric with masepic zones; weak argillans along voids and ped faces; common root traces and biocasts/pellets; iron depletions along channels; clear smooth boundary (S/Si/C – 14.3/22/63.6).

Bw2 50-130 cm; pale olive (5Y 6/3) clay; moderate coarse subangular blocky structure; common prominent yellowish red (5YR 5/8) iron oxide stains; few fine black (N 2.5/) root traces and biocasts; non-calcareous; porphyroskelic insepic/skelesepic microfabric with masepic zones; weak argillans along voids and ped faces; common root traces and biocasts/pellets; iron depletions along channels; clear smooth boundary (S/Si/C – 17.3/20.6/62).

Bss1 130-175 cm; dark olive gray (5Y 3/2) clay; strong medium wedge structure; common prominent strong brown (7.5YR 5/6) iron oxide stains; very few fine black (N 2.5/) root traces and biocasts; non-calcareous; porphyroskelic masepic microfabric with skelesepic zones; few biocasts/pellets; iron oxide hypocoats along ped faces, few matrix-shifted argillans; gradual smooth boundary (S/Si/C – 3/16.6/80.3).

Bss2 175-245 cm; very dark gray (5Y 3/1) clay; strong medium/coarse wedge structure; common prominent strong brown (7.5YR 5/6) iron oxide stains; very few fine black (N 2.5/) root traces and biocasts; non-calcareous; porphyroskelic masepic/clinobimasepic microfabric; few biocasts/pellets; iron oxide hypocoats along ped faces, few matrix-shifted argillans; clear smooth boundary (S/Si/C – 8.3/18.3/73.3).

BC 245-300 cm; very dark gray (5Y 3/1) clay; moderate medium/coarse subangular blocky structure; common prominent strong brown (7.5YR 4/6) iron oxide stains; non-calcareous; porphyroskelic argillasepic microfabric; few biocasts/pellets. (S/Si/C – 22/28.6/49.3)

USDA Classification for Type Paleosol PS16:
Epipedon:
Ochric

- Fails to meet definition for any other epipedon

Endopedon:

Cambic

- Texture of vf sand, loamy vf sand, or finer
- Soil structure, roots
- Evidence of alteration in the form of:
  - Higher clay content (Bss1) than underlying horizons (Bss2)
- No argillic (lack of argillans), kandic, oxic, or spodic horizon
- No cementation or induration
- A lower depth of 25 cm or more from the mineral soil surface

Order:

Vertisol (A layer 25 cm+ thick, upper boundary within 100 cm of the soil surface (not in the case of the type soil, may be an overdeepened microlow), intersecting slickensides, over 30% clay in the soil, cracks)

- Udert – Meets no other definition for suborders
- Hapludert (if pH was 4.5 or more) Dystrudert (if pH is 4.5 or less)
- Typic Dystrudert- Meets no other definition for subgroup, no carbonate.

Paleosols in the Trochu Pedotype:
C11PS3 – A-Bw-Btss-Bss-BC
C11PS4 – A-Bw-Btss1-Btss2-Bss-BC
PS16- A-Bw1-Bw2-Bss1-Bss2-BC

Characteristics of Paleosols in the Trochu Pedotype:

Trochu paleosols are all moderately well developed Vertisols that occur in the upper Horseshoe Canyon (Carbon 11 zone) and Scollard Formations (Figures 12 and 17). Slickensides and infilled cracks in Trochu paleosols indicate pronounced wet/dry seasonality. Trochu paleosols also posses developmental features such as ferriargillans and well developed root and biological traces that suggest longer exposure history than the morphologically similar Ramp paleosols. While Trochu vertisols display evidence for clay translocation, none of the Trochu paleosols have well developed argillans or eluvial horizons.

Geochemistry (absolute values by Retallack, 1997):

- Clay Formation: Absolute values indicate little clay formation has taken place in Trochu paleosols. Use of the mass transport function for mobile constituents associated with clays (potassium and aluminum) does, however, suggest that lessivage has occurred, with clay being removed from Bw Horizons and Moved to Bss horizons.
- Calcification: Absolute values indicate little calcification has taken place in Trochu paleosols. The mass transport function indicates slight enrichment in calcium in surface horizons and slight depletion of calcium in Bss horizons.
- Weathering: Soluble products of hydrolytic weathering are most concentrated in the surface horizons of Trochu paleosols. Absolute values of weathering

ratios indicate little appreciable weathering has taken place in Trochu paleosols.

- Salinization- Absolute values for salinization are inordinantly large for all paleosols that were investigated. This may be due to excess sodium in feldspar being mistakenly counted as Na_2O in the weathering ratio. The mass transport function indicates slightly more sodium in the surface horizon of the type paleosol than in the rest of the profile. This may be due to the weathering of sodium in feldspar at the surface.
- Oxidation- The molecular weathering ratio for ferric iron is not indicative of a recognizable depth trend. The mass transport function also indicates that there is a slight increase in iron with depth in the upper half of the paleosol. This may be a function of oxidation of iron during dry season in the surface horizons.
- Leaching- Ba/Sr ratios throughout the profile are not indicative of strong leaching.
- Organic Carbon- Organic carbon levels peak in the surface horizon of the type Trochu paleosol. The absolute value of organic carbon indicates a greater accumulation of organic material in Trochu paleosols than in Ramp paleosols, either because Trochu paleosols had a longer developmental history or because surficial conditions were wetter and more conducive to organic matter preservation in Trochu paleosols. Input of organic matter is the probable cause of positive strain (dilation) in the surface horizons. At depth, organic carbon levels begin to rise, which may be the signature of an early composite soil, or remnant depositional organic material in the parent material.

Paleoclimatic implications-

- No pedogenic carbonate; MAP of at least 125-150 cm (Birkeland,
- 1999).
- Sepic fabric indicates wet/dry seasonality.
- Argillans/Argillic indicate drainage and/or seasonality (Retallack, 2001).
- Bss / surface cracks indicate pronounced wet/dry seasonality (Retallack, 2001).

Paleobiology:

- Fine roots penetrate over 2 meters into Trochu paleosols, indicating pronounced seasonality, or that the paleosol was well-drained.

Paleotopography:

- Flat, seasonally wet overbank plain

Parent Material:

- Clay-rich overbank/floodplain sediments.

Time of Formation:

- 1000+ years, estimated from development of cambic horizon, argillans, and well-developed slickensides (Birkeland, 1999).

Raw chemical data for Trochu pedotype (PS16)

SAMPLE DESCRIPTION	Ag ppm	Al %	As ppm	Ba ppm	Be ppm	Bi ppm	Ca %	Cd ppm	Co ppm	Cr ppm	Cu ppm	Fe %	K %	Mg %	Mn ppm	Mo ppm	Na %	Ni ppm	P ppm	Pb ppm	S %	Sb ppm	Sr ppm	Ti %	V ppm	W ppm	Zn ppm	SiO_2 % fusion
PS16A	<0.5	6.54	20	740	1.5	2	0.79	<0.5	19	64	40	3.54	1.6	0.69	145	1	1.56	52	330	20	0.06	5	258	0.34	90	<10	76	55.6
PS16Bw1	<0.5	6.5	<5	690	1	2	0.59	<0.5	9	76	33	3.96	1.7	0.75	130	<1	1.46	38	330	20	0.03	<5	194	0.35	115	<10	76	59.6
PS16Bw2	<0.5	6.62	<5	680	0.5	<2	0.5	<0.5	14	87	40	4.18	1.57	0.87	170	1	1.44	51	500	18	0.05	5	180	0.35	126	<10	88	59.9
PS16Bss1	<0.5	6.6	<5	790	1	<2	0.45	<0.5	15	87	44	4.39	1.8	0.86	150	<1	1.16	52	460	20	0.03	5	151	0.35	163	<10	104	57.7
PS16Bss2	<0.5	6.54	<5	670	1	<2	0.44	<0.5	12	84	54	3.88	1.92	0.89	160	<1	1.2	55	400	22	0.03	<5	144	0.37	148	<10	102	58.2
PS16BC	<0.5	6.52	<5	740	1	<2	0.53	<0.5	43	90	46	3.48	1.67	0.88	205	2	1.32	71	530	16	0.04	5	174	0.38	127	<10	108	57.9

Major Elements Oxide Mass

Depth (cm)	Al_2O_3	CaO	Fe_2O_3	K_2O	MgO	Na_2O	SiO_2	TiO
0	12.36	1.1	5.06	1.93	1.14	2.1	55.6	0.45
40	12.29	0.83	5.67	2.05	1.24	1.97	59.6	0.47
90	12.51	0.7	5.98	1.89	1.44	1.94	59.9	0.47
160	12.48	0.63	6.28	2.17	1.43	1.56	57.7	0.47
230	12.48	0.62	5.55	2.31	1.48	1.62	58.2	0.49
300	12.44	0.74	4.98	2.01	1.46	1.78	57.9	0.51

Elemental Ratios

Depth (cm)	Al_2O_3/SiO_2	$CaO+MgO/Al_2O_3$	$CaO+MgO+K2O+NaO/Al_2O_3$	Na_2O/K_2O	Fe_2O_3/SiO_2	Ba/Sr
0	0.13	0.397	0.843	1.7	0.034	1.84
40	0.122	0.38	0.826	1.45	0.036	2.28
90	0.123	0.39	0.805	1.55	0.037	2.27
160	0.127	0.377	0.77	1.09	0.041	3.34
230	0.126	0.393	0.811	1.04	0.036	2.98
300	0.127	0.4	0.811	1.38	0.032	2.71

Mass Transport

Depth (cm)	Al	Ca	Fe	K	Mg	Na	SiO_2	Ti
0	0.12	0.66	0.135	0.069	-0.125	0.32	0.072	-0.0015
40	0.082	0.208	0.235	0.105	-0.075	0.2	0.117	-0.0005
90	0.102	0.024	0.3	0.02	0.073	0.184	0.123	-0.00033
160	0.099	-0.078	0.37	0.171	0.061	-0.046	0.082	0.00023
230	0.03	-0.15	0.15	0.181	0.039	-0.066	0.032	0.00005
300	0	0	0	0	0	0	0	0

Organic Carbon

Depth (cm)	OC %
0	1.37
10	1.26
20	1.37
30	0.9
40	0.6
50	0.3
60	0.27
70	0.28
80	0.34
90	0.26
100	0.34
110	0.32
120	0.32
130	0.36
140	0.32
150	0.37
160	0.33
170	0.38
180	0.38
190	0.35
200	0.4
210	0.45
220	0.5
230	0.5
240	0.6
250	0.78
260	0.8
270	0.83
280	1.21
290	0.92
300	0.87

Strain

Depth	BD	Strain
0	1.86	0.35
40	2.18	0.12
90	2.21	0.105
160	2.29	0.067
230	2.31	0.0004
300	2.25	0

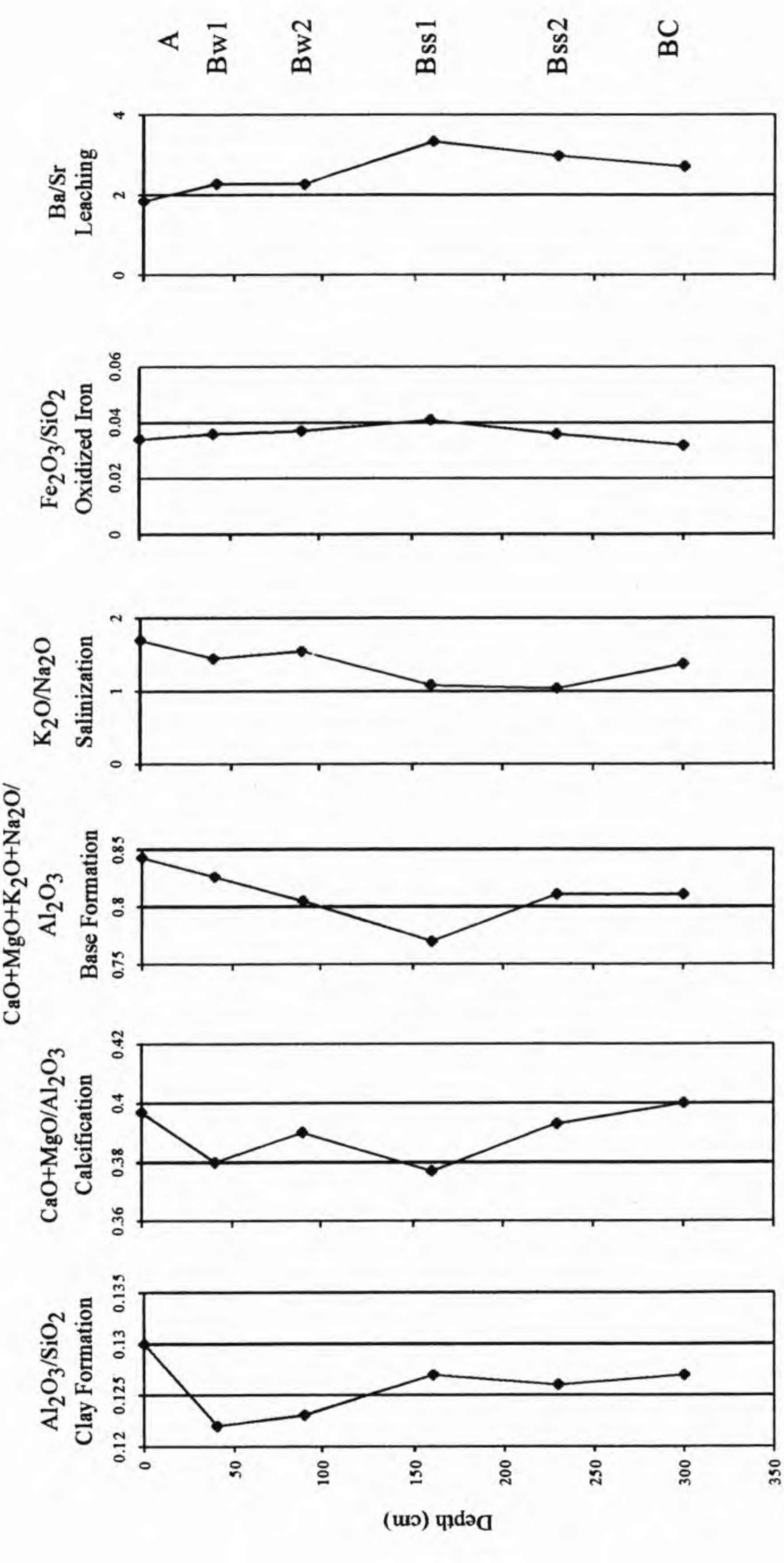
A
Bw1
Bw2
Bss1
Bss2
BC
Ba/Sr
Leaching
Fe2O3/SiO2
Oxidized Iron
K2O/Na2O
Salinization
CaO+MgO+K2O+Na2O/
Al2O3
Base Formation
CaO+MgO/Al2O3
Calcification
Al2O3/SiO2
Clay Formation
Depth (cm)
0
50
100
150
200
250
300
350

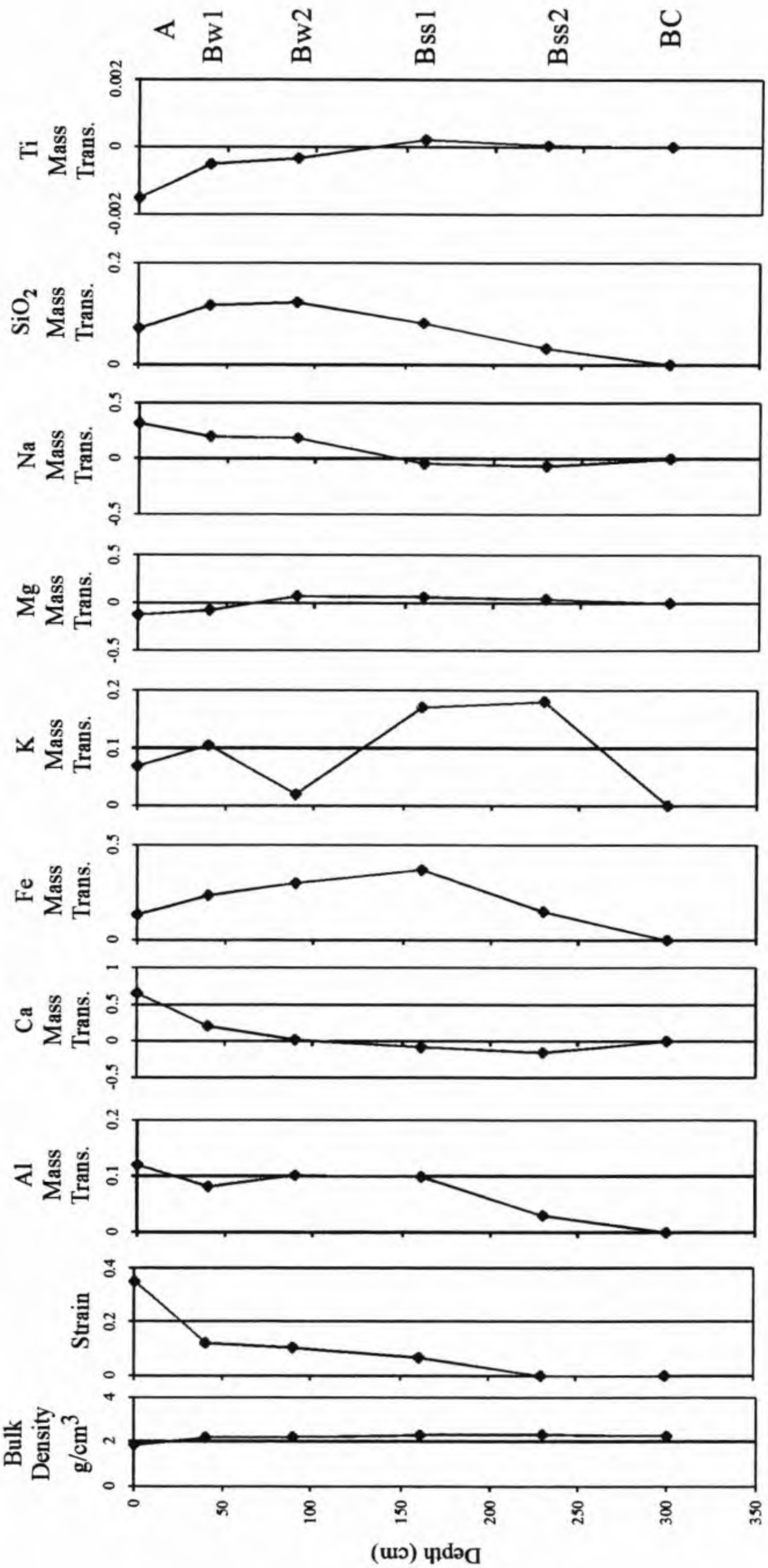
A
Bw1
Bw2
Bss1
Bss2
BC
Ti Mass Trans.
SiO2 Mass Trans.
Na Mass Trans.
Mg Mass Trans.
K Mass Trans.
Fe Mass Trans.
Ca Mass Trans.
Al Mass Trans.
Strain
Bulk Density g/cm3
Depth (cm)
0
50
100
150
200
250
300
350

APPENDIX D

Cow 1 Pedotype

USDA Taxonomic Classification for PS14
Epipedon:
    Ochric
    - Fails to meet definition for any other epipedon.

Endopedon:
    Cambic (no argillic because of lack of evidence for pronounced clay translocation)
    - Texture of very fine sand, loamy very fine sand, or finer
    - Soil structure
    - Alteration in the form of:
        - No evidence of aquic conditions, higher clay content (Bt2) than underlying horizons (BC)
    - No argillic, kandic, oxic, or spodic horizon
    - No cementation or induration
    - A lower depth of 25 cm or more from the mineral soil surface

Order:
    Inceptisol (Cambic horizon)
    - Udept (assuming udic moisture regime)
    - Dystrudept - Meets no other definition for great group
    - Typic Dystrudept – Meets no other definition for subgroup
    - Note- Although a true argillic horizon could not be identified in representative paleosol PS14, it is probable that Cow 1 paleosols represent an integrade between inceptisols and alfisols given the abrupt clay increases between horizons.

Paleosols in Cow 1 Pedotype:
T12PS2 – A-Bt1-Bt2-Bt3-BC-C
PS7 – Scalped-Bt1-Bt2-BC
PS8 – A-Bt-BC1-BC2-C
PS9/10 – A-Bt1-Bt2-BC
PS11 – A1-A2-Bt-C
PS12 – A-Bt-BC-C
PS13 – A1-A2-Bt1-Bt2-BC
PS14 – A-Bt1-Bt2-Bt3-BC-C
PS21 – A1-A2-Bt-BC-C
PS22 – A1-A2-Bt1-Bt2-BC
PS23 – A-Bw-Bt1-Bt2-BC

Characteristics of paleosols in Cow 1 Pedotype:

Cow 1 Paleosols are most common in the low to middle Scollard formation, particularly in coal-free intervals. Cow 1 paleosols are well developed Dystrudepts that border on being classified as Alfisols (Figure 18). Argillans and lack of pedogenic carbonate indicate a humid climate in a well-drained setting.

Geochemistry (absolute values by Retallack, 1997):

- Clay Formation: Absolute values indicate little clay formation has taken place in Cow 1 paleosols. However, weathering ratios do suggest slight increases in clay formation in Bt horizons relative to weathering ratios in the parent material. Mass transport calculations for mobile constituents associated with clays (potassium and aluminum) suggests slight increases in potassium and aluminum in Bt horizons, which is consistent with other indicators of clay translocation, including clay films. Bw horizons do contain a greater percentage of clay than do Bt horizons, but this is likely due to depositional fining-up because of the greater proportion of argillans in Bt horizons.
- Calcification: The relative depth trend for calcification indicates general decrease of calcification in the surface of the profile. Absolute values indicate that little calcification has taken place in the type Cow 1 paleosol. Slight depletion in calcium relative to parent material (mass transport function) provides evidence for slight carbonate removal Cow 1 paleosols.
- Weathering: A relative depth trend indicates a very slight increase in soluble products of hydrolytic weathering with depth. However, absolute values of weathering ratios also indicate little weathering has taken place in Cow 1 paleosols.
- Salinization- Absolute values for salinization are inordinantly large for all paleosols that were investigated. This may be due to excess sodium in feldspar being mistakenly counted as Na_2O in the weathering ratio, which shows a general increase in Na_2O with depth below the surface horizon. The mass transport function indicates that sodium has been leached from upper horizons relative to the parent material, as would be expected in a well drained soil in a humid climate.
- Oxidation- The molecular weathering ratio for ferric iron indicates a slightly higher proportion of oxidized iron in Bt horizons relative to the rest of the profile. The mass transport function also indicates an increase in iron concentration in Bt horizons, possibly associated with the formation of ferriargillans.
- Leaching- Ba/Sr ratios indicate low levels of leaching.
- Organic Carbon- Organic carbon levels peak in the surface horizon of the Cow 1 type paleosol, although the absolute value of organic carbon does not indicate a significant accumulation of organic material.

Paleoclimatic implications:

- No pedogenic carbonate; humid climate with MAP of at least 125 cm (Birkeland, 1999).
- Sepic fabric indicates moderate wet/dry seasonality.
- MAP of approximately 73 cm using the equation of Ready and Retallack (1995) where MAP (mm) = -759(bases/alumina)+1300.
- Argillans indicate drainage and/or seasonality (Retallack, 2001).

Paleobiology:

- Roots typically penetrate 60 cm+ in Cow 1 paleosols, and in some instances into the parent material, indicating many prolonged periods of free drainage.

Paleotopography:

- Clay-rich overbank/floodplain sediments with free drainage.

Time of Formation:

- At least 3,000-5,000 years, estimated from development of cambic horizon, argillans, and well-developed slickensides (Birkeland, 1999).

Raw chemical data for Cow 1 pedotype (PS14)

SAMPLE DESCRIPTION	Ag ppm	Al %	As ppm	Ba ppm	Be ppm	Bi ppm	Ca %	Cd ppm	Co ppm	Cr ppm	Cu ppm	Fe %	K %	Mg %	Mn ppm	Mo ppm	Na %	Ni ppm	P ppm	Pb ppm	S %	Sb ppm	Sr ppm	Ti %	V ppm	W ppm	Zn ppm	SiO2 % fusion
PS14A	0.5	7.36	<5	610	1.5	<2	0.55	<0.5	10	82	32	3.42	1.44	0.69	105	1	1.33	29	70	30	0.03	5	197	0.32	83	<10	74	59.5
PS14Bw	<0.5	6.71	<5	590	1	<2	0.5	<0.5	11	73	19	3.83	1.46	0.67	110	<1	1.24	34	60	28	0.03	<5	175	0.31	106	<10	62	58.4
PS14Bt1	<0.5	6.43	<5	770	0.5	2	0.56	<0.5	11	85	18	4.23	1.57	0.63	115	<1	1.39	35	300	20	0.02	5	189	0.31	110	<10	60	58.8
PS14Bt2	<0.5	6.84	<5	1180	0.5	<2	0.59	<0.5	11	79	18	4.29	1.61	0.65	125	1	1.46	35	370	22	0.03	5	212	0.32	108	<10	68	58.5
PS14BC	<0.5	6.21	<5	780	0.5	2	0.63	<0.5	12	81	23	3.97	1.63	0.6	130	<1	1.56	37	500	20	0.03	<5	197	0.32	98	<10	108	58.4
PS14C	0.5	6.91	<5	890	0.5	<2	0.71	<0.5	13	91	24	4.16	1.71	0.66	155	<1	1.67	42	570	20	0.02	5	245	0.35	103	<10	82	60.6

Major Elements Oxide Mass

Depth (cm)	Al_2O_3	CaO	Fe_2O_3	K_2O	MgO	Na_2O	SiO_2	TiO
0	13.91	0.77	4.89	1.73	1.14	1.79	59.5	0.43
10	12.68	0.7	5.48	1.76	1.11	1.67	58.4	0.41
30	12.16	0.78	6.05	1.89	1.04	1.87	58.8	0.41
40	12.93	0.83	6.14	1.94	1.08	1.97	58.5	0.43
70	11.74	0.88	5.68	1.96	1	2.1	58.4	0.43
80	13.06	0.99	5.95	2.06	1.09	2.25	60.6	0.47

Organic Carbon

Depth	OC %
0	0.47
10	0.27
20	0.23
30	0.13
40	0.26
50	0.21
60	0.2
70	0.19
80	0.2

Strain

Depth	BD	Strain
0	1.72	0.33
10	2.03	0.16
30	2.18	0.08
40	2.18	0.05
70	2.15	0.06
80	2.09	0

Elemental Ratios

Depth (cm)	Al_2O_3/SiO_2	$CaO+MgO/Al_2O_3$	$CaO+MgO+K2O+NaO/Al_2O_3$	Na_2O/K_2O	Fe_2O_3/SiO_2	Ba/Sr
0	0.137	0.309	0.654	1.61	0.031	1.97
10	0.128	0.323	0.694	1.42	0.035	2.15
30	0.121	0.336	0.756	1.5	0.039	2.6
40	0.131	0.331	0.748	1.52	0.039	3.55
70	0.119	0.357	0.835	1.62	0.037	2.52
80	0.127	0.352	0.805	1.64	0.037	2.31

Mass Transport

Depth (cm)	Al	Ca	Fe	K	Mg	Na	SiO_2	Ti
0	0.17	-0.15	-0.1	-0.078	0.14	-0.128	0.075	0.0007
10	0.094	-0.21	0.037	-0.038	0.144	-0.163	0.086	-0.002
30	0.048	-0.11	0.145	0.034	0.075	-0.062	0.093	-0.002
40	0.084	-0.09	0.129	0.031	0.079	-0.043	0.057	0.0013
70	-0.02	-0.032	0.041	0.039	-0.009	0.019	0.051	-0.003
80	0	0	0	0	0	0	0	0

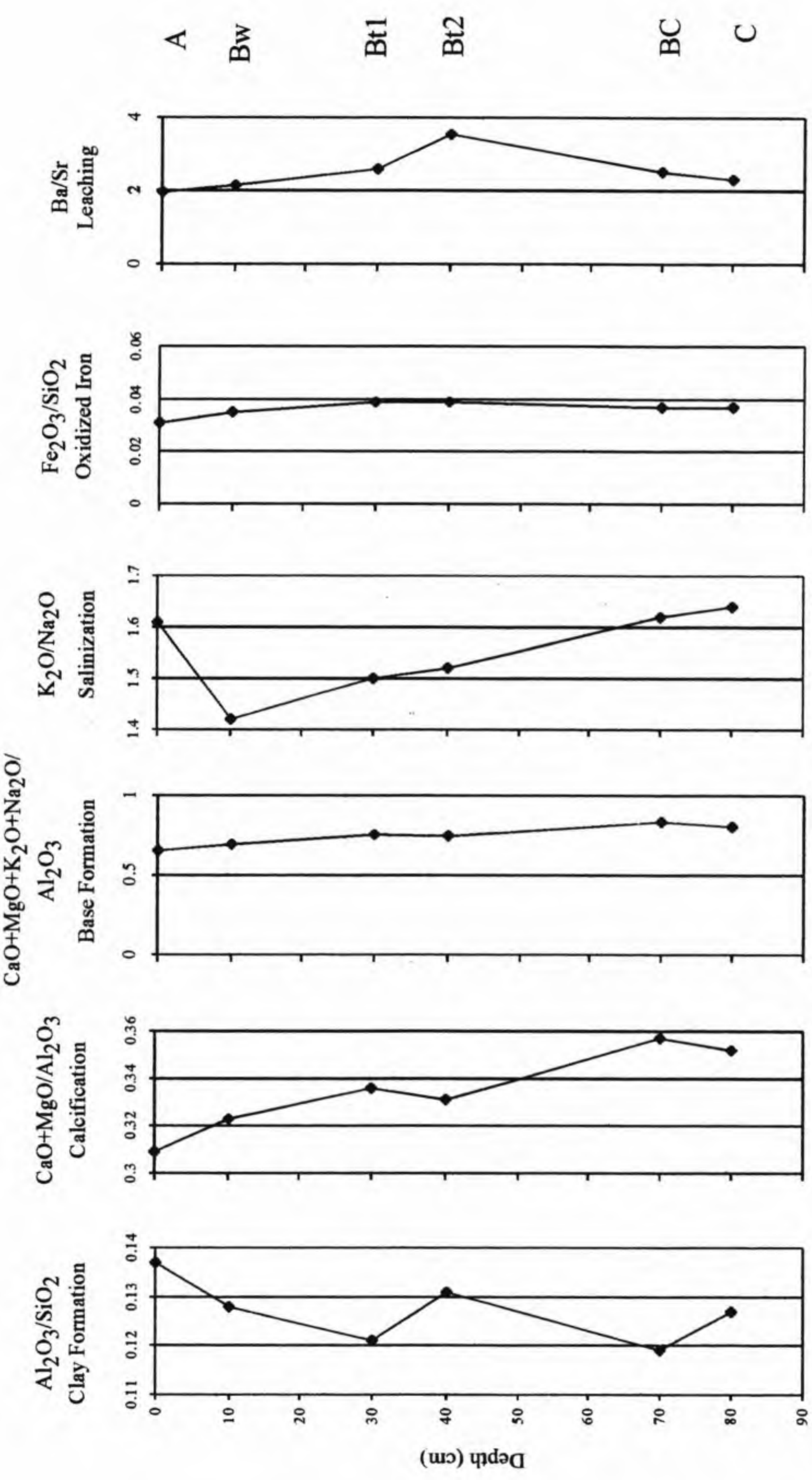

A
Bw
Bt1
Bt2
BC
C
Ba/Sr
Leaching
Fe_2O_3/SiO_2
Oxidized Iron
K_2O/Na_2O
Salinization
$CaO+MgO+K_2O+Na_2O/$
Al_2O_3
Base Formation
$CaO+MgO/Al_2O_3$
Calcification
Al_2O_3/SiO_2
Clay Formation
Depth (cm)

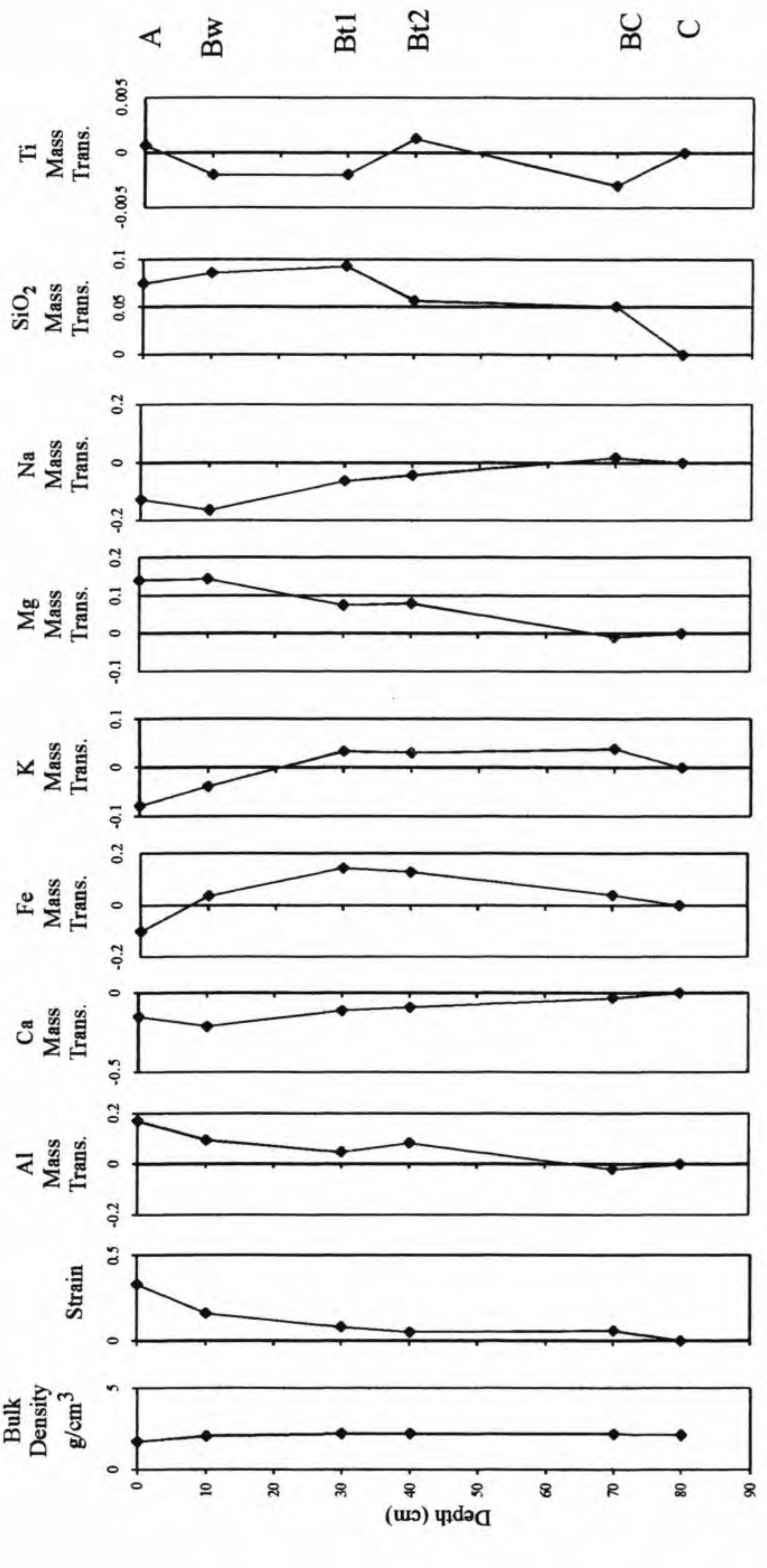
A
Bw
Bt1
Bt2
BC
C
Ti Mass Trans.
SiO2 Mass Trans.
Na Mass Trans.
Mg Mass Trans.
K Mass Trans.
Fe Mass Trans.
Ca Mass Trans.
Al Mass Trans.
Strain
Bulk Density g/cm3
Depth (cm)
0
10
20
30
40
50
60
70
80
90

APPENDIX E

Oreo Pedotype

PS27 Type Paleosol in Oreo Pedotype

OA 0-9 cm; black (N 2.5/) carbonaceous clay; strong very fine/fine angular blocky structure; non-calcareous; few fine black (N 2.5/) root traces and biocasts; porphyroskelic lattisepic microfabric, large biocasts; abrupt smooth boundary (S/Si/C – 9.3/28.3/62.3).

Bg 9-23 cm; light olive gray (5Y 6/2) clay; moderate fine/medium subangular blocky structure; common prominent yellowish red (5YR 5/8) iron oxide stains; non-calcareous; few fine black (N 2.5/) root traces and biocasts; porphyroskelic masepic microfabric; large biocasts/pellets; iron reductions and stains along pores, few argillans along voids; gradual smooth boundary (S/Si/C – 12/33/55).

Btg1 23-35 cm; dark greenish gray (10Y 4/1) clay; moderate medium angular blocky structure; common prominent yellowish red (5YR 5/8) iron oxide stains; non-calcareous; few fine black (N 2.5/) root traces and biocasts; common dark gray (5Y4/1) clay films; porphyroskelic masepic/clinobimasepic microfabric; argillans along voids; Clear smooth boundary (S/Si/C – 3.3/26.3/70).

Btg2 35-48 cm; dark greenish gray (10Y 4/1) clay; moderate medium angular blocky structure; common prominent yellowish red (5YR 5/8) iron oxide stains; non-calcareous; few fine black (N 2.5/) root traces and biocasts; few very dark gray (5Y3/1) clay films; porphyroskelic masepic microfabric; ew argillans along voids; clear smooth boundary (S/Si/C – 3.3/30.6/66).

BC 48 cm+; light olive gray (5Y 6/2) clay; moderate medium/coarse angular blocky structure; common prominent yellowish red (5YR 5/8) iron oxide masses; non-calcareous; few fine black (N 2.5/) root traces and biocasts; porphyroskelic microfabric; faint relict bedding preserved. (S/Si/C – 11/24.3/64.6).

USDA Taxonomic Classification for Type Paleosol PS27

Endopedon:

Ochric

- Fails to meet definition for any other epipedon.

Endopedon:

Argillic

- The argillic horizon (Btg1) has over 8% more clay than the overlying horizon.
- The argillic horizon is at least one tenth the thickness of the entire soil.
- Pronounced, well-developed clay films along surfaces of peds (macro and micro scale).

Order: Alfisol (argillic horizon)

- Aqualf – At least 50% redox depletions (gley) with a chroma of 2 or less in the matrix.
- Ednoaqualf – Meets no other great group definition.
- Typic Endoaqualf – Meets no other subgroup definition.

Paleosols in the Oreo Pedotype:
PS2 – OA-Bg1-Bg2-Btg1-Btg2-C
PS3 – OA1-OA2-Btg-BC
PS4 – A-Bg-Btg1-Btg2-C
PS5 – OA-Btg1-Btg2-Btg3-BC-C
PS6 – OA-Bg-Bt1-Bt2-C
PS27 – OA-Bg-Btg1-Btg2-BC
PS30 – O/A1-OA2-Bt-BC

Characteristics of paleosols in the Oreo pedotype:

Paleosols in the Oreo pedotype are well developed aquic alfisols that generally occur in intervals of transition from poorly drained conditions to moderate or well-drained conditions (Figure 19). Oreo paleosols do show evidence of periodic drainage, including argillans along voids and ped faces and roots that penetrate into subsurface horizons (50 cm+). Oreo paleosols also have gleyed subsurface horizons and thin surficial horizons that are organic-rich. Oreo paleosols are similar to Gloom paleosols, but have a better-developed history of drainage.

Geochemistry (absolute values by Retallack, 1997):

- Clay Formation: Absolute values indicate that little clay formation has taken place in Oreo paleosols. Use of the mass transport function for mobile constituents associated with clays (potassium and aluminum) indicates that these mobile constituents have been lost from upper horizons and transported downward in the profile. This may be evidence for pre-inundation or periodic lessivage.
- Calcification: Absolute values indicate very little calcification has taken place in Oreo paleosols, with a slight trend indicating a decrease in calcification towards the soil surface. The mass transport function indicates a slight increase in calcium concentration in the organic surface horizon as well as calcium removal in horizons of clay accumulation.
- Weathering: Soluble products of hydrolytic weathering do not follow a specific trend in Oreo paleosols. Absolute values of weathering ratios indicate little weathering has taken place in Oreo paleosols.
- Salinization- Absolute values for salinization are inordinantly large for all paleosols that were investigated. This may be due to excess sodium weathering from feldspar in surface horizons being mistakenly counted as Na_2O in the weathering ratio. The mass transport function does not provide any reasonable trends in sodium loss or accumulation.
- Oxidation- The molecular weathering ratio for ferric iron indicates the iron oxide occurs in greatest abundance in both the surface horizon and illuviated

clay horizons of the type paleosol. The mass transport function indicates a similar trend, which may be related to iron in translocated clays.
- Leaching- Ba/Sr ratios indicate little leaching.
- Organic Carbon- Organic carbon levels peak in the surface horizon of the type Oreo paleosol. Input of organic matter is the probable cause of positive strain (dilation) in the surface horizons.

Paleoclimatic implications-
- No pedogenic carbonate, either because of lack of development or because of MAP of at least 125-150 cm (Birkeland, 1999).
- MAP of approximately 72 cm using the equation of Ready and Retallack (1995) where MAP (mm) = -759(bases/alumina)+1300.
- Gley features indicate either poor drainage overprint over previous well-drained conditions, or seasonal flooding. While MAP is similar to Cow 1 paleosols, Oreo paleosols may not have been as well drained
- Sepic fabric indicates wet/dry seasonality.
- Argillans indicate drainage and/or seasonality such that clay could be moved through the profile (Retallack, 2001)

Paleobiology:
- Fine roots penetrate nearly 50 cm (up to 75% of soil thickness) into Oreo paleosols, indicating either wet/dry seasonality or a pre-inundation history.

Paleotopography:
- Flat, seasonally flooded overbank plain.

Parent Material:
- Clay-rich overbank/floodplain sediments.

Time for Formation:
- At least 5,000 years, based on argillic/alfisol development (Birkeland, 1999). Paleosols without a true argillic horizon are likely younger.

Raw chemical data for Oreo pedotype (PS27)

SAMPLE DESCRIPTION	Ag ppm	Al %	As ppm	Ba ppm	Be ppm	Bi ppm	Ca %	Cd ppm	Co ppm	Cr ppm	Cu ppm	Fe %	K %	Mg %	Mn ppm	Mo ppm	Na %	Ni ppm	P ppm	Pb ppm	S %	Sb ppm	Sr ppm	Ti %	V ppm	W ppm	Zn ppm	SiO_2% fusion
PS27O/A	0.5	7.01	<5	350	1.5	<2	0.63	<0.5	4	48	20	2.82	0.85	0.6	150	3	1.33	15	40	32	0.04	<5	170	0.26	67	<10	54	54.2
PS27Bg	<0.5	6.58	<5	570	1	<2	0.64	<0.5	6	66	16	2.3	1.13	0.55	70	<1	1.49	18	40	28	0.03	<5	223	0.26	53	<10	46	64.7
PS27Btg1	<0.5	6.46	<5	560	1.5	2	0.55	<0.5	22	64	17	3.42	1.46	0.65	65	<1	1.46	73	100	24	0.05	<5	194	0.3	88	<10	60	59.8
PS27Btg2	<0.5	6.68	<5	420	2	2	0.53	<0.5	13	64	19	3.51	1.13	0.72	70	<1	1.24	43	80	20	0.03	5	184	0.25	81	<10	68	54.5
PS27BC	<0.5	6.35	<5	1040	1.5	2	0.63	<0.5	18	74	19	3.17	1.26	0.65	80	1	1.4	43	280	26	0.04	<5	211	0.28	82	<10	70	56.5

Major Elements Oxide Mass

Depth (cm)	Al_2O_3	CaO	Fe_2O_3	K_2O	MgO	Na_2O	SiO_2	TiO
0	13.25	0.88	4.03	1.02	1	1.79	54.2	0.35
10	12.44	0.9	3.29	1.36	0.91	2.01	64.7	0.35
30	12.21	0.77	4.89	1.76	1.08	1.97	59.8	0.4
40	12.63	0.74	5.02	1.36	1.19	1.67	54.5	0.33
50	12	0.88	4.34	1.52	1.08	1.89	56.5	0.37

Organic Carbon

Depth (cm)	OC %
0	0.31
10	0.22
20	0.18
30	0.17
40	0.23
50	0.24

Strain

Depth	BD	Strain
0	2.07	0.087
10	2.19	0.028
30	2.14	-0.088
40	2.13	0.099
50	2.09	0

Elemental Ratios

Depth (cm)	Al_2O_3/SiO_2	$CaO+MgO/Al_2O_3$	$CaO+MgO+K2O+NaO/Al_2O_3$	Na_2O/K_2O	Fe_2O_3/SiO_2	Ba/Sr
0	0.144	0.315	0.623	2.64	0.028	1.31
10	0.113	0.32	0.697	2.29	0.019	1.63
30	0.121	0.34	0.767	1.68	0.031	1.85
40	0.137	0.347	0.677	1.93	0.034	1.46
50	0.126	0.364	0.754	1.88	0.029	3.14

Mass Transport

Depth (cm)	Al	Ca	Fe	K	Mg	Na	SiO_2	Ti
0	0.19	0.077	-0.042	-0.27	-0.006	0.023	0.033	-0.0003
10	0.116	0.094	-0.22	-0.034	-0.089	0.146	0.234	0.0002
30	-0.05	-0.185	0.0075	0.082	-0.066	-0.026	-0.0116	0.0005
40	0.18	-0.058	0.24	0.0045	0.24	-0.008	0.08	0.00003
50	0	0	0	0	0	0	0	0

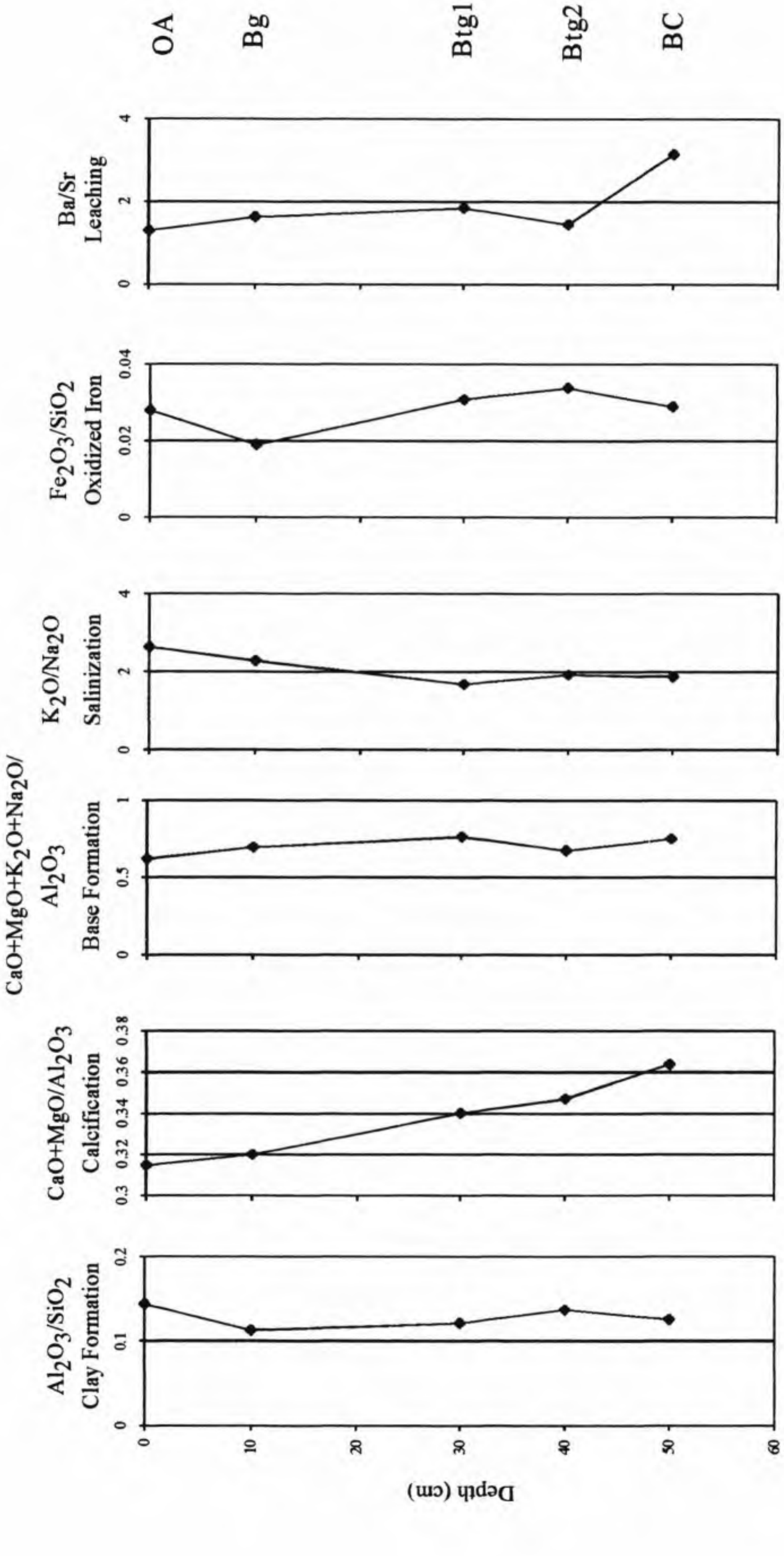
OA
Bg
Btg1
Btg2
BC
Ba/Sr
Leaching
Fe_2O_3/SiO_2
Oxidized Iron
K_2O/Na_2O
Salinization
$CaO+MgO+K_2O+Na_2O/$
Al_2O_3
Base Formation
$CaO+MgO/Al_2O_3$
Calcification
Al_2O_3/SiO_2
Clay Formation
Depth (cm)

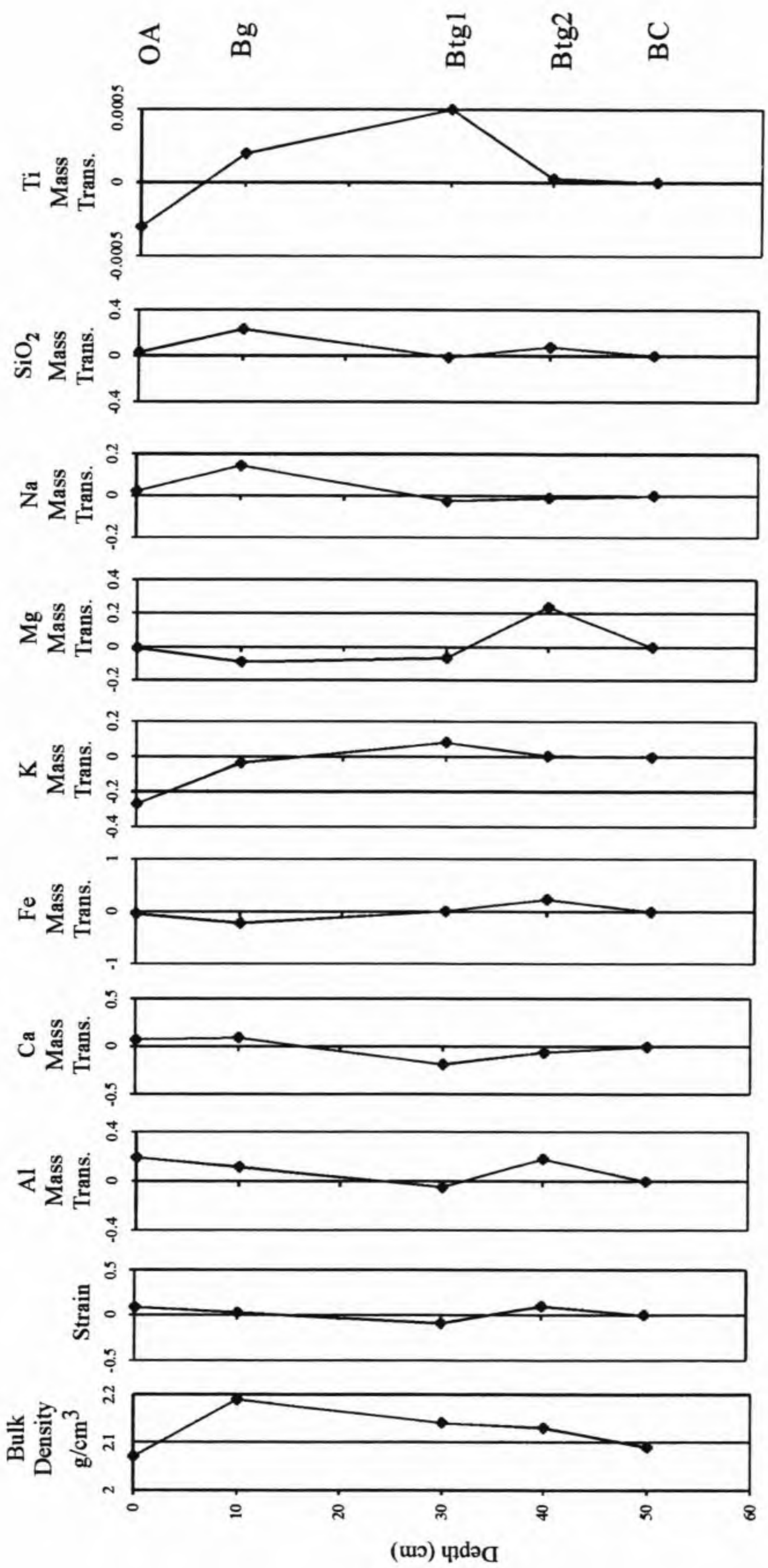
OA
Bg
Btg1
Btg2
BC
Ti Mass Trans.
SiO2 Mass Trans.
Na Mass Trans.
Mg Mass Trans.
K Mass Trans.
Fe Mass Trans.
Ca Mass Trans.
Al Mass Trans.
Strain
Bulk Density g/cm3
0
10
20
30
40
50
60
Depth (cm)

APPENDIX F

Cow 2 Pedotype

PS15 Type Clay Paleosol for Cow 2 Pedotype

A 0-23 cm; black (5Y 2.5/1) clay; moderate fine/medium angular blocky structure; common prominent strong brown (7.5YR 5/6) iron oxide stains; many fine black (N 2.5/) root traces; non-calcareous; porphyroskelic insepic/skelesepic microfabric, common root traces and biocasts/pellets; clear smooth boundary (S/Si/C – 15.3/35.3/49.3).

Bw 23-45 cm; pale olive (5Y 6/3) clay; strong coarse subangular blocky structure; common prominent yellowish red (5YR 5/8) iron oxide stains. Many fine black (N 2.5/) root traces; non-calcareous; porphyroskelic insepic/skelesepic microfabric, common root traces and biocasts/pellets; clear smooth boundary (S/Si/C – 30.3/19.6/50).

Bt1 45-57 cm; very dark gray (5Y 3/1) clay; moderate coarse subangular blocky structure; common prominent yellowish red (5YR 5/8) iron oxide stains; common fine black (N 2.5/) root traces; few light yellowish brown (2.5Y 6/4) clay films; non-calcareous; porphyroskelic patchy insepic/masepic microfabric; few argillans along voids and transported into matrix; clear smooth boundary (S/Si/C – 7.6/22.3/70).

Bt2 57-100 cm; olive gray (5Y 4/2) clay; moderate medium/coarse subangular blocky structure; common prominent yellowish red (5YR 4/6) iron oxide stains; few fine black (N 2.5/) root traces; few light yellowish brown (2.5Y 6/4) clay films; non-calcareous; porphyroskelic masepic microfabric; few argillans along voids walls; clear smooth boundary (S/Si/C – 24/22.6/50.3).

BC 100-120 cm; pale olive (5Y 6/3) clay; moderate coarse subangular blocky structure; few prominent yellowish red (5YR 5/8) iron oxide stains. Very few fine black (N 2.5/) root traces; non-calcareous; agglomeroplasmic patchy insepic microfabric with depositional stratification present; few oxide pore linings (S/Si/C – 24.6/24.6/50.6).

USDA Taxonomic Classification for PS15
Epipedon:

Ochric

- Fails to meet definition for any other epipedon.

Endopedon:

Argillic

- The argillic horizon (Bt1) has over 8% more clay than the overlying horizon (Bw).
- The argillic horizon is at least one tenth the thickness of the entire soil.

- Clay films along surfaces of peds.

Order: Alfisol (argillic horizon)

- Udualf – Meets no other suborder definition.
- Hapludalf – Meets no other great group definition.
- Typic Hapludalf – Meets no other subgroup definition.

Paleosols in Cow 2 Pedotype:
PS15 – A-Bw-Bt1-Bt2-BC
PS19 – A-Bw-Bt1-Bt2-Bt3-BC

Characteristics of paleosols in Cow 2 pedotype:

Cow 2 Paleosols are most common in the middle Scollard formation and are associated with seasonally drained vertisols and inceptisols of the Cow 1 pedotype (Figure 20). Cow 2 paleosols are moderately developed Alfisols with true argillic horizons. Abundant argillans and lack of pedogenic carbonate indicate a humid climate in a well-drained setting. Cow 2 paleosols are morphologically similar to Cow 1 paleosols, but are better developed.

Geochemistry (absolute values by Retallack, 1997):

- Clay Formation: Absolute values indicate little clay formation has taken place in Cow 2 paleosols. However, weathering ratios do suggest slight increases in clay formation near the surface of the paleosol. Mass transport calculations for mobile constituents associated with clays (potassium and aluminum) suggests that slight increases in potassium and aluminum in Bt horizons, which is consistent with other indicators of clay translocation, including clay films.
- Calcification: The relative depth trend for calcification indicates s general increase in calcification with depth. However, absolute values indicate that little true calcification has taken place in the type Cow 2 paleosol. Use of mass transport calculations for calcification does not reveal a clear trend in gains or losses through the profile.
- Weathering: A relative depth trend indicates a very slight increase in soluble products of hydrolytic weathering with depth. However, absolute values of weathering ratios indicate little true weathering has taken place in Cow 2 paleosols.
- Salinization- Absolute values for salinization are inordinantly large for all paleosols that were investigated. This may be due to excess sodium in feldspar being mistakenly counted as Na_2O in the weathering ratio. The mass transport function does not indicate a clear trend in sodium gains or losses in the profile.
- Oxidation- The molecular weathering ratio for ferric iron indicates nearly constant concentrations of oxidized iron in the profile. The mass transport function also indicates little variability in iron gains and losses relative to the parent material. If reducing conditions never existed during pedogenesis, then

it would follow that iron would not have been mobilized and moved through the profile.
- Leaching- Ba/Sr ratios indicate little leaching.
- Organic Carbon- As expected, organic carbon levels peak in the surface horizon of the Cow 2 type paleosol, although the absolute value of organic carbon indicates a greater amount and depth of accumulation of organic material as compared with Cow1 paleosols.

Paleoclimatic implications-
- No pedogenic carbonate; MAP of at least 125-150 cm (Birkeland,
- 1999).
- Sepic fabric indicates moderate wet/dry seasonality.
- Argillans/Argillic indicate drainage and/or seasonality (Retallack, 2001).
- MAP of approximately 72cm using the equation of Ready and Retallack (1995) where MAP (mm) = -759(bases/alumina)+1300.

Paleobiology:
- Roots penetrate in excess of 1 meter in Cow 2 paleosols, in some instances into the parent material, indicating periods of free drainage.

Paleotopography:
- Clay-rich overbank/floodplain sediments with free drainage.

Time of Formation:
- At least 5,000 years, possibly 10,000 years; estimated from development of true argillic horizon (Birkeland, 1999).

Raw chemical data for Cow 2 pedotype (PS15)

SAMPLE DESCRIPTION	Ag ppm	Al %	As ppm	Ba ppm	Be ppm	Bi ppm	Ca %	Cd ppm	Co ppm	Cr ppm	Cu ppm	Fe %	K %	Mg %	Mn ppm	Mo ppm	Na %	Ni ppm	P ppm	Pb ppm	S %	Sb ppm	Sr ppm	Ti %	V ppm	W ppm	Zn ppm	SiO_2 % fusion
PS15A	<0.5	6.65	<5	660	1.5	<2	0.47	<0.5	15	94	45	3.22	1.78	0.62	85	2	1.37	36	150	18	0.04	5	176	0.34	115	<10	78	60
PS15Bw	<0.5	7.3	5	820	1	<2	0.59	<0.5	16	83	29	3.92	1.71	0.7	140	<1	1.5	46	230	24	0.04	5	226	0.34	114	<10	118	59.5
PS15Bt1	<0.5	6.3	<5	660	0.5	<2	0.47	<0.5	12	81	39	3.54	1.63	0.73	130	1	1.23	46	420	20	0.03	<5	168	0.33	118	<10	92	59.6
PS15Bt2	<0.5	6.48	<5	670	1.5	<2	0.79	<0.5	16	87	42	3.81	1.86	0.74	160	<1	1.5	52	1080	22	0.03	5	209	0.34	111	<10	108	59.5
PS15BC	<0.5	6.34	<5	650	0.5	<2	0.59	<0.5	14	91	34	3.73	1.65	0.84	175	<1	1.36	51	690	24	0.02	5	181	0.35	119	<10	88	57.8

Major Elements Oxide Mass

Depth (cm)	Al_2O_3	CaO	Fe_2O_3	K_2O	MgO	Na_2O	SiO_2	TiO
0	12.57	0.66	4.61	2.14	1.03	1.85	60	0.45
30	13.8	0.83	5.61	2.06	1.16	2.02	59.5	0.45
50	11.91	0.66	5.06	1.96	1.21	1.66	59.6	0.44
70	12.25	1.1	5.45	2.24	1.23	2.02	59.5	0.45
120	11.98	0.83	5.34	1.99	1.39	1.83	57.8	0.47

Organic Carbon

Depth (cm)	OC %
0	1.4
10	1.41
20	1.24
30	0.36
40	0.31
50	0.33
60	0.42
70	0.37
80	0.39
90	0.27
100	0.28
110	0.32
120	0.35
130	0.3

Strain

Depth	BD	Strain
0	2.09	0.1
30	2.21	0.04
50	2.26	0.04
70	2.28	0.008
120	2.2	0

Elemental Ratios

Depth (cm)	Al_2O_3/SiO_2	$CaO+MgO/Al_2O_3$	$CaO+MgO+K2O+NaO/Al_2O_3$	Na_2O/K_2O	Fe_2O_3/SiO_2	Ba/Sr
0	0.123	0.309	0.74	1.3	0.029	2.39
30	0.136	0.326	0.73	1.5	0.035	2.31
50	0.118	0.359	0.769	1.29	0.032	2.51
70	0.121	0.425	0.9	1.38	0.034	2.04
120	0.122	0.419	0.855	1.43	0.034	2.29

Mass Transport

Depth (cm)	Al	Ca	Fe	K	Mg	Na	SiO_2	Ti
0	0.096	-0.17	-0.098	0.13	-0.23	0.053	0.085	0.015
30	0.2	0.045	0.098	0.083	-0.13	0.15	0.075	0.015
50	0.062	-0.15	0.014	0.055	-0.072	-0.034	0.1	0.0073
70	0.068	0.4	0.067	0.18	-0.08	0.15	0.075	0.015
120	0	0	0	0	0	0	0	0

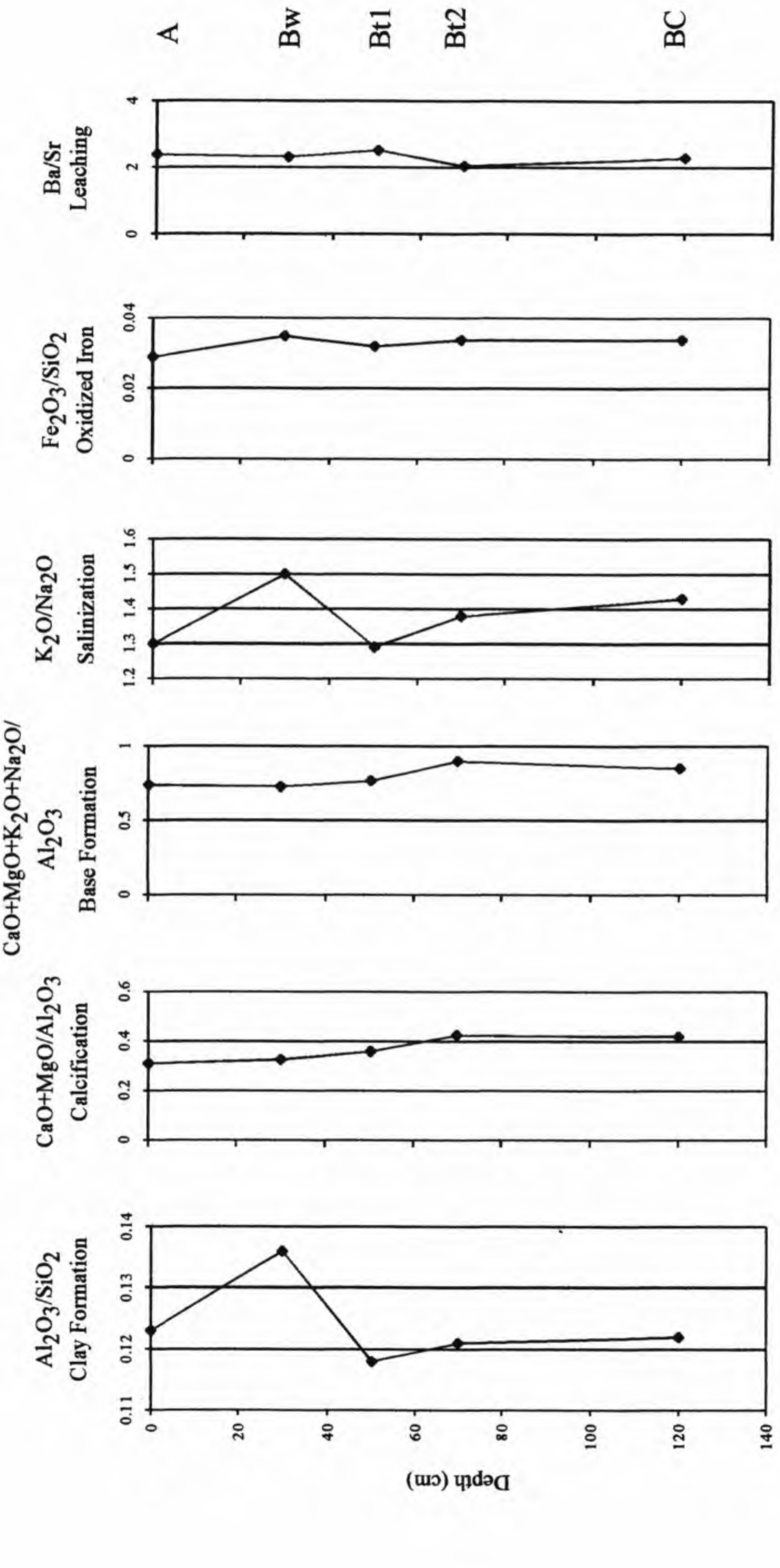
A
Bw
Bt1
Bt2
BC
Ba/Sr
Leaching
Fe2O3/SiO2
Oxidized Iron
K2O/Na2O
Salinization
CaO+MgO+K2O+Na2O/
Al2O3
Base Formation
CaO+MgO/Al2O3
Calcification
Al2O3/SiO2
Clay Formation
Depth (cm)

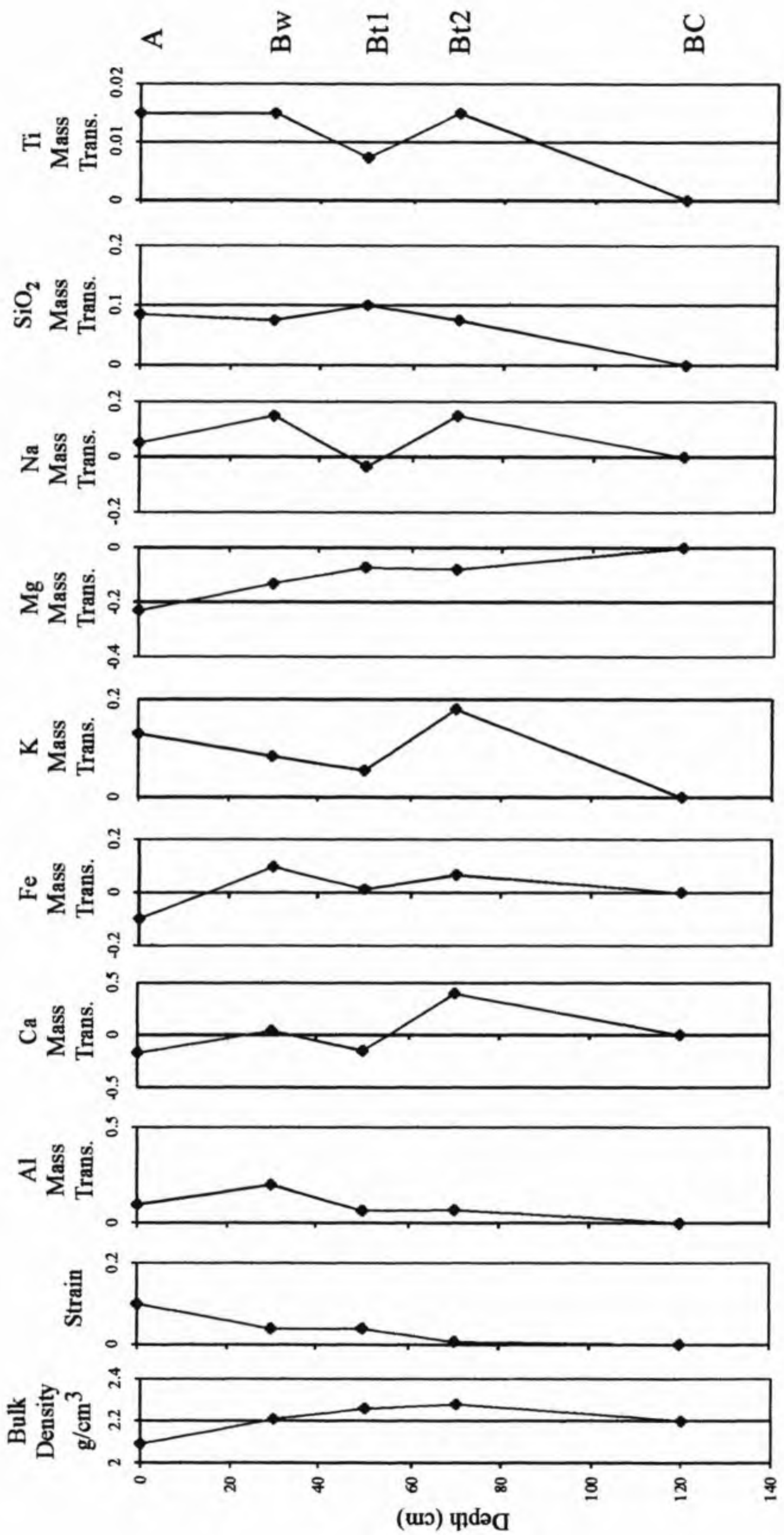
A
Bw
Bt1
Bt2
BC
Ti Mass Trans.
SiO2 Mass Trans.
Na Mass Trans.
Mg Mass Trans.
K Mass Trans.
Fe Mass Trans.
Ca Mass Trans.
Al Mass Trans.
Strain
Bulk Density g/cm3
Depth (cm)
0
20
40
60
80
100
120
140

APPENDIX G

Ramp Pedotype

PS25 Type Clay Paleosol for Ramp Pedotype

A 0-12 cm; dark gray (5Y 4/1) clay; moderate medium angular blocky structure; common prominent yellowish red (5YR 4/6) iron oxide stains; common fine black (N 2.5/) root traces and biocasts; non-calcareous; porphyroskelic insepic microfabric; common root traces and biocasts/pellets; clear smooth boundary (S/Si/C 3/27.6/69.3).

Bss1 12-22 cm; gray (5Y 5/1) clay; moderate fine wedge structure; common prominent red (2.5YR 5/8) iron oxide stains; few fine black (N 2.5/) root traces and biocasts, common masticated organic material; non-calcareous; porphyroskelic insepic microfabric; few root traces and biocasts/pellets, iron oxide hypocoats on peds; clear smooth boundary (S/Si/C 2.6/25.3/72).

Bss2 22-53 cm; gray (5Y 5/1) clay; strong medium wedge structure; common prominent yellowish red (5YR 5/8) iron oxide stains; few fine black (N 2.5/) root traces and biocasts; non-calcareous; porphyroskelic insepic microfabric; few root traces and biocasts/pellets; iron depletions along void walls, iron oxide hypocoats on peds; clear smooth boundary (S/Si/C 2.6/35.3/72).

Bss3 53-120 cm; dark gray (5Y 4/1) clay; moderate coarse angular blocky structure; common prominent reddish brown (2.5YR 4/4) iron oxide stains; very few fine black (N 2.5/) root traces and biocasts; non-calcareous. porphyroskelic insepic microfabric; few root traces and biocasts/pellets; iron depletions along void walls, iron oxide hypocoats on peds; clear smooth boundary (S/Si/C 2/27.3/70.6).

BC 120-135 cm; very dark gray (5Y 3/1) clay; moderate coarse subangular blocky structure; common distinct olive (5Y 5/6) oxide stains; very few fine black (N 2.5/) root traces and biocasts; non-calcareous; porphyroskelic argillasepic microfabric; iron depletions along voids, few thin oriented clay films on ped surfaces; clear smooth boundary (S/Si/C 10.6/27.3/62).

C 135 cm+; pale olive (5Y 6/3) clay; weak coarse subangular blocky structure; common prominent strong brown (7.5YR 5/8) iron oxide stains; non-calcareous; agglomeroplasmic microfabric. (S/Si/C 29/27/44)

USDA Taxonomic Classification for Type Paleosol PS25:
Epipedon:

Ochric

- Fails to meet definition for any other epipedon.

Endopedon:

Cambic

- Texture of vf sand, loamy vf sand, or finer
- Soil structure, roots
- Evidence of alteration in the form of:
    - o Higher clay content (Bss3) than underlying horizons (BC)
- No argillic, kandic, oxic, or spodic horizon
- No cementation or induration, a lower depth of 25 cm or more from the mineral soil surface

Order:

Vertisol (A layer 25 cm+ thick with upper boundary within 100 cm of the soil surface having intersecting slickensides, over 30% clay in the soil, cracks-implied)

- Udert – Meets no other definition for suborders, no evidence for ustic conditions (no carbonate).
- Hapludert (if pH was 4.5 or more), Dystrudert (if pH is 4.5 or less)
- Typic Dystrudert- Meets no other definition for subgroup.

Paleosols in the Ramp Pedotype:
PS20 – A-Bss1-Bss2-Bss3-C
PS24 – A1-A2-Bss1-Bss2-BC
PS25 – A-Bss1-Bss2-Bss3-BC-C

Characteristics of paleosols in the Ramp pedotype:

Ramp paleosols are all moderately developed Vertisols that occur in the upper Scollard Formation above a series of moderately developed Alfisols and below a series of Histosols and gleyed Inceptisols (Figure 17). Slickensides in Ramp paleosols indicate pronounced wet/dry seasonality, although lack of carbonate suggests that the climate was humid. Ramp paleosols likely formed on clay-rich parent material due to a lack of evidence for in-situ clay formation. Occurrence of primary weatherable minerals such as mica in thin section also suggest pedogenic immaturity for Ramp paleosols.

Geochemistry (absolute values by Retallack, 1997):

- Clay Formation: Absolute values indicate little or no clay formation has taken place in Ramp paleosols. Use of the mass transport function for mobile constituents associated with clays (potassium and aluminum) does not suggest that lessivage has occurred.
- Calcification: Absolute values indicate little or no calcification has taken place in Ramp paleosols. Slight depletion in calcium relative to parent material (mass transport function) provides evidence for slight carbonate removal Ramp paleosols.
- Weathering: No true depth trend was established for soluble products of hydrolytic weathering in Ramp paleosols. Absolute values of weathering ratios indicate little weathering has taken place in Ramp paleosols.
- Salinization- Absolute values for salinization are inordinantly large for all paleosols that were investigated. This may be due to excess sodium in

feldspar being mistakenly counted as Na_2O in the weathering ratio. The mass transport function indicates that sodium has been leached from upper horizons relative to the parent material, as would be expected in a seasonally wet soil.
- Oxidation- The molecular weathering ratio for ferric iron is not indicative of a recognizable depth trend. The mass transport function also indicates that there is slightly more iron in upper horizons than in the parent material. While this may be a function of oxidation of iron during dry season in the surface horizons, it may also be true that there is a greater density of iron-rich clays in the upper horizons relative to the parent material.
- Leaching- Ba/Sr ratios indicate that Ramp paleosols were moderately leached.
- Organic Carbon- Organic carbon levels peak in the surface horizon of the type Ramp paleosol, although the absolute value of organic carbon does not indicate a significant accumulation of organic material, either because Ramp paleosols are not well developed or because surficial conditions were not conducive to organic matter preservation. Input of organic matter is the probable cause of positive strain (dilation) in the surface horizons.

Paleoclimatic implications:
- No pedogenic carbonate, either because of lack of development or because of MAP of at least 50-60cm (Birkeland, 1999).
- Sepic fabric and iron depletions along voids are indicative of moderate wet/dry seasonality.
- Bss indicates pronounced wet/dry seasonality (Retallack, 2001).

Paleobiology:
- Fine roots penetrate over 1 meter into Ramp paleosols, indicating fluctuation of water table, possibly associated with seasonality.

Paleotopography:
- Flat, seasonally wet overbank plain

Parent Material:
- Clay-rich overbank/floodplain sediments.

Time of Formation:
- At least 1,000 years, estimated from development of cambic horizon and slickensides (Birkeland, 1999).

Raw chemical data for Ramp pedotype (PS25)

SAMPLE DESCRIPTION	Ag ppm	Al %	As ppm	Ba ppm	Be ppm	Bi ppm	Ca %	Cd ppm	Co ppm	Cr ppm	Cu ppm	Fe %	K %	Mg %	Mn ppm	Mo ppm	Na %	Ni ppm	P ppm	Pb ppm	S %	Sb ppm	Sr ppm	Ti %	V ppm	W ppm	Zn ppm	SiO_2 % fusion
PS25A	<0.5	6.81	<5	670	1.5	2	0.36	0.5	13	86	58	3.62	2.01	0.87	140	<1	1	54	410	24	0.04	<5	132	0.34	162	<10	116	56.2
PS25Bss1	<0.5	6.64	<5	650	1	<2	0.37	<0.5	12	87	47	4.17	2.02	0.85	140	<1	1.03	53	410	20	0.03	<5	126	0.35	164	<10	106	58
PS25Bss2	<0.5	6.55	<5	910	1	<2	0.38	0.5	14	97	62	4.08	1.94	0.81	145	1	1.13	57	410	22	0.04	<5	144	0.38	161	<10	112	58.6
PS25Bss3	0.5	6.65	<5	620	1	<2	0.32	<0.5	11	96	49	3.63	1.93	0.69	100	<1	1.01	41	170	18	0.03	<5	125	0.36	148	<10	100	58.2
PS25BC	0.5	6.91	<5	770	1	<2	0.36	<0.5	21	112	45	4.09	1.98	0.77	145	<1	1.18	62	250	20	0.04	<5	138	0.39	155	<10	94	59.1
PS25C	<0.5	7.38	5	840	1	<2	0.47	<0.5	23	117	35	3.84	1.89	0.85	175	2	1.35	80	460	16	0.04	5	173	0.38	140	<10	116	60.2

Major Elements Oxide Mass

Depth (cm)	Al_2O_3	CaO	Fe_2O_3	K_2O	MgO	Na_2O	SiO_2	TiO
10	12.87	0.5	5.18	2.42	1.44	1.35	56.2	0.45
20	12.55	0.52	5.97	2.43	1.41	1.39	58	0.47
40	12.38	0.53	5.84	2.34	1.34	1.52	58.6	0.51
90	12.57	0.45	5.19	2.33	1.14	1.36	58.2	0.48
130	13.06	0.5	5.85	2.39	1.28	1.59	59.1	0.52
140	13.95	0.66	5.49	2.28	1.41	1.82	60.2	0.51

Organic Carbon

Depth (cm)	OC %
10	1.03
20	0.62
30	0.68
40	0.73
50	0.67
60	0.63
70	0.68
80	0.77
90	0.66
100	0.71
110	0.68
120	0.59
130	0.51
140	0.46

Strain

Depth	BD	Strain
10	2.18	0.11
20	2.22	0.06
40	2.2	-0.014
90	2.24	0.023
130	2.19	0.035
140	2.17	0

Elemental Ratios

Depth (cm)	Al_2O_3/SiO_2	$CaO+MgO/Al_2O_3$	$CaO+MgO+K_2O+NaO/Al_2O_3$	Na_2O/K_2O	Fe_2O_3/SiO_2	Ba/Sr
10	0.135	0.357	0.738	0.85	0.034	3.23
20	0.127	0.358	0.748	0.85	0.038	3.28
40	0.124	0.347	0.76	1	0.038	4.04
90	0.127	0.293	0.675	0.88	0.033	3.16
130	0.13	0.32	0.719	1.04	0.038	3.57
140	0.137	0.343	0.73	1.21	0.034	3.11

Mass Transport

Depth (cm)	Al	Ca	Fe	K	Mg	Na	SiO_2	Ti
10	0.029	-0.146	0.051	0.186	0.141	-0.174	0.041	-0.0023
20	-0.024	-0.146	0.178	0.159	0.084	-0.173	0.045	-0.0012
40	-0.113	-0.192	0.062	0.026	-0.047	-0.163	-0.027	-0.0004
90	-0.048	-0.281	-0.00175	0.078	-0.143	-0.21	0.021	0.0004
130	-0.022	-0.2	0.113	0.094	-0.054	-0.087	0.025	0.072
140	0	0	0	0	0	0	0	0

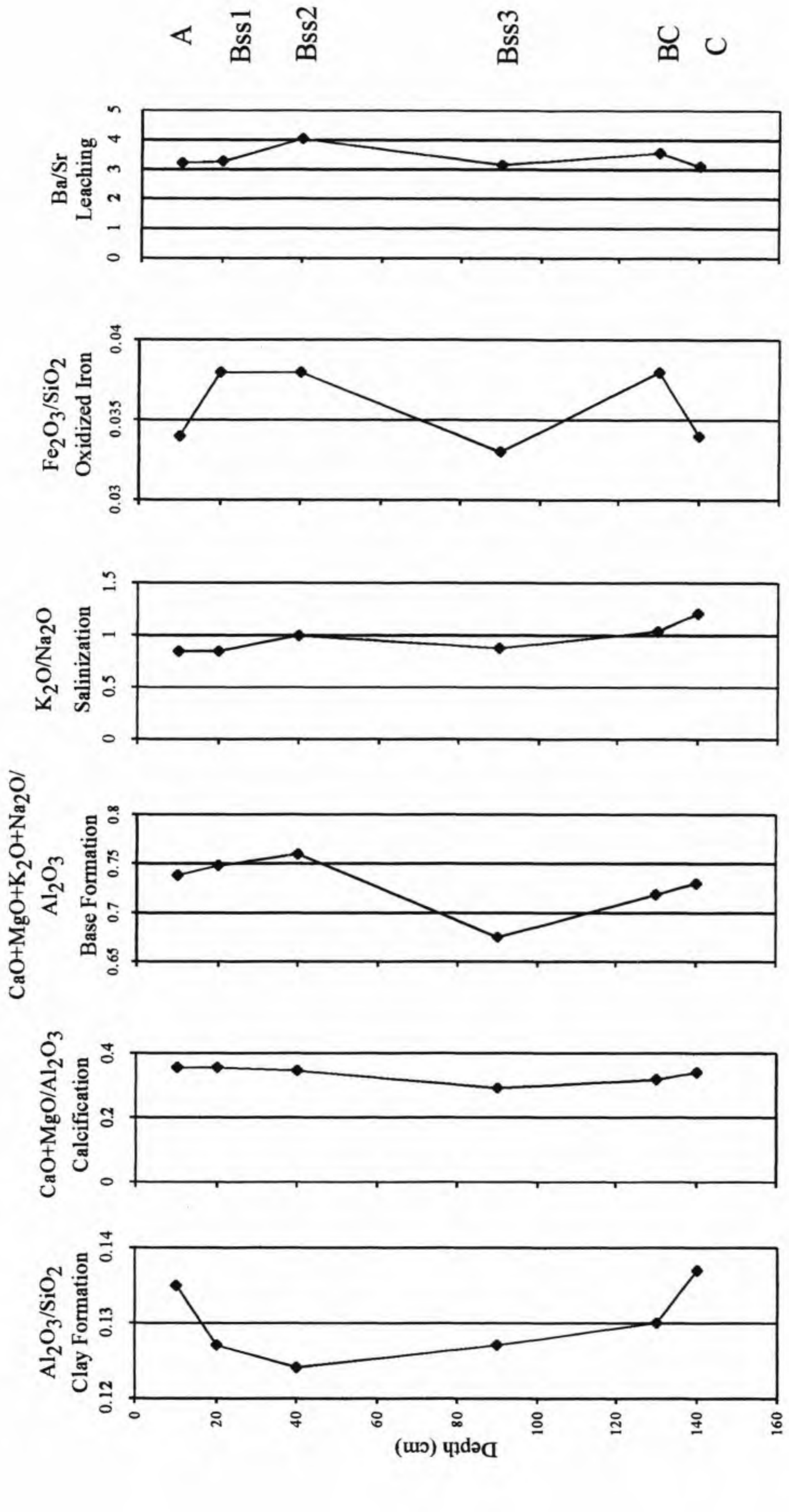
A
Bss1
Bss2
Bss3
BC
C
Ba/Sr
Leaching
Fe2O3/SiO2
Oxidized Iron
K2O/Na2O
Salinization
CaO+MgO+K2O+Na2O/
Al2O3
Base Formation
CaO+MgO/Al2O3
Calcification
Al2O3/SiO2
Clay Formation
Depth (cm)

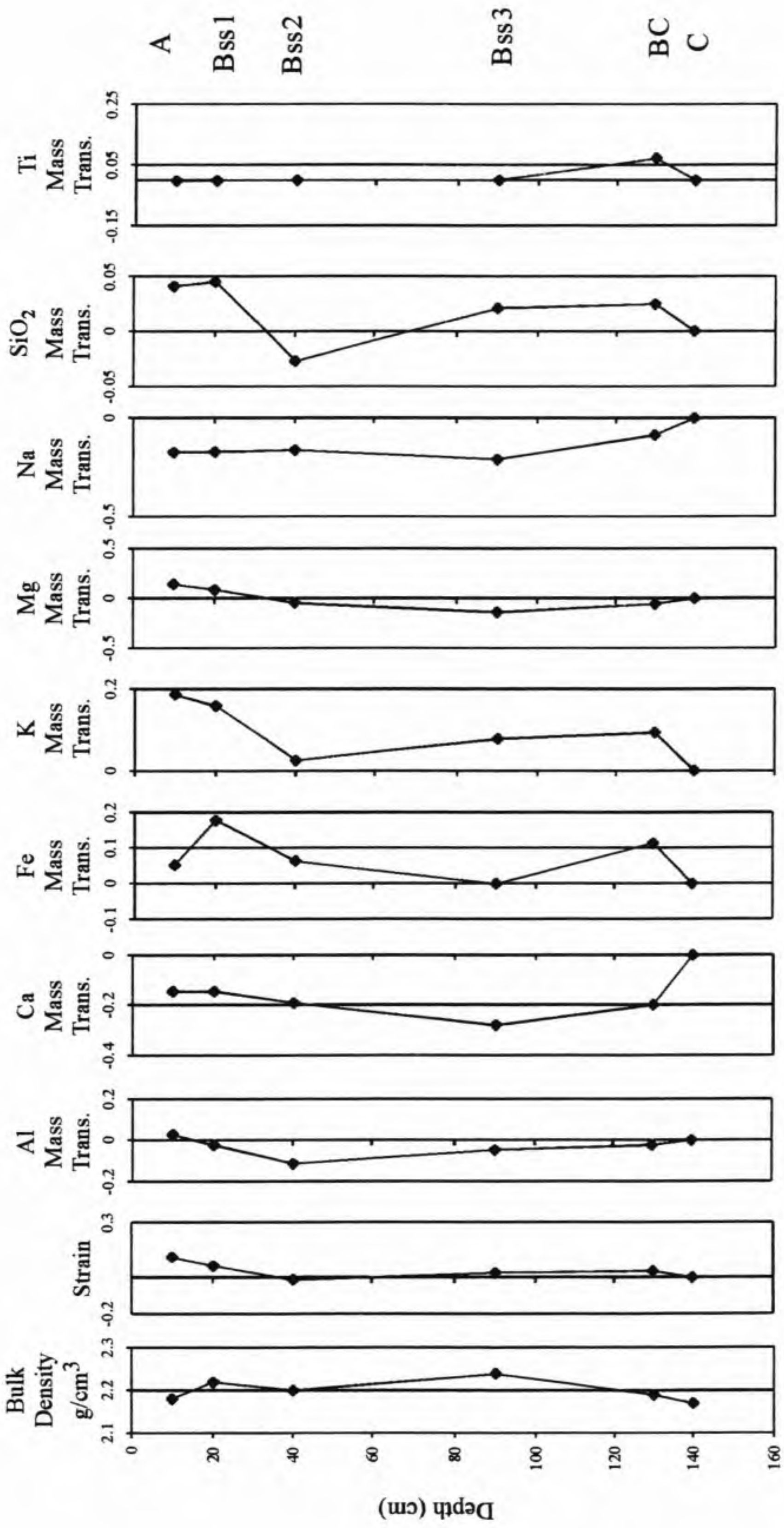
A
Bss1
Bss2
Bss3
BC
C
Ti Mass Trans.
SiO_2 Mass Trans.
Na Mass Trans.
Mg Mass Trans.
K Mass Trans.
Fe Mass Trans.
Ca Mass Trans.
Al Mass Trans.
Strain
Bulk Density g/cm^3
Depth (cm)
0
20
40
60
80
100
120
140
160

APPENDIX H

Doom Pedotype

PS28 Type Coal Paleosol for Doom Pedotype

O1 0-17 cm; black (N 2.5/) coal; strong medium/coarse angular blocky parting to thin platy structure; non-calcareous; very fine sand-size quartz grains present in thin section; abrupt smooth boundary.

Clay 17-20 cm; dusky red (10R 3/3) clay; moderate medium angular blocky parting to medium platy structure; few prominent yellowish red (5YR 5/8) iron oxide stains; few fine black (N 2.5/) root traces; non-calcareous; abrupt smooth boundary. The clay composing the KT fallout layer identified at Knudson's Farm is vermicular kaolinite (Wilding, personal contact, 2002). The portion of the claystone viewed in this section likely represents the 'fireball' claystone described by Hildebrand and Boynton (1988).

O2 20-31 cm; black (N 2.5/) coal; moderate strong medium/coarse angular blocky parting to thin platy structure; non-calcareous; clear smooth boundary.

Bg 31-43 cm; very dark gray (5Y 3/1) clay, moderate medium subangular blocky structure; common prominent yellowish red (5YR 5/8) iron oxide stains; common fine to medium black (N 2.5/) root traces; non-calcareous; porphyroskelic weak insepic/skelesepic microfabric; common root traces and biocasts/pellets, clear smooth boundary (S/Si/C – 38.3/17.3/44.3).

BC 43-60 cm; dark gray (5Y 4/1), strong coarse subangular blocky structure; few prominent red (10R 4/6) iron oxide stains; few fine to medium black (N 2.5/) root traces; non-calcareous; porphyroskelic, with weak insepic/skelesepic microfabric; few root traces and biocasts/pellets (S/Si/C – 42/22.6/35.3).

USDA Taxonomic Classification for Type Paleosol PS28
Epipedon:

Ochric

- Meets no other definition for soil order, reconstructed orgainic surface layer is well over 60 cm thick (not histic).
- Assuming coal compaction of 0.1 times former thickness, original O would have been 280 cm+ thick.

Endopedon:

Cambic

- Texture of vf sand, loamy vf sand, or finer
- Soil structure
- Evidence of alteration in the form of:
    - Evidence of aquic conditions, 50% of chroma is 2 or less, redox features present.

- No argillic, kandic, oxic, or spodic horizon
    - No cementation or induration
    - A lower depth of 25 cm or more from the mineral soil surface.

Order: Histosol (No andic soil properties, likely saturated with water for at least 6 month per year)
- Saprists – Meets no other suborder classification.
- Troposaprist – If there was less than a 5° difference between mean summer and mean winter soil temperatures at a depth of 30 cm

Or
- Medisaprists – Meets no other great group classification
- Likely Typic Troposaprist or Typic Medisaprist – meets no other subgroup classification.

Paleosols in the Doom Pedotype:
C11PS2 – O-Bg1-Bg2-Bg3-C
C11PS5 – O-OA-Bg-BC
T12PS1 – O-OA-Bg1-Bg2-BC
PS28KT – O1-CLAY-O2-Bg-BC

Characteristics of paleosols in the Gloom pedotype:

Paleosols in the Doom pedotype are well developed Histosols that occur at intervals of gleyed, poorly drained paleosols (Figure 22). Doom paleosols typically have rooting that penetrates into subsurface horizons (1m+). However, the dominant features of Doom paleosols are gleyed subsurface horizons and thick (30-60cm) surficial coals.

Geochemistry (absolute values by Retallack, 1997):
- Clay Formation: Absolute values indicate that little clay formation has taken place in most Doom paleosols. However, analysis of sample from PS28 indicates an excess of Al_2O_3 relative to SiO_2. This excess may be related to deposition and reworking of fallout from extraterrestrial impact. Use of the mass transport function for mobile constituents associated with clays (potassium and aluminum) indicates that potassium has been lost from upper horizons relative to the parent material. Aluminum ratios are similar, except for anomalously high values of aluminum in the surface horizon of PS28, possibly associated with fallout. There is no evidence for lessivage in Doom paleosols.
- Calcification: Absolute values indicate very little calcification has taken place in Doom paleosols. Both the calcification weathering ratio and mass transport function indicate that the largest amounts of calcium are found in the organic surface horizon.
- Weathering: Soluble products of hydrolytic weathering occur in the greatest abundance in the surface horizons of the type Doom paleosol. This is most likely due to weathering and alteration of fallout following an extraterrestrial impact (Hildebrand and Boynton, 1988). Absolute values of weathering ratios

indicate little weathering has taken place in the subsurface horizons of Doom paleosols.

- Salinization- Absolute values for salinization are inordinantly large for all paleosols that were investigated. The mass transport function indicates that sodium and potassium have been leached from upper horizons relative to the parent material.
- Oxidation- The molecular weathering ratio for ferric iron indicates the greatest amount of iron oxide occurs in the organic horizons of Doom paleosols. However, the mass transport function indicates that iron has been depleted from upper horizons relative to the parent material, which would be expected for a soil in reducing conditions.
- Leaching- Ba/Sr ratios indicate little leaching in PS28, with moderate leaching in the fallout layer.
- Organic Carbon- Organic carbon levels peak in the surface horizon of the type Gloom paleosol, with the absolute value of organic carbon indicating a significant accumulation of organic material (in excess of 50% organic carbon), and is considered coal. Input of organic matter is the probable cause of positive strain (dilation) in the surface horizons. Position of the PS28 fallout claystone corresponds to a sharp drop in organic carbon levels that rebound in the overlying coal.

Paleoclimatic Implications:

- Thick coal surface horizon indicates 250 cm+ MAP (Retallack, 2001).
- Sepic fabric in the subsoil indicates periodic drainage.
- Abundant primary mineral content in lower horizons indicates a non-oxidizing environment.

Paleobiology:

- Fine roots penetrate nearly 1 meter (up to 75% of soil thickness) into Doom paleosols, indicating periodic drainage.
- PS28 records the change from a pre-impact suite of both angiosperm and gymnosperm species to a post-impact opportunistic angiosperm-dominated plant community (Sweet and Braman, 1992). Most Doom paleosols contain palynological evidence for angiosperms, gymnosperms and algae (Sweet and Braman, 1992).

Paleotopography:

- Flat, flooded overbank plain.

Parent Material:

- Clay-rich overbank/floodplain sediments.

Time for Formation:

- 3,000-6,000 years *or* 6,000-12,000 years, depending on coal thickness assuming coal compaction of 0.1 times former thickness and peat accumulation of 0.5-1.0mm/yr (Retallack, 1997).

Raw chemical data for Doom pedotype (PS28)

SAMPLE DESCRIPTION	Ag ppm	Al %	As ppm	Ba ppm	Be ppm	Bi ppm	Ca %	Cd ppm	Co ppm	Cr ppm	Cu ppm	Fe %	K %	Mg %	Mn ppm	Mo ppm	Na %	Ni ppm	P ppm	Pb ppm	S %	Sb ppm	Sr ppm	Ti %	V ppm	W ppm	Zn ppm	SiO_2 % fusion
PS28O1	<0.5	1.48	5	320	1.5	<2	0.27	<0.5	4	11	10	0.86	0.17	0.13	20	8	0.38	11	40	8	0.26	5	110	0.06	24	<10	12	16.15
PS28CLAY	<0.5	8.6	<5	550	<0.5	2	0.4	<0.5	5	14	8	2.14	0.22	0.43	85	<1	0.82	9	40	28	0.07	<5	110	0.45	28	<10	26	45
PS28O2	<0.5	2.2	<5	390	4	<2	0.83	0.5	7	53	47	0.58	0.08	0.15	35	4	0.7	14	30	14	0.31	15	188	0.16	113	<10	10	8.84
PS28Bg	1	7.08	<5	2400	0.5	2	0.9	<0.5	7	74	18	2.7	1.55	0.61	135	<1	1.82	17	60	20	0.09	5	332	0.33	84	10	54	61.6
PS28BC	<0.5	6.62	10	920	0.5	<2	0.97	<0.5	11	95	19	2.72	1.56	0.62	125	1	1.79	32	330	18	0.04	<5	345	0.32	88	<10	74	61.9

Major Elements Oxide Mass

Depth (cm)	Al_2O_3	CaO	Fe_2O_3	K_2O	MgO	Na_2O	SiO_2	TiO
0	2.8	0.38	1.23	0.2	0.22	0.51	16.15	0.08
17	16.26	0.56	3.06	0.27	0.71	1.11	45	0.6
25	4.16	1.16	0.83	0.096	0.25	0.94	8.84	0.21
40	13.38	1.26	3.86	1.87	1.01	2.45	61.6	0.44
60	12.51	1.36	3.89	1.88	1.03	2.41	61.9	0.43

Organic Carbon

Depth (cm)	OC %
0	47.6
5	46
10	30
15	2.73
17	1.5
20	24.7
25	46.5
30	20.3
40	1.3
50	1
60	0.78

Strain

Depth	BD	Strain
0	1.26	7.8
17	1.8	-0.18
25	1.27	2.28
40	2.01	0.0035
60	2.08	0

Elemental Ratios

Depth (cm)	Al_2O_3/SiO_2	$CaO+MgO/Al_2O_3$	$CaO+MgO+K2O+NaO/Al_2O_3$	Na_2O/K_2O	Fe_2O_3/SiO_2	Ba/Sr
0	0.1	0.44	0.81	4	0.03	1.85
17	0.213	0.175	0.31	6	0.025	3.18
25	0.273	0.66	1.05	15	0.033	1.32
40	0.127	0.359	0.82	2	0.023	4.49
60	0.119	0.407	0.89	1.95	0.023	1.7

Mass Transport

Depth (cm)	Al	Ca	Fe	K	Mg	Na	SiO_2	Ti
0	0.192	0.484	0.685	-0.42	0.118	0.132	0.39	-0.00048
17	-0.078	-0.71	-0.44	-0.9	-0.51	-0.67	-0.48	-0.0021
25	-0.334	0.714	-0.57	-0.9	-0.52	-0.22	-0.714	0.0013
40	0.037	-0.1	-0.037	-0.036	-0.046	-0.014	-0.035	0.00003
60	0	0	0	0	0	0	0	0

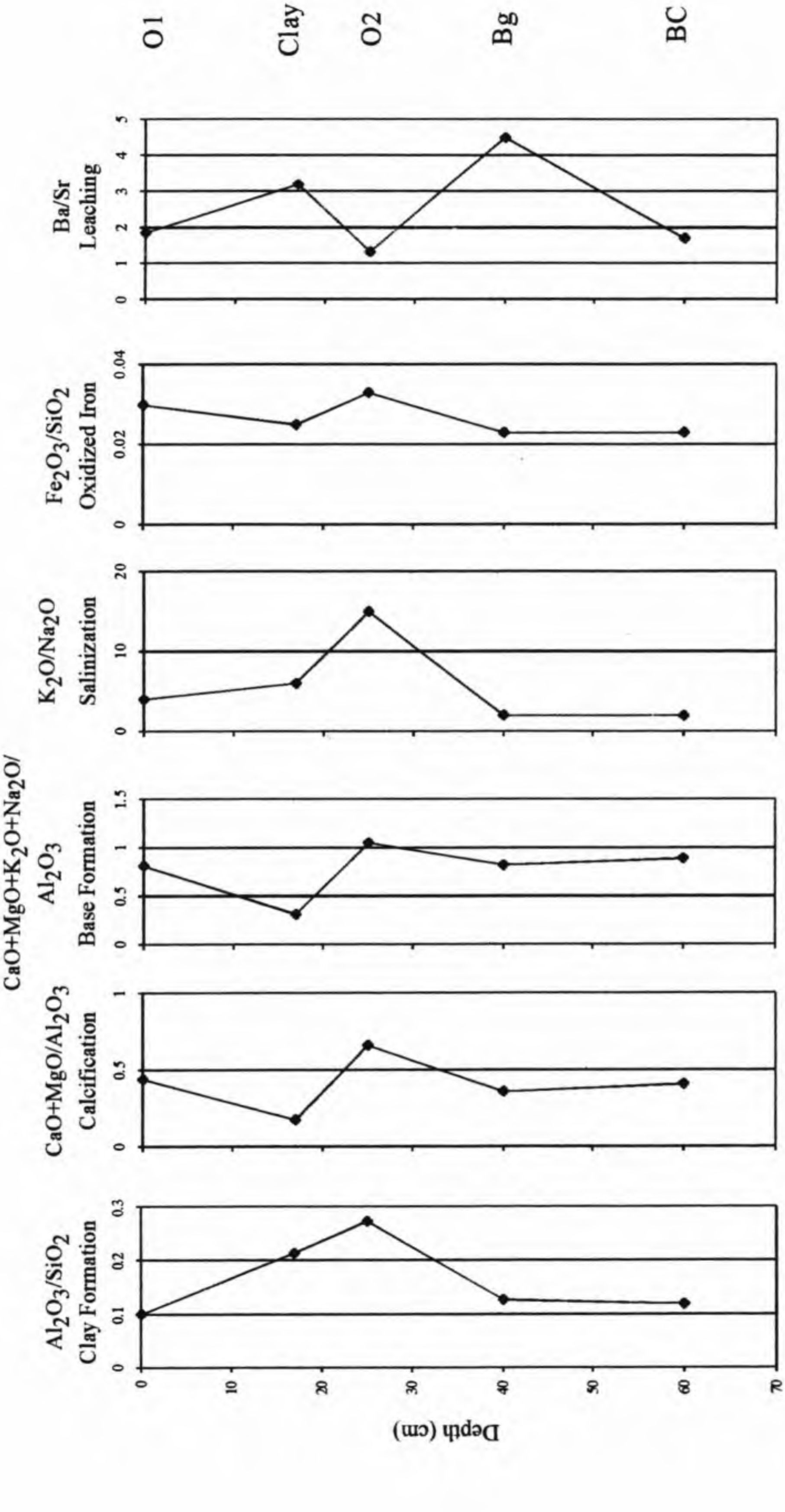
O1
Clay
O2
Bg
BC
Ba/Sr
Leaching
Fe_2O_3/SiO_2
Oxidized Iron
K_2O/Na_2O
Salinization
$CaO+MgO+K_2O+Na_2O/$
Al_2O_3
Base Formation
$CaO+MgO/Al_2O_3$
Calcification
Al_2O_3/SiO_2
Clay Formation
Depth (cm)

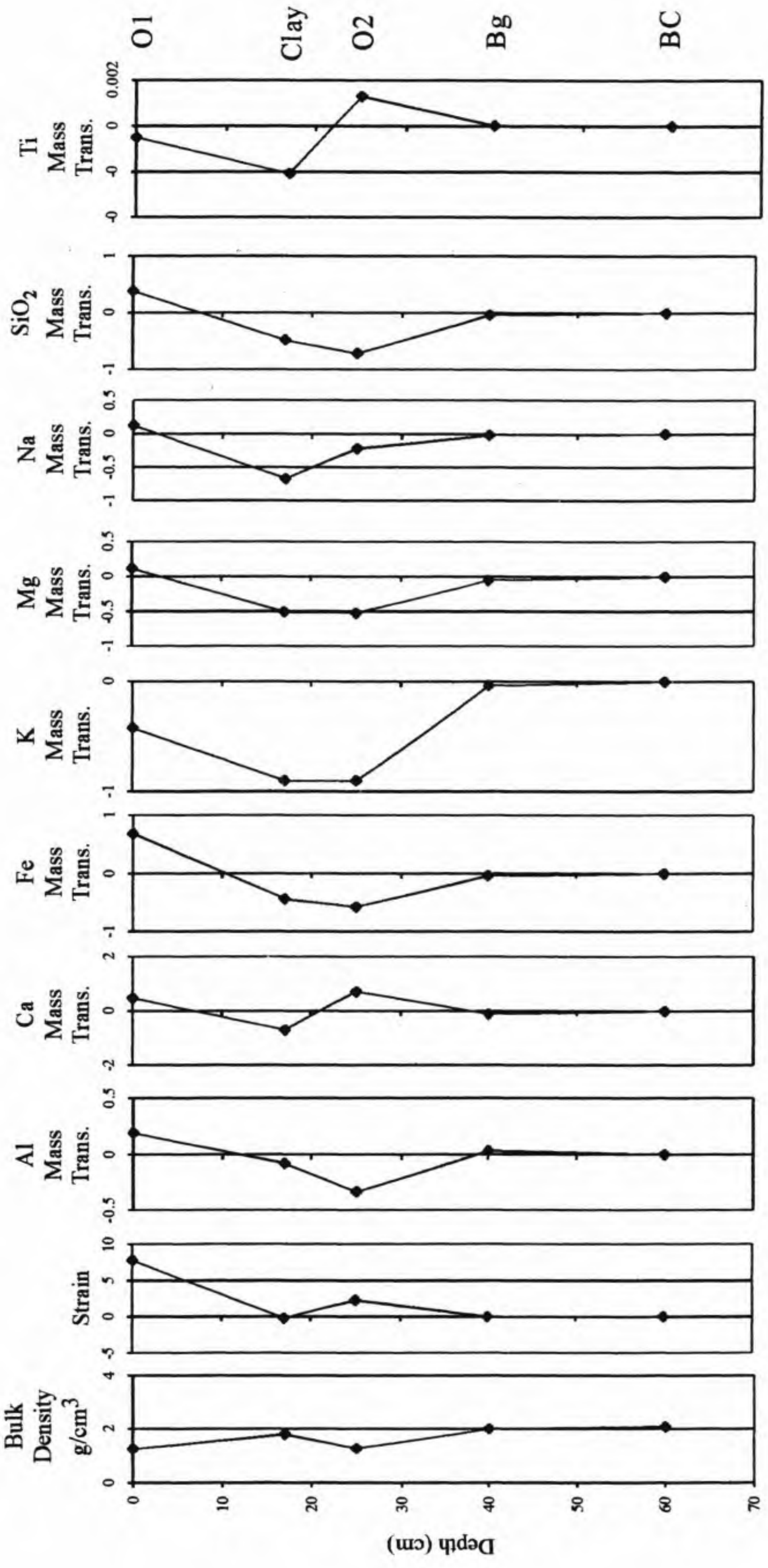

O1
Clay
O2
Bg
BC
Ti Mass Trans.
SiO_2 Mass Trans.
Na Mass Trans.
Mg Mass Trans.
K Mass Trans.
Fe Mass Trans.
Ca Mass Trans.
Al Mass Trans.
Strain
Bulk Density g/cm^3
Depth (cm)

REFERENCES

Binda, P.L., 1992. The Battle Formation: a lacustrine episode in the late Maastrichtian of western Canada, *in* Mateer, N. and Chen, P.J., eds., Aspects of Nonmarine Cretaceous Geology: China Ocean Press, Beijing. p. 220-236.

Birkeland, P.W., 1999, Soils and Geomorphology, third edition. Oxford University Press, New York, 430 p.

Blake, G.R., and Hartge, K.H., 1986, Bulk Density, *in* Klute, A., ed., Methods of soil analysis, part 1, physical and mineralogical methods, second edition. Agronomy series, No. 9, part 1: Soil Science Society of America, Inc., publishers, Madison, Wisconsin, USA, p. 363-376.

Blum, M.D., and Tornqvist, T.E., 2000, Fluvial responses to climate and sea-level change: a review and look forward: Sedimentology, v. 47, suppl. 1, p. 2-48.

Brewer, R., 1976, Fabric and mineral analysis of soils. Robert E. Krieger Pub. Co., Huntington, New York.

Buol, S.W., Hole, F.D., McCracken, R.J., and Southard, R.J., 1997, Soil Genesis and Classification, Fourth Edition: Iowa State University Press, Ames, Iowa. 527 p.

Caldwell, W.G.E., 1984, Early Cretaceous transgressions and regressions in the southern Interior plains. *In* Stott, D.F., and Glass, L.J., eds., The Mesozoic of Middle North America: Canadian Society of Petroleum Geologists, Memoir 9, p. 173-203.

Cant, D.J., and Stockmal, G.S., 1989, The Alberta foreland basin: relationship between stratigraphy and Cordilleran terrane-accretion events: Canadian Journal of Earth Science, v. 26, p. 1964-1975.

Catuneanu, O., Sweet, A.R., and Miall, A.D., 1997, Reciprocal architecture of Bearpaw T-R sequences, uppermost Cretaceous, Western Canada Sedimentary Basin: Bulletin of Canadian Petroleum Geology, v. 45, no. 1, p. 75-94.

Catuneanu, O., and Sweet, A.R., 1999, Maastrichtian-Paleocene foreland-basin stratigraphies, western Canada: a reciprocal sequence architecture: Canadian Journal of Earth Sciences, v. 36, p. 685-703.

Catuneanu, O., Sweet, A.R., and Miall, A.D., 2000, Reciprocal stratigraphy of the Campanian-Paleocene Western Interior of North America: Sedimetary Geology, v. 134, p. 235-255.

Chadwick, O.A., Brimhall, G.H., and Hendricks, D.M., 1990, From a black to a gray box- a mass balance interpretation of pedogenesis: Geomorphology, v. 3, p. 369-390.

Cherven, V.B., and Jacob, A.F., 1985, Evolution of Paleogene depositional systems, Williston Basin, in response to global sea level changes. *In* Flores, F.M., and Kaplan, S.S., Cenozoic paleogeography of the west-central United States: SEPM Symposium No. 3, p. 127-170.

Driese, S.G., Mora, C.I., Stiles, C.A., Joeckel, R.M., and Nordt, L.C., 2000, Mass-balance reconstruction of a modern Vertisol: implications for interpreting the geochemistry and burial history of paleo-Vertisols: Geoderma, v.95, p. 179-204.

Eberth, D.A., and O'Connell, S.C., 1995, Notes on changing paleoenvironments across the Cretaceous-Tertiary boundary (Scollard Formation) in the Red Deer River valley of southern Alberta: Bulletin of Canadian Petroleum Geology, v. 43, p. 44-53.

Fastovsky, D.E., and McSweeney, K., 1987, Paleosols spanning the Cretaceous-Paleogene transition, eastern Montana and western North Dakota: Geological Society of America Bulletin, v. 99, p. 66-77.

Energy, Mines and Resources Canada, 1989, Trochu sheet, 82 P/14, Edition 4, 1:50,000. Canada Centre for Mapping, Department of Energy, Mines and Resources.

Geologic Highway Map of Canada, 1975, Canadian Society of Petroleum Geologists.

Gibson, D.W., 1977, Upper Cretaceous and Tertiary coal-bearing strata in the Drumheller-Ardley region, Red Deer River valley, Alberta: Geological Survey of Canada Paper 76-35.

Gill, J.R., and Cobban, W.A., 1973, Stratigraphy and geologic history of the Montana Group and equivalent rocks, Montana, Wyoming, and North and South Dakota: United States Geological Survey Professional Paper 776, 37 p.

Harland, W.B., Cox, A.V., Llewellyn, P.G., Pickton, C.A.G., Smith, A.G., and Walters, R., 1982, A Geologic Time Scale: Cambridge University Press, p. 4-80.

Hansen, T. A., Farrand, R., Montgomery, H., and Billman, H., Sedimentology and extinction patterns across the Cretaceous-Tertiary boundary interval, Brazos River Valley, East Texas: American Association of Petroleum Geologists Field Trip Guidebook, p. 21-36.

Haq, B.U., Hardenbol, J., and Vail, P.R., 1988, Mesozoic and Cenozoic chronostratigraphy and cycles of sea-level change. *In* Sea-Level changes – an integrated approach. SEPM Special Publication No. 42.

Hildebrand, A.R., and Boynton, W.V., 1988, Provenance of the K/T boundary layers. *In* Global catastrophies in earth history: an interdisciplinary conference on impacts, volcanism, and mass mortality: Lunar and Planetary Institute contribution No. 673, p. 78-79.

Irish, E.J.W., 1970, The Edmonton Group of south-central Alberta: Bulletin of Canadian Petroleum Geology, v. 18, p. 125-155.

Izett, G.A., 1990, The Cretaceous/Tertiary boundary interval, Raton Basin, Colorado and New Mexico: Geological Society of America Special Paper 249. 100 p.

Jenny, H., 1941, Factors of Soil Formation: McGraw-Hill, New York. 288 p.

Jerzykiewicz, T., 1985, Stratigraphy of the Saunders Group in the central Alberta Foothills-a progress report: Geological Survey of Canada, Paper 85-1B, p. 247-258.

Jerzykiewicz, T., and Sweet, A.R., 1988, Sedimetological and palynological evidence of regional climatic changes in the Campanian to Paleocene sediments of the Rocky Mountain Foothills, Canada: Sedimentary Geology, v. 59, p. 29-76.

Jerzykiewicz, T., 1997, Stratigraphic framework of the uppermost Cretaceous to Paleocene strata of the Alberta basin: Geological Survey of Canada Bulletin 510.

Kraus, M.J., 1988, Integration of channel and floodplain suites II. Vertical relations of alluvial paleosols: Journal of Sedimentary Petrology, v.57, no.4, p. 602-612.

Lerbekmo, J.F., and Coulter, K.C., 1983, Late Cretaceous to early Tertiary magnetostratigraphy of a continental sequence: Red Deer Valley, Alberta: Canadian Journal of Earth Science, v. 22, p. 567-583.

Lerbekmo, J.F., Demchuk, T.D., Evans, M.E., and Hoye, G.S., 1992, Magnetostratigraphy and biostratigraphy of the continental Paleocene of the Red Deer Valley, Alberta, Canada: Bulletin of Canadian Petroleum Geology, v. 40, no. 1, p. 24-35.

Lerbekmo, J.F., Sweet, A.R., and Braman, D.R., 1995, Magnetobiostratigraphy of late Maastrichtian to earlt Paleocene strata of the Hand hills, south central Alberta, Canada: Bulletin of Canadian Petroleum Geology, v. 43, no. 1, p. 35-43.

Ludvigson, G.A., Gonzalez, L.A., Metzger, R.A., Witzke, B.J., Brenner, R.L., Murillo, A.P., and White, T.S., 1998, Meteoric sphaerosiderite lines and their use for paleohydrology and paleoclimatology: Geology, v. 26; no. 11, p. 1039-1042.

Mack, G.H., 1992, Paleosols as an indicator of climatic change at the early-late Cretaceous boundary, southwestern New Mexico: Journal of Sedimentary Petrology, v. 62, no. 3, p. 483-494.

McCarthy, P.J., Faccini, U.F., and Plint, A.G., 1999, Evolution of an ancient coastal plain: paleosols, interfluves, and alluvial architecture in a sequence stratigraphic f ramework, Cenomanian Dunvegan Formation, NE British Columbia, Canada: Sedimentology, v. 46, p. 861-891.

McCarthy, P.J., and Plint, A.G., 1998, Recognition of interfluve sequence boundaries: Integrating paleopedology and sequence stratigraphy: Geology, v. 26, p. 387-390.

Miall, A.D., 1985, Architectural-element analysis: a new method of facies analysis applied to fluvial deposits: Earth Science Review, vol. 22, p. 261-308.

Miall, A.D., 1992, Alluvial Deposits. *In* Walker, R.G., and James, N.P., eds., Facies Models: response to sea level change: Geological Association of Canada, St. John's, Newfoundland, p. 119-142.

Miall, A.D., 1996, The Geology of Fluvial Deposits: Springer-Verlag Publishers, New York. 582 p.

Nambudiri, E.M.V., and Binda, P.L., 1991, Paleobotany, palynology and depositional environment of the Maastrichtian Whitemud Formation in Alberta and Saskatchewan, Canada: Cretaceous Research, v. 12, p. 579-596.

Posamentier, H.W., and Allen, G.P., 1993, Siliciclastic sequence stratigraphic patterns in foreland ramp-type basins: Geology, v. 21, p. 455-458.

Posamentier, H.W., and Vail, P.R., 1988, Eustatic controls on clastic deposition II– Sequence and systems tract models. *In* Sea-Level changes – an integrated approach: SEPM Special Publication No. 42.

Ready, C.D., and Retallack, G.J., 1995, Chemical composition as a guide to paleoclimate of paleosols: Geological Society of America Abstracts, v. 27, A237.

Retallack, G.J., Leahy, G.D., and Spoon, M.D., 1987, Evidence from paleosols for ecosystem changes across the Cretaceous/Tertiary boundary in eastern Montana: Geology, v. 15, p. 1090-1093.

Retallack, G.J., Dugas, D.P., and Bestland, E.A., 1990, Fossil soils and grasses of the middle Miocene, East African grassland: Science, v. 247, p. 1325-1328.

Retallack, G.J., 1994, A pedotype approach to latest Cretaceous and earliest Tertiary paleosols in eastern Montana: Geological Society of American Bulletin, v. 106, p. 1377-1397.

Retallack, G.J., 1996, Paleosols: record and engine of past global change: Geotimes, v. 41, no. 6, p. 25-28

Retallack, G.J., Veevers, J.J., and Morante, R., 1996, Global early Triassic coal gap between Late Permian extinction and Middle Triassic recovery of peat-forming plants: Geological Society of America Bulletin, v. 108, p. 195-207.

Retallack, G.J., 1997, A Colour Guide to Paleosols: John Wiley & Sons, New York, 174 p.

Retallack, G.J., 2001, Soils of the Past, second edition: Blackwell Science, Malden, MA, 404 p.

Richardson, R.J.H., Strobl, R.S., MacDonald, D.E., Nurkowski, J.R., McCabe, P.J., and Bosman, A., 1988, An evaluation of the coal resourcesof the Ardley coal zone, to a depth of 400 m, in the Alberta plains area: Alberta Geological Survey, Open File Report, v. 2, 96 p.

Russell, L.S., 1983, Evidence for an unconformity at the Scollard-Battle contact, Upper Cretaceous strata, Alberta: Canadian Journal of Earth Sciences, v. 20, p. 544-568.

Schumm, S.A., 1993, River response to baselevel change: Implications for sequence stratigraphy: The Journal of Geology, v. 101, p. 279-294.

Schwans, P., 1995. Controls on sequence stacking and fluvial shallow marine architecture in a foreland basin. *In* Van Wagoner, J.C., and Bertram, G.T., eds., Sequence stratigraphy of foreland basin deposits – outcrops and subsurface examples from the Cretaceous of North America: American Association of Petroleum Geologists Memoir 64. p. 55-102.

Shanley, K.W., and McCabe, P.J., 1994, Perspectives on the sequence stratigraphy of continental strata: American Association of Petroleum Geologists Bulletin, v. 78, no. 4, p. 544-568.

Soil Survey Staff, 1998, Keys to Soil Taxonomy, seventh edition: U.S. Department of Agriculture, Natural Resources Conservation Service, 643 p.

Stockmal, G.S., Cant, D.J., and Bell, J.S., 1992, Relationship of the stratigraphy of the Western Canada foreland basin to cordilleran tectonics: Insights from geodynamic models. *In* MacQueen, R.W., and Leckie, D.A., eds., Foreland Basins and Fold Belts: American Association of Petroleum Geologists, Memoir 55, p. 107-124.

Sweet, A.R., 2001, Plants, a yardstick for measuring the environmental consequences of the Cretaceous-Tertiary boundary event: Geoscience Canada, v. 28, no. 3, p. 127-138.

Sweet, A.R., Braman, D.R., and Lerbakmo, J.F., 1990, Palynofloral response to K/T boundary events; A transitory interruption within a dynamic system. *In* Sharpton, V.L., and Ward, P.D., eds., Global catastrophies in Earth history; An interdisciplinary on inputs, volcanism, and mass mortality: Geological Society of America Special Paper 247.

Sweet, A.R., and Braman, D.R., 1992, The K-T boundary and contiguous strata and western Canada: interactions between paleoenvironments and palynological assemblages: Cretaceous Research, v. 13, p. 31-79.

Walker, R.G., and James, N.P., 1992, Facies models: response to sea level change: Geological Association of Canada, St. John's, Newfoundland.

Wilding, L.P., and Puentes, R., eds., 1988, Vertisols: Technical Monograph No. 18, Soil Management Support Services. Texas A&M University Printing Center, College Station, TX. 193 p.

Zaitlin, B.A., Dalrymple, R.W., and Boyd, R., 1994, The stratigraphic organization of incised-valley systems associated with relative sea-level change: SEPM Special Publication No. 51, p. 45-60.